UNIVERSITY OF CALIFORNIA, SAN DIEGO

Iron distribution and phytoplankton iron limitation in the southern California Current System

A Dissertation submitted in partial satisfaction of the
Requirements for the degree in Doctor of Philosophy

in

Oceanography

by

Andrew Luke King

Committee in charge:

Professor Katherine Barbeau, Chair
Professor Nigel Crawford
Professor Michael Landry
Professor B. Greg Mitchell
Professor Clinton Winant

2008

The Dissertation of Andrew Luke King is approved, and it is acceptable in quality and form for publication on microfilm:

_____

_____

_____

_____

_____
Chair

University of California, San Diego

2008

Dedication

For Mom and Dad,

and for Mike Mullin.

Table of Contents

List of Tables

List of Figures

Acknowledgements

I would like to thank my mentors/advisors for the last ten years of my training in oceanography: Mike Mullin, Ken Smith, and Kathy Barbeau. In particular, Kathy Barbeau has been an exceptional mentor and advisor, and has provided paramount interdisciplinary expertise, consistent funding for research, and unfaltering patience and emotional support during my time in her lab. I would also like to thank my committee members for their intellectual contributions and time commitments: Nigel Crawford, Michael Landry, Greg Mitchell, and Clinton Winant.

The Barbeau Lab has been a unique research environment due to the varying backgrounds of undergraduates, graduate students, postdocs, visiting researchers, and technicians we have had over the years. Brian Hopkinson, especially, has been a wonderful labmate. Brian and I began graduate school together, worked on similar research projects, and sailed together on several research cruises. The work presented in this dissertation would not be possible without valuable discussions with him and his willingness to help and teach. Kelly Roe, Chris Dupont, and Kristen Buck also provided great help and discussion with work presented in this dissertation.

A bulk of this research has been a piece of larger research programs: CalCOFI (California Cooperative Oceanic Fisheries Investigations), CCE-LTER (California Current Ecosystem-Long Term Ecological Research), and SAFe (Standardization and Analysis of Fe). I would like to thank the Chief Scientists on cruises I have sailed on including Mike Landry, Neil Driscoll, Elizabeth Venrick, Dave Wolgast, Jim Wilkinson, Ron Dotson, and Amy Hays. I would also like to acknowledge the hard

work or fellow scientists, technicians, and research vessel officers and crew for sample collection and analysis.

Lastly, I would like to thank my family and friends who have always supported my pursuit of science.

This research has been funded by NASA New Investigator Program (NAG5-12535), the California Current Ecosystem Long-Term Ecological Research program (NSF/OCE-0417616), and OCE-0550302.

Chapter 2 has been submitted to Limnology and Oceanography: Methods as: King, Andrew L., and Katherine A. Barbeau. Determination of dissolved iron in seawater using iron(II) sulfite reduction with nitriloacetic acid resin preconcentration and chemiluminescent flow injection analysis. Chapter 3 of this dissertation has been published elsewhere as: King, Andrew L., and Katherine A. Barbeau. Evidence for phytoplankton iron limitation in the southern California Current System. 2007. Marine Ecology Progress Series. 342:91-103. I was the primary researcher and author of this article. Chapter 4 is in preparation for publication as: King, Andrew L., and Katherine A. Barbeau. Iron distribution in the southern California Current System and relation to macronutrients and phytoplankton.

Vita

1998-2001	Undergraduate Researcher, Scripps Institution of Oceanography, University of California, San Diego
1999	Summer Student Fellow/Minority Trainee, Woods Hole Oceanographic Institution
2000	Research Associate, Hawaii Institute of Marine Biology, University of Hawaii, Manoa
2000	B.S., Biology: Ecology, Behavior and Evolution, University of California, San Diego
2001-2008	Graduate Student Researcher, Scripps Institution of Oceanography, University of California, San Diego
2005	Teaching Assistant, California State Summer School for Mathematics and Science, Jacobs School of Engineering, University of California, San Diego
2006	Co-Instructor, California State Summer School for Mathematics and Science, Jacobs School of Engineering, University of California, San Diego
2008	Ph.D. Oceanography, Scripps Institution of Oceanography, University of California, San Diego

Publications

King, A.L. and K. Barbeau. 2007. Evidence for phytoplankton iron limitation in the southern California Current System. *Marine Ecology Progress Series*, 342:91-103.

Johnson, K.S., E. Boyle, K. Bruland, K. Coale, C. Measures, J. Moffett, A. Aguilar-Islas, K. Barbeau, B. Bergquist, A. Bowie, K. Buck, Y. Cai, Z. Chase, J. Cullen, T. Doi, V. Elrod, S. Fitzwater, M. Gordon, **A.L. King**, P. Laan, L. Laglera-Baquer, W. Landing, M. Lohan, J. Mendez, A. Milne, H. Obata, L. Ossiander, J. Plant, G. Sarthou, P. Sedwick, G. Smith, B. Sohst, S. Tanner, C. van den Berg, and J. Wu. 2007. Developing standards for dissolved iron in seawater. *Eos Transactions AGU*, 88:131–132.

King, A.L. and E. La Casella. 2003. Seasonal variations in abundance, distribution, and population structure of *Metridia gerlachei* in Port Foster, Deception Island, Antarctica. *Deep-Sea Research II*, 50:1753-1763.

Kaufmann, R.S., E.C. Fisher, W.H. Gill, **A.L. King**, M. Laubacher, and B. Sullivan. 2003. Temporal patterns in the distribution, biomass and community structure of macrozooplankton and micronekton within Port Foster, Deception Island, Antarctica. *Deep-Sea Research II*, 50: 1765-1785.

Sturz, A.A., S.C. Gray, K. Dykes, **A.L. King**, and J. Radtke. 2003. Seasonal changes of dissolved nutrients within and around Port Foster, Deception Island, Antarctica. *Deep-Sea Research II*, 50:1685-1705.

Beaulieu, S.E., M.M. Mullin, S. Pyne, V. Tang, **A.L. King** and B.S. Twining. 1999. Using an optical plankton counter to determine size distributions of preserved zooplankton samples. *Journal of Plankton Research*, 21:1939-1956.

Awards

1999	Two - National Science Foundation Research Experience for Undergraduates Award
2000	National Science Foundation Antarctica Service Medal
1999-2000	David Marc Belkin Research Scholarship
2004	Best Student Poster in session, American Society of Limnology and Oceanography/The Oceanography Society Ocean Research Conference
2005	Best Student Poster (3rd) overall, The Oceanography Society/United Nations Education, Scientific and Cultural Organization International Ocean Research Conference
2006	Best Oral Presentation in session, North Pacific Marine Science Organization, XV Annual Meeting

ABSTRACT OF THE DISSERTATION

Iron distribution and phytoplankton iron limitation in the southern California Current System

by

Andrew Luke King

Doctor of Philosophy in Oceanography

University of California, San Diego, 2008

Professor Katherine Barbeau, Chair

The research presented in this dissertation focuses on the distribution of dissolved iron (<0.4 μm) and its biogeochemical consequences in the southern California Current System (sCCS). Trace metal clean oceanographic techniques were used to conduct iron addition bottle experiments and collect samples for dissolved iron on ten research cruises between 2002 and 2007. The concentration of dissolved iron from both mixed layer and water column samples was determined using a new and improved flow injection method with preconcentration of iron(II) on nitriloacetic acid

and luminol chemiluminescence detection (detection limit of 0.02 nM iron). Spatially and temporally, elevated dissolved iron concentrations were found to be generally associated with coastal upwelling processes in the northern coastal domain of the study area, and thus corresponded with elevated macronutrient and chlorophyll a concentrations. However, at the fringes and outside of the northern coastal domain (~10-100 km from the coast) during April 2003, April 2004, July 2003, July 2004, and April 2007, dissolved iron concentrations dropped rapidly below ~0.5 nM and were found to be lower relative to macronutrients, especially nitrate. This was supported by regional and mesoscale synoptic observations during California Cooperative Oceanic Fisheries Investigations (CalCOFI) survey cruises and mesoscale Lagrangian drifter studies during California Current Ecosystem-Long Term Ecological Research (CCE-LTER) cruises. The spatial extent of the nitrate-dissolved iron decoupling was as far as ~100 km offshore in April 2003 and 2004 and as far as ~250 km offshore in July 2003 and 2004. Iron addition bottle experiments conducted in relatively high nitrate-low dissolved iron mixed-layer water masses in July 2003 and 2004 indicated that phytoplankton nitrate-utilization, and therefore growth, was limited by iron availability. Somewhat analogous to the spatial decoupling between dissolved iron and nitrate in the mixed layer, the ferricline (defined as the depth where dissolved iron is >0.2 nM) was found to be deeper than the nitracline (defined as the depth where nitrate is >1 μM) on several occasions in July 2007. Based on these findings and the results of other studies in nearby systems, the distribution of dissolved iron has important biological and geochemical implications for the sCCS.

Chapter 1

Introduction

1.1. Background

Recent research, driven in part by the development of trace metal clean techniques, has recognized the low concentrations and biological importance of transition metals in the ocean (Butler 1998; Morel and Price 2003). Arguably the most important relationship which has arisen is between iron (as a micronutrient) and phytoplankton. Like all transition metals, iron has a d-electron configuration which readily undergoes reduction-oxidation transitions between iron(II) and iron(III) at physiological redox potentials. Iron is primarily used for electron transport and has been found to be an obligate requirement for phytoplankton - central to metalloproteins and metalloenzymes in photosynthesis, respiration, and nitrogen assimilation. The photosynthetic electron transport chain, including photosynthetic proteins and superoxide dismutase (an enzyme that mediates oxidative stress), accounts for about 80% of phytoplankton cellular iron (Raven 1990). The requirement for iron by phytoplankton also depends on the type of nitrogen that is utilized. Both neritic and oceanic phytoplankton cultured with ammonium, a reduced and bioavailable form of nitrogen, have been shown to require 30-40% less iron than phytoplankton grown on nitrate (Raven et al. 1992; Maldonado and Price 1996).

It has been hypothesized that photosynthesis evolved in an anoxic ocean in which iron(II) was abundant. The eventual expansion of photosynthetic organisms resulted in the oxygenation of the surface layer of the oceans and consequently low dissolved iron concentrations. While iron(II) is soluble in seawater, oxygen quickly oxidizes iron(II) to the thermodynamically-stable and insoluble iron(III) oxidation state. Indeed, due to scavenging and biological uptake the modern surface oceans are

very low in dissolved iron. The concentration of dissolved iron decreases as much as 100-fold from coastal to oceanic waters. Dissolved iron input is high in coastal regions due to the proximity of the continental shelf, although the transition from iron-replete (up to 10 nM) to low iron (<0.2 nM) waters can occur within 50 km (Johnson et al. 1997; Bruland et al. 2001), and at times within the boundary of the continental shelf (Johnson et al. 1999) or the continental slope (Chase et al. 2002). The open ocean relies primarily on atmospheric dust deposition and/or upwelling of deep water as sources of iron (Duce and Tindale 1991; Coale et al. 1997). The high phytoplankton iron requirement relative to dissolved iron concentrations, the similarity in vertical profile shapes of dissolved iron and macronutrients nitrate and phosphate, and observations of remote ocean regions enriched in macronutrients with low phytoplankton standing stock have prompted researchers to examine iron as a potentially limiting nutrient for phytoplankton productivity (Martin 1989). Mesoscale iron fertilization experiments in high nutrient, low chlorophyll (HNLC; chlorophyll is a proxy for phytoplankton standing stock) regimes in the Southern Ocean and the equatorial and subarctic Pacific Ocean have confirmed that phytoplankton productivity is iron-limited (Coale et al. 1996; Boyd et al. 2000; Tsuda et al. 2003; Coale et al. 2004). In HNLC regions spanning at least 20% of the oceans (Coale 2000), low iron availability controls phytoplankton size structure, resulting in communities dominated by smaller cells at low standing stock, maintained by microzooplankton grazing pressure (Landry et al. 1997).

Similar HNLC conditions have also been observed in other oceanic regions including eastern boundary current (EBC) upwelling regimes, such as the California

Current System (CCS) and the Peru Upwelling region. These areas are traditionally thought to be very productive due to intense wind-driven coastal upwelling of macronutrients nitrate, phosphate, and silicic acid, in addition to a nearby continental source of iron. Continental margins represent <1% of the world's ocean surface area but disproportionately account for over 10% of global ocean primary productivity (Chavez and Toggweiler 1995). However, HNLC conditions due to iron limitation of phytoplankton productivity have recently been observed in some regions of EBCs, including the CCS off central and northern California (Hutchins and Bruland 1998; Bruland et al. 2001; Johnson et al. 2001; Firme et al. 2003; Fitzwater et al. 2003), and in the Peru Upwelling region (Hutchins et al. 2002; Bruland et al. 2005). Iron limitation arises due to the reduced supply of iron relative to macronutrients via coastal upwelling along narrow continental shelves. In contrast, upwelling along wide continental shelves entrains a significant source of iron from the associated benthic boundary layer.

In comparison to the central and northern California EBC systems, the southern California Current System (sCCS) is quite different due to its complex circulation and weaker, broader nutrient supply regime. Since 1949, the sCCS has been studied by the California Cooperative Oceanic Fisheries Investigations (CalCOFI; see Fig. 1.2 for map of study area and station locations). Situated between the United States-Mexico border and Point Conception, California, the sCCS is a unique biogeographical niche high in physical and biological mesoscale variability, and serves as an important nursery ground for epipelagic fish of the entire CCS. Included in a large suite of physical, biological, and chemical measurements, the

CalCOFI dataset of phytoplankton chlorophyll and productivity and macronutrient concentrations has contributed to understanding the link between upwelling and phytoplankton growth (e.g. Hayward and Venrick 1998). The largest and most well-understood component of surface macronutrient enrichment is wind-driven coastal upwelling, although this upwelling is considerably weaker in magnitude compared to typical EBC systems due to the curtailing of northerly winds by the southern Californian topography (see Fig. 1.2; Eppley and Peterson 1979; Wilkerson and Dugdale 1987). Strong spring and summer-time equatorward winds near Point Conception and the Santa Barbara Channel upwell nutrient-rich waters typically within 10 km of the coast and support massive diatom blooms (Venrick 1998). Another supply of macronutrients to surface waters ~50-250 km offshore is the shoaling of isopycnals observed to be associated with Ekman pumping due to large wind stress curl, high eddy kinetic energy, and the boundary of the CC jet (Chelton 1982; Winant and Dorman 1997; Hayward and Venrick 1998; Di Lorenzo et al. 2003).

Work from the CalCOFI program and the Southern California Bight Studies (SBCS) in the 70's and 80's has identified nitrate as the limiting nutrient for phytoplankton new production and an as an important factor controlling the distribution of phytoplankton standing stock (Eppley et al. 1979; Eppley and Holm-Hansen 1986). The upwelling of nitrate to surface waters in the sCCS was found to be a dominant source of biological variability, often perturbing oligotrophic-type conditions and resulting in shifts to larger phytoplankton community structure, higher standing stock and greater primary productivity. However, the analysis of archived CalCOFI data indicates that there were times, especially in spring and summer, when

the spatial distribution of nitrate and chlorophyll a were decoupled (Fig. 1.3). Among many possible processes, the limitation by a nutrient other than nitrate could explain this observation. The distribution of dissolved iron and the role of iron as a micronutrient, although likely to be pertinent to phytoplankton in the sCCS, has not yet been assessed. This dissertation presents evidence for phytoplankton iron limitation in the sCCS transition zone during summer and describes the distribution of iron and its biogeochemical consequences from ten cruises between 2002 and 2007.

1.2. Organization of the dissertation

Chapter 2 contains a detailed description of a new and improved analytical method developed for determining dissolved iron in the sub-nM range. Results from this work have accompanied an article published in *Marine Ecology Progress Series* (King and Barbeau 2007; Chapter 3) and work related to the Standardization and Analysis of Fe seawater reference samples was included in an article in *Eos Transactions* (Johnson et al. 2007). This description and assessment of the method has been submitted to *Limnology and Oceanography: Methods*.

Chapter 3 describes shipboard iron addition bottle experiments at ten CalCOFI stations during July 2003 and July 2004 in the sCCS. The biological and chemical results of these experiments are discussed in the context of phytoplankton iron limitation and biogeochemical cycles in the region. This chapter was published in 2007 in *Marine Ecology Progress Series* (King and Barbeau 2007).

Chapter 4 presents distributions of dissolved iron from ten research cruises. Both mixed layer distribution of iron and vertical iron profiles are described and

discussed in the context of sources of iron, processes that could explain observed patterns, and biogeochemical consequences for the sCCS. The contents of Chapter 4 are in preparation for publication.

Chapter 5 summarizes findings from the previous chapters and discusses future directions for iron biogeochemistry in the sCCS.

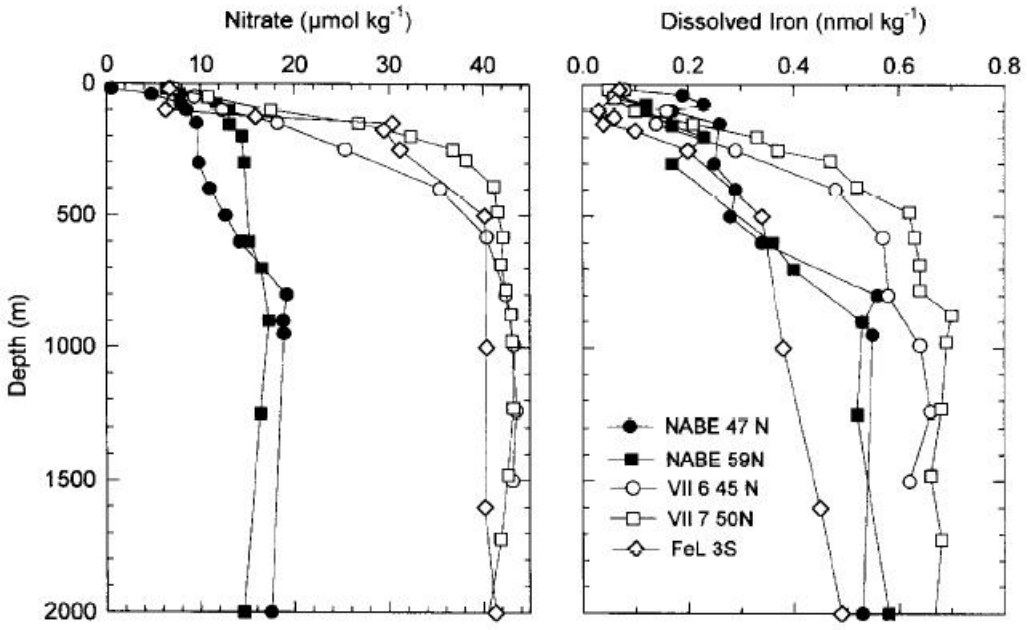

Figure. 1.1. Nitrate and dissolved iron concentrations from the north Atlantic (filled symbols) and equatorial Pacific (open symbols); nmol $kg^{-1} \approx$ nmol L^{-1}. From Coale et al. (1997).

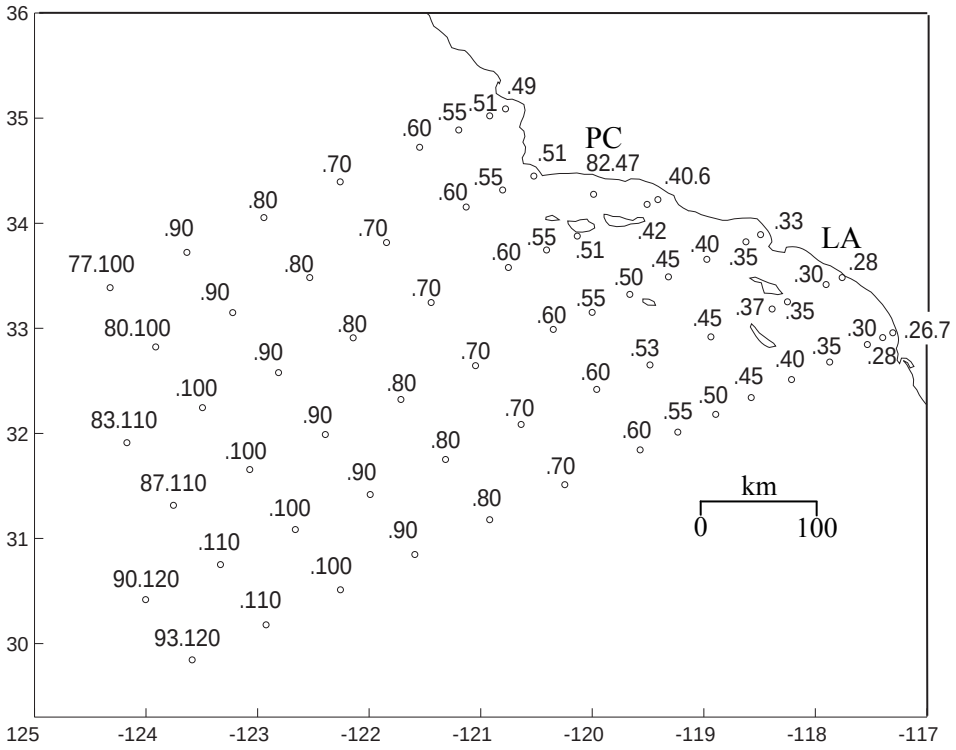

Figure. 1.2. Station locations of hydrographic surveys conducted by the California Cooperative Oceanic Fisheries Investigations (CalCOFI) as of 1984. For geographic reference, Point Conception (PC) and Los Angeles (LA), CA are labeled. Line numbers are designated to the left of decimal point and station numbers are to the right, i.e. 90.53 = line 90, station 53.

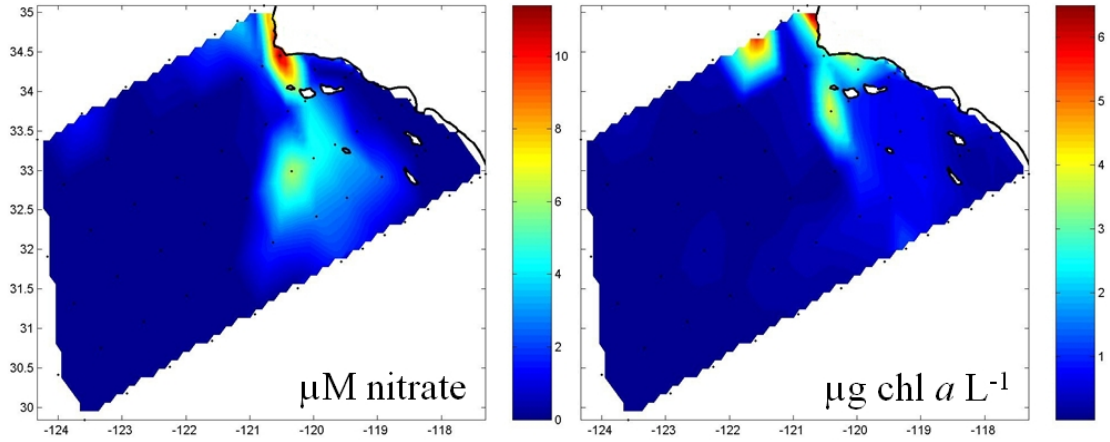

Figure. 1.3. Synoptic view of nitrate and chlorophyll a during June 2000 CalCOFI cruise. Actual data were interpolated between stations marked with black dots. Note the decoupled distribution of high nitrate (1-4 µM) relative to low chlorophyll (<1 µg chl L^{-1}) in the southern offshore region.

1.3. Literature cited

Boyd, P.W, A.J. Watson, C.S. Law, E.R. Abraham, T. Trull, R. Murdoch, D.C.E. Bakker, A.R. Bowie, K.O. Buesseler, H. Chang, M. Charette, P. Croot, K. Downing, R. Frew, M. Gall, M. Hadfield, J. Hall, M. Harvey, G. Jameson, J. LaRoche, M. Liddicoat, R. Ling, M.T. Maldonado, R.M. McKay, S. Nodder, S. Pickmere, R. Pridmore, S. Rintoul, K. Safi, P. Sutton, R. Strzepek, K. Tanneberger, S. Turner, A. Waite and J. Zeldis. 2000. A mesoscale phytoplankton bloom in the polar Southern Ocean stimulated by iron fertilization. Nature 407: 695-702.

Bruland, K.W., E.L. Rue, and G.J. Smith. 2001. Iron and macronutrients in California coastal upwelling regimes: Implications for diatom blooms. Limnol. Oceanogr. 46: 1661-1674.

Bruland, K.W., E.L. Rue, G.J. Smith, G.R. DiTullio. 2005. Iron, macronutrients and diatom blooms in the Peru upwelling regime: brown and blue waters of Peru. Marine Chemistry 93:81-103.

Butler, A. 1998. Acquisition and utilization of transition metal ions by marine organisms. Science 281: 207-210.

Chase, Z., A. van Geen, P.M. Kosro, J. Marra, and P.A. Wheeler. 2002. Iron, nutrient, and phytoplankton distributions in Oregon coastal waters. J. Geophys. Res. 107, doi:10.1029/2001JC000987.

Chavez, F.P. and J.R. Toggweiler. 1995. In C.P. Summerhayes et al. [eds.], Upwelling in the Ocean: Modern Processes and Ancient Records. Wiley, Chichester.

Chelton, D.B. 1982. Large-scale response of the California Current to forcing by the wind stress curl. Rep. - Calif. Coop. Ocean. Fish. Invest. 23: 130-148.

Coale, K.H., K.S. Johnson, S.E. Fitzwater, R.M. Gordon, S. Tanner, F.P. Chavez, L. Ferioli, C. Sakamoto, P. Rogers, F. Millero, P. Steinberg, P. Nightingale, D. Cooper, W.P. Cochlan, M.R. Landry, J. Constantinou, G. Rollwagen, A. Trasvina and R. Kudela.1996. A massive phytoplankton bloom induced by an ecosystem-scale iron fertilization experiment in the equatorial Pacific Ocean. Nature 383: 495-501.

Coale, K.H., S.E. Fitzwater, R.M. Gordon, K.S. Johnson, and R.T. Barber. 1997. Control of community growth and export production by upwelled iron in the equatorial Pacific Ocean. Nature 379: 621-624.

Coale, K.H. 2000. Nutrient Cycling: Iron Fertilization. In J. Steele, K. Turekian, and S. Thorpe [eds.], Encyclopedia for Ocean Sciences. Academic Press.

Coale, K.H., K.S. Johnson, F.P. Chavez, K.O. Buesseler, R.T. Barber, M.A. Brzezinski, W.P. Cochlan, F.J. Millero, P.G. Falkowski, J.E. Bauer, R.H. Wanninkhof, R.M. Kudela, M.A. Altabet, B.E. Hales, T. Takahashi, M.R. Landry, R.R. Bidigare, X. Wang, Z. Chase, P.G. Strutton, G.E. Friederich, M.Y. Gorbunov, V.P. Lance, A.K. Hilting, M.R. Hiscock, M. Demarest, W.T. Hiscock, K.F. Sullivan, S.J. Tanner, R.M. Gordon, C.N. Hunter, V.A. Elrod, S.E. Fitzwater, J.L. Jones, S. Tozzi, M. Koblizek, A.E. Roberts, J. Herndon, J. Brewster, N. Ladizinsky, G. Smith, D. Cooper, D. Timothy, S.L. Brown, K.E. Selph, C.C. Sheridan, B.S. Twining, and Z.I. Johnson. 2004. Southern Ocean iron enrichment experiment: carbon cycling in high- and low-Si waters. Science 304: 408-414.

Di Lorenzo, E. 2003. Seasonal dynamics of the surface circulation in the Southern California Current System. Deep-Sea Res. II 50: 2371-2388

Duce, R.A. and N.W. Tindale. 1991. Atmospheric transport of iron and its deposition in the ocean. Limnol. Oceanogr. 36: 1715-1726.

Eppley, R. and B. Peterson. 1979. Particulate organic matter flux and planktonic new production in the deep ocean. Nature 282: 677-680.

Eppley, R.W., E.H. Renger and W.G. Harrison. 1979. Nitrate and phytoplankton production in Southern California coastal waters. Limnol. Oceanogr. 24: 483-494.

Eppley, R.W. and O. Holm-Hansen. 1986. Primary production in the Southern California Bight, pp. 176-215. In R.W. Eppley [ed.], Plankton Dynamics of the Southern California Bight. Lecture Notes on Coastal and Estuarine Studies, 15. Springer-Verlag.

Firme, G.F.; E.L. Rue, D.A Weeks, K.W. Bruland, and D.A. Hutchins. 2003. Spatial and temporal variability in phytoplankton iron limitation along the California coast and consequences for Si, N, and C biogeochemistry. Global Biogeochem. Cycles 17: 10.1029/2001GB001824.

Hayward, T.L. and E.L.Venrick. 1998. Nearsurface pattern in the California Current: coupling between physical and biological structure. Deep-Sea Res. II 45: 1617-1638.

Hutchins, D.A. and K.W. Bruland. 1998. Iron-limited diatom growth and Si:N uptake ratios in a coastal upwelling regime. Nature 393: 561-564.

Hutchins, D.A., C.E. Hare, R.S. Weaver, Y. Zhang, G.F. Firme, G.R. DiTullio, M.B. Alm, S.F. Riseman, J.M. Maucher, M.E. Geesey, C.G. Trick, G.J. Smith, E.L.

Rue, J.Conn, and K.W. Bruland. 2002. Phytoplankton iron limitation in the Humboldt Current and Peru Upwelling. Limnol. Oceanogr. 47: 997-1011.

Johnson, K.S., R.M. Gordon, and K.H. Coale. 1997. What controls dissolved iron concentrations in the world ocean? Mar. Chem. 57: 137-161.

Johnson, K.S., F.P. Chavez, and G.E. Friederich. 1999. Continental-shelf sediment as a primary source of iron for coastal phytoplankton. Nature 398: 697-700.

Johnson, K.S., F.P. Chavez, V.A. Elrod, S.E. Fitzwater, J.T. Pennington, K.R. Buck, and P.M. Waltz. 2001. The annual cycle of iron and the biological response in the central California coastal waters. Geophys. Res. Lett. 28: 1247-1250.

Johnson, K.S., E. Boyle, K. Bruland, K. Coale, C. Measures, J. Moffett, A. Aguilar-Islas, K. Barbeau, B. Bergquist, A. Bowie, K. Buck, Y. Cai, Z. Chase, J. Cullen, T. Doi, V. Elrod, S. Fitzwater, M. Gordon, A. King, P. Laan, L. Laglera-Baquer, W. Landing, M. Lohan, J. Mendez, A. Milne, H. Obata, L. Ossiander, J. Plant, G. Sarthou, P. Sedwick, G. Smith, B. Sohst, S. Tanner, C. van den Berg, and J. Wu. 2007. Developing standards for dissolved iron in seawater. EOS 88:131-132

King, A.L., and K.A. Barbeau. 2007. Evidence for phytoplankton iron limitation in the southern California Current System. Mar. Ecol. Prog. Ser. 342:91-103.

Landry, M.R., R.T. Barber, R.R. Bidigare, F. Chai, K.H. Coale, H.G. Dam, M.R. Lewis, S.T. Lindley, J.J. McCarthy, M.R. Roman, D.K. Stoecker, P.G. Verity, and J.R. White. 1997. Iron and grazing constraints on primary production in the central equatorial Pacific: An EqPac synthesis. Limnol. Oceangr. 42:405-418.

Maldonado, M.T. and N.M. Price. 1996. Influence of N substrate on Fe requirements of marine centric diatoms. Mar. Ecol. Prog. Ser. 141: 161-172.

Martin, J.H., R.M. Gordon, W.W. Broenkow. 1989. VERTEX: phytoplankton/iron studies in the Gulf of Alaska. Deep-Sea Res. 36: 649-680.

Morel, F.M.M. and N.M. Price. 2003. The biogeochemical cycles of trace metals in the oceans. Science 300: 944-947.

Raven, J.A. 1990. Predictions of Mn and Fe use efficiencies of phototrophic growth as a function of light availability for growth and C assimilation pathway. New Phytol. 116: 1-18.

Raven, J.A., B. Wollenweber, and L.L. Handley. 1992. A comparison of ammonium and nitrate as nitrogen sources for photolithotrophs. New Phytol. 121: 19-32.

Rue, E.L. and K.W. Bruland. 1995. Complexation of iron(III) by natural organic ligands in the Central North Pacific as determined by a new competitive ligand equilibration/adsorptive cathodic stripping voltammetric method. Mar. Chem. 50: 117-138.

Sunda, W.G. and S.A. Huntsman. 1995. Iron uptake and growth limitation in oceanic and coastal phytoplankton. Mar. Chem. 50: 189-206.

Tsuda, A., S. Takeda, H. Saito, J. Nishioka, Y. Nojiri, I. Kudo, H. Kiyosawa, A. Shiomoto, K. Imai, T. Ono, A. Shimamoto, D. Tsumune, T. Yoshimura, T. Aono, A. Hinuma, M. Kinugasa, K. Suzuki, Y. Sohrin, Y. Noiri, H. Ogawa, K. Fukami, K. Kuma, and T. Saino. 2003. A mesoscale iron enrichment in the western subarctic Pacific induces a large centric diatom bloom. Science 300:958-961.

Venrick, E.L. 1998. Spring in the California Current, the distribution of phytoplankton species in April 1993 and April 1995. Mar. Ecol. Prog. Ser. 167: 73-88.

Wilkerson, F.P. and R.C. Dugdale. 1987. Use of large shipboard barrels and drifters to study the effects of coastal upwelling on phytoplankton dynamics. Limnol. Oceanogr. 32: 362-382.

Winant, C. D. and C. E. Dorman, 1997. Seasonal patterns of surface wind stress and heat flux over the Southern California Bight. J. Geophys. Res. - Oceans 102, 5641-5653.

Chapter 2

Determination of dissolved iron in seawater using iron(II) sulfite reduction with nitriloacetic acid resin preconcentration and chemiluminescent flow injection analysis

2.1. Abstract

Dissolved iron (<0.4 µm) in seawater samples acidified to pH 1.8 was determined by measuring iron(II) preconcentrated on a nitriloacetic acid (NTA) chelating resin coupled with luminol chemiluminescence detection. This method is a substantial modification of previously described sulfite reduction methods for measuring iron (Powell et al. 1995; Bowie et al. 1998). The use of commercially-available NTA chelating resin included modifications to sulfite and luminol solutions, and the use of pH 1.8 Milli-Q water and pH 1.8 trace metal-free ultraviolet-irradiated seawater (UVSW) for blank corrections. pH 1.8 Milli-Q and UVSW were found to be comparable, incorporating instrumental and reagent blank corrections for the method into one measurement. Dissolved iron profiles from a nearshore and an offshore location in the southern California Current System are presented, as well as the analysis of surface and deep seawater reference standards from the Sampling and Analysis of Fe (SAFe) international intercalibration project. The described apparatus is portable and easy to use, and the method is sensitive enough to measure dissolved iron concentrations in the 0.1 nM range (with a 0.02 nM detection limit).

2.2. Introduction

Dissolved iron (operationally defined by a <0.2 or 0.4 μm cutoff) exists at very low concentrations in the world's oceans due to its relatively low solubility and the high biological demand for iron by autotrophic and heterotrophic marine organisms. Low iron concentrations have been shown to limit phytoplankton growth in both the open and coastal ocean (Martin and Fitzwater 1988; Hutchins and Bruland 1998). The adequate analysis of dissolved iron in marine systems has been hindered by the extremely low concentrations of iron present and the risk of contamination during collection and processing (Bruland and Rue 2001, review and references therein). The early benchmark technique for measuring low concentrations of dissolved iron in seawater involved using extractive chelation preconcentration followed by graphite furnace atomic absorption spectrometry analysis (GFAAS) (Landing and Bruland 1987). More recent methods for measuring dissolved iron include isotope dilution with high resolution inductively-coupled plasma mass spectroscopy (ID-HR-ICPMS) (Wu and Boyle 1998), voltammetry (Gledhill and Van de Berg 1994; Rue and Bruland 1995; Wu and Luther 1995), and flow injection (FI) analysis (Elrod et al. 1991; Obata et al. 1993; Powell et al. 1995; Measures et al. 1995). FI analysis systems are advantageous because in general they are portable, adaptable, require minimal sample handling, and analyses can be made on relatively small sample volumes over short time periods. Several FI methods for measuring oceanic levels of iron have been developed using preconcentration with coupled chemiluminescence (CL) (e.g. Elrod et al. 1991) or colorimetric detection (e.g. Measures et al. 1995). Currently, most FI-CL methods for measuring oceanic levels of iron use the chelating resin 8-

hydroxyquinoline (8-HQ) (Landing et al. 1986, Dierssen et al. 2001; e.g. Obata et al. 1993, Measures et al. 1995, Bowie et al. 1998) for the concentration and separation of iron from major seawater salts that interfere with the CL reaction. Recently, the commercially-available nitriloacetic acid (NTA) resin was studied and characterized in detail (Lohan et al. 2005, 2006) and used as an alternative to 8-HQ for iron preconcentration. Lohan et al. (2005) reported the successful use of NTA for preconcentration of iron(III) with subsequent analysis by inductively-coupled plasma optical emission spectroscopy, GFAAS, and FI-HR-ICP-MS using an iron(III)-hydrogen peroxide method. NTA resin was also used to determine iron(III) concentrations with the N,N-dimethyl-p-phenylenediamine dihydrocholoride (DPD) FI colorimetric method (Lohan et al. 2006), similar to Measures et al. (1995). A detailed report has not yet been published regarding the use of NTA with an FI-CL method or for the preconcentration of iron(II).

This article describes a new method using NTA resin preconcentration with significant modifications to the iron(II) sulfite reduction FI-CL method developed by Powell et al. (1995) and adapted by Bowie et al. (1998). Briefly, the method includes adding sulfite to an acidified seawater sample for reduction of iron(III) to iron(II), preconcentrating iron(II) on to 8-HQ resin, eluting and mixing iron(II) with a luminol buffer, and measuring production of light at 425 nm from the resulting oxidation of luminol. During the Standardization and Analysis of Fe (SAFe) cruise in 2006, iron(II) sulfite reduction FI methods gave inconsistent results in comparison to other shipboard methods (Johnson et al. 2007). The method described in this paper uses NTA resin for preconcentration (Lohan et al. 2005), a pH 1.8 Milli-Q and pH 1.8 trace

metal-free ultraviolet-irradiated seawater blank correction, adjustments to the preparation and formulation of the luminol buffer solution, a lower concentration of sulfite for the reduction of iron(III) to iron(II), and reduced column rinsing time following sample loading. We also investigated the possibility of interference by reduced vanadium species as reported by a non-preconcentration luminol CL method (Hopkinson and Barbeau 2007) and the effect of a strong iron-binding ligand (desferrioxamine B) on NTA iron recovery. This method was tested by measuring SAFe surface and deep seawater reference standards, in addition to nearshore and offshore samples collected in the southern California Current System (CCS).

2.3. Materials and Procedures

2.3.1. Reagents

Ultrapure Milli-Q water (Millipore) was used for the preparation of all solutions. Solutions were made with high purity reagents and were not purified further. A luminol-NH_3OH buffer was prepared by adding 250 ml of 2 M ultrapure NH_3OH (OmniTrace Ultra grade, EMD Chemicals) to 250 ml 1.2 M ultrapure HCl (Optima Ultra grade, EMD Chemicals; or Optima grade, Fisher Chemical; or Ultrex II grade, JT Baker) with a final volume of 500 ml and a pH >9.5. Luminol sodium salt (5-amino-2,3-dihydro-1,4-phthalazinedione, Sigma-Aldrich) was added to a final concentration of 0.7 mM. The luminol-NH_3OH buffer was made 12 hrs in advance and, as tested by analytical response, was stable for up to 3 d. A 4 M ammonium acetate buffer was prepared by slowly adding 250 ml 8 M ultrapure glacial acetic acid (Optima grade, Fisher Chemical) to 250 ml 8 M NH_3OH with a final volume of 500

ml and adjusted to pH 8.6. The 4 M ammonium acetate was stored at 5 °C and diluted to a 2 M working solution with Milli-Q water on the day of use. 0.15 M ultrapure HCl was used as a carrier/elution solution and was prepared at least one day in advance. A reducing sulfite solution was prepared daily by dissolving 0.05 g sodium sulfite salt (Sigma Ultra grade, Sigma-Aldrich) in 50 ml Milli-Q water. The solution was shaken until the solute was dissolved and added to samples within one hour. A 180 µM stock solution of iron(III) was made by diluting a 17.98 mM atomic absorption standard solution (Sigma-Aldrich) in 0.016 M ultrapure HCl every six months. A 0.36 µM iron(III) working stock was prepared daily in 0.016 M ultrapure HCl. Typically, standard additions of 0.2, 0.4, 0.6, 0.8 nM were prepared, and if necessary for analysis of high concentrations, 1.2, 1.6, 3.2, and 10 nM standard additions.

2.3.2. Cleaning protocols and sample collection

Low density and high density polyethylene bottles (LDPE, HDPE; Nalgene) for seawater samples and for sample analysis were cleaned with acidic soap (Citranox), 2 M Trace Metal grade HCl (Fisher Chemical), and 2 M Trace Metal grade HNO_3 (Fisher Chemical), with several rinses with Milli-Q water between steps. Each acid cleaning step was at either 25 °C for weeks, or 60 °C for one day. Bottles were then stored in 0.01 M ultrapure HCl (~1-6 months) until rinsed and filled with seawater samples. Sample analysis bottles (60 ml HDPE) were used for sample aliquots during sulfite reduction and analysis. These bottles were periodically cleaned between uses by soaking in 0.016 M Trace Metal grade HCl for 24 h.

Seawater samples for dissolved iron were collected using either a ~7 m long trace-metal clean pole sampler, GO-FLO bottles (General Oceanics), or a Teflon diaphragm pump (Cole-Parmer) system. Samples were filtered using 0.4 µm acid-cleaned polycarbonate filters (Isopore, Millipore), acidified to pH ~1.8 with ultrapure HCl, and stored in acid-cleaned LDPE bottles for six months or longer. Dissolved iron concentrations were determined using a FeLume flow injection analysis system (Waterville Analytical), using a method modified from Powell et al. (1995) and Bowie et al. (1998) and NTA chelating resin described by Lohan et al. (2005). Teflon tubing and tygon peristaltic tubing for the FI system were cleaned by slowly pumping 1.5 M ultrapure HCl through the system for at least 6 h prior to initial use. On a daily basis, tubing and wetted parts of the FI system were cleaned with 1.5 M ultrapure HCl for 10 min.

2.3.3. Apparatus

A schematic of the flow injection system is shown in Figure 2.1. The basic system was designed and assembled by Waterville Analytical (King et al. 1995). This included an electronically-actuated 10-port stream select valve (Valco Instruments), an electronically-actuated 10-port injection valve (Valco Instruments), an eight-channel peristaltic pump (Rainin Instruments), and a photomultiplier tube (PMT; Hamamatsu Photonics HC-135-11, 875 volts). These components were controlled via serial-to-USB connection to a laptop PC (Dell) running Microsoft Windows operating system using a LabView-based program (National Instruments) written by Waterville Analytical. The PMT was housed in a light-resistant plastic bag and positioned over a

reaction coil (~3 cm in diameter) that was constructed using rigid ~1.6 mm (1/16") OD, 0.75 mm ID Teflon FEP tubing (Upchurch Scientific) and a PEEK t-connector (Upchurch Scientific) fixed to a cardboard backing using small zip-ties. The apparatus in its entirety has been used shipboard and is portable. The only requirements are a source of electricity and a class-100 clean benchtop working area.

Solutions were pumped through the system using peristaltic tygon tubing with 1.3 mm and 0.38 mm ID (Tygon formulation R-3603, Cole-Parmer). Peristaltic tubing was replaced once per month or when wear was evident (either via physical examination or reduced flow performance). Rigid ~1.6 mm OD, 0.75 mm ID Teflon FEP tubing (Upchurch Scientific) was connected to 1.3 mm ID tygon tubing using peristaltic tubing adapters and ¼-28 PEEK flangeless fittings and Tefzel ferrules (Upchurch Scientific). The smaller (0.38 mm ID) tubing was connected to ~1.6 mm OD Teflon tubing using a ~1 cm long piece of 1.3 mm ID tygon. Teflon tubing was connected to stream select and injection valves using ¼-28 PEEK flangeless fittings and Tefzel ferrules (Upchurch Scientific). Non-metallic check valves (PEEK and a perfluoroelastomer; Upchurch Scientific) were used to prevent backwash of ammonium acetate buffer into the sampling line. All Teflon tubing was translucent except for the luminol-NH_3OH buffer tubing, which was black to prevent possible luminol-light interactions (Rose and Waite 2001).

We used a 1 cm long, conically-shaped mini-column with an 85 µl internal volume (Global FIA) that was fitted with non-metallic frits (Global FIA) (Lohan et al. 2005). The column was filled with NTA resin (Superflow, Qiagen) using a syringe and column fitting adapter (Global FIA) to about 90% capacity and cleaned with 1.5

M HCl prior to use. We did not fill the column completely to avoid overpacking and overpressure. The column was attached to the injection valve so that sample loading and injection would occur in reversing directions to improve elution peak shape. Before use each day, the column was cleaned with 1.5 M ultrapure HCl for 5 min. In between uses, the NTA column was stored filled with Milli-Q at 5 °C. Columns were refilled with NTA if stored for prolonged periods (>3 months).

Reagents were placed in a class-100 laminar flow bench (AirClean 600 PCR Workstation, AirClean Systems), while the instrument was under normal laboratory conditions. Carrier and Milli-Q rinse solutions were stored in polycarbonate bottles, luminol-buffer solution in an amber HDPE bottle, sample buffer solution in a polypropylene container, and sulfite and seawater samples in HDPE bottles.

2.3.4. Procedure

Seawater samples (pH 1.8), usually 20 or 30 ml aliquots, were poured into 60 ml HDPE bottles. Iron in the sample was reduced to iron(II) for 12 h by adding sodium sulfite to a final concentration of 2 µM. Seawater samples reduced with sulfite were stable for up to 48 h. Prior to sample loading, the column was eluted with 0.15 M ultrapure HCl carrier solution. The seawater sample was then buffered in-line to pH ~6 with the addition of 2 M ammonium acetate (~0.2 ml/min, resulting in a mixture ratio of ~90% sample:10% buffer) and iron(II) was preconcentrated on the NTA column at a rate of ~2.4 ml/min for 30 sec (for higher sensitivity, a longer load time can be used). About 15 s elapsed between the buffering of the acidified seawater sample to pH ~6 to when it was loaded onto the column. To determine whether

samples and buffer were mixing sufficiently using the in-line buffering system, we compared the signal response of in-line buffered samples with a subset of samples buffered by manually with ammonium acetate. When the manually-buffered sample was analyzed immediately after buffering, the differences between the two buffering protocols were undetectable. Extended time between manually buffering and analysis of sample gave inconsistent results. At pH ~6, iron(II) recovery was shown to be near 100% on NTA, and quantitative only above pH 5.5 (Lohan et al. 2005). This was confirmed for this work by testing iron(II) standard additions with seawater samples (data not shown). Following sample loading, the column was then rinsed for 5 s with Milli-Q water and iron(II) was eluted with 0.15 M HCl carrier solution (at 2.4 ml/min) and mixed in the reaction coil with the luminol-NH_3OH buffer (at 2.4 ml/min). The final pH of the carrier/luminol-NH_3OH mixture was >9.0. Radical intermediates produced by the oxidation of iron(II) oxidize luminol and produce light at 425 nm (Rose and Waite 2001), which was detected by the PMT. We used pH 1.8 MQ water and pH 1.8 trace metal-free ultraviolet-irradiated seawater (UVSW; obtained from K. Bruland) as analytical blank measurements. The UVSW was prepared as described by Donat and Bruland (1988), with the following resin-filled column sequence: 1 - Duolite S-587 (Diamond Shamrock), 1 - Bio-Beads SM-2 (BioRad), 1 - Amberlite XAD16 (Sigma-Aldrich), 3 - Chelex 100 (BioRad), and 1 - C18 (Sep-Pak). Sulfite was added to blanks and they were run according to the same procedure as seawater samples. Generally, iron(III) standard additions were run in the beginning and end of the analysis period (usually twice per day) and used to generate a standard curve. Iron

concentration was determined by average peak height and subtracting out blank and baseline signals.

2.4. Assessment

2.4.1. Typical system response

A customized sampling protocol was created in conjunction with the Waterville Analytical LabView program to automate loading and elution so that three triplicate measurements of one sample took about 6 min using ~1.5 ml of sample for each measurement. Elution spectra were typically characterized by a baseline signal produced by the mixing of 0.15 M carrier HCl solution and luminol-NH_3OH buffer, then an increase to the signal peak, followed by a small peak tailing (Fig. 2.2). The peak tails were removed by rinsing between loading steps with 0.15 M ultrapure HCl. The column was checked to be clean by monitoring the signal from column elution between runs. Standard additions usually resulted in curvilinear responses - there was a larger ratio of signal to iron added with higher iron concentrations (Fig. 2.3). The increased sensitivity with higher iron concentrations is consistent with modeled iron(II)-luminol interactions (Rose and Waite 2001). A polynomial regression was fit to the standard addition curve and used to calculate the concentration of the sample and determine iron concentration of subsequent samples.

2.4.2. Sulfite reduction

Previously described methods for iron(III) reduction used 25 µM (Powell et al. 1995) and 100 µM sulfite addition (Bowie et al. 1998), followed by a 1 and 4 h

reduction period, respectively. With our method, sulfite additions to 100 µM generated poor and irreproducible results (possibly due to an unknown interaction between sulfite and NTA). Therefore, we tested lower sulfite additions in the range of <10 µM (W. Landing, pers. comm.). Sulfite reduction of iron(III) in seawater was found to be first order with a variety of iron(III) and sulfite concentrations (Millero et al. 1995). These authors found that with the addition of ~2.7 µM sulfite (1 M NaCl, pH 3.5, 25 °C), the half-life of 100 nM iron(III) was ~30 min. Theoretically, at pH <2 with 2 µM sulfite addition, 0.1 and 5 nM iron(III) in seawater would be reduced to iron(II) on the timescale of ~10 min and ~8 hrs, respectively (Millero et al. 1995). We tested 2 µM sulfite additions and 12 hr reduction periods with iron(II) and iron(III) standard additions and found they yielded similar results. Another factor that may aid in iron reduction is that storage at pH <2 over time (weeks to months) results in some reduction of iron(III) and tends to stabilize iron(II) (Bruland and Rue 2000; Johnson et al. 2002; Lohan et al. 2005).

2.4.3. Luminol-NH_3OH buffer

Previously described luminol buffers include borate/NaOH (Powell et al. 1995), Na_2CO_3/NaOH (Bowie et al. 1998), and NH_3OH/HCl solutions (Rose and Waite 2001). We chose to use a NH_3OH buffer because it is commercially available in an ultrapure grade. We found no signal enhancement with Na_2CO_3 addition (Xiao et al. 2002). We found that the pH of the luminol-NH_3OH buffer is important for minimizing the CL signal baseline, while at the same time providing a high enough pH to oxidize iron(II) in the reaction coil. Although previous methods documented the

use of luminol solutions at pH >10 for millisecond time-scale oxidation of iron(II) (Powell et al. 1995; King et al. 1995), luminol-NH_3OH buffer at pH 9.5-10 provided the largest signal-to-baseline ratio (conceptually similar to signal-to-noise ratio), and thus highest sensitivity, for our method. Higher pH luminol (>10) solutions resulted in higher signal baseline while lower pH solutions (<9.2) resulted in lower sensitivity for iron(II). Parenthetically, we attempted to substitute Trace Metal grade NH_3OH and Trace Metal grade HCl (Fisher Chemical) in the place of ultrapure reagents in our luminol-NH_3OH buffer. We found that it was adequate for iron measurements in the >1 nM range, but below the ~1 nM threshold, an interfering peak of unknown origin eluted just prior to the iron(II) peak.

2.4.4. Blank correction and detection limit

A critical component of our analysis is our blank correction. Instead of calculating an instrumental blank (contribution from tubing, valves and other wetted parts within apparatus) and a reagent blank (addition of sulfite, ammonium acetate, HCl), we determine a summed blank by using the same load/elute protocol for seawater analysis with pH 1.8 Milli-Q water (0.016 M ultrapure HCl and checked with pH meter, pH stable for weeks) and pH 1.8 UVSW for blank measurements. This method for blank determination combines both instrumental and reagent blanks into one measurement. Both pH 1.8 Milli-Q water and pH 1.8 UVSW were independently measured for iron and found to be below detection limit (K. Buck, pers. comm.). The addition of sulfite to seawater samples had no measurable effect on the signal blank - there was no significant difference between 2 and 4 µM sulfite additions. Also, based

on the certificate of analysis provided by manufacturers (Fisher Chemical, EMD Chemicals, JT Baker) and the amount added to seawater samples, ultrapure HCl would have a minimal impact on the blank signal (<0.4 pM). We were unable to use an alternate method (such as double-spiking for sulfite) for measuring reagent blanks of ammonium acetate buffer due to the sensitive relationship between loading pH and iron(II) recovery. For example, a doubling of the concentration of ammonium acetate buffer would result in a sample pH >7, which would then compromise an adequate comparison to a sample with a single addition of buffer loaded at pH 6. The use of pH 1.8 Milli-Q water and UVSW resulted in a mean blank value of 0.126 nM (n=27) with a detection limit of 0.02 nM (three times the standard deviation of blank).

2.4.5. NTA column rinse

After loading samples on chelating resins, rinsing of the column is needed to ensure that any seawater and buffer remaining in the column and adjacent tubing do not enter the reaction coil and interfere with the signal produced by the luminol. Bowie et al. (1998), when using a ~24 µl column filled with 8-HQ chelating resin, reported a Milli-Q water rinse volume of ~0.6 ml. We found that this amount of rinsing of our 85 µl column with Milli-Q affected sensitivity, potentially due to some degree of elution of iron(II) from NTA by the Milli-Q water rinse. While some rinsing of the column was necessary, we decreased the Milli-Q rinse step to about ~0.2 ml, a volume similar to that reported by Lohan et al. (2006).

2.4.6. Signal interference by reduced vanadium

In a non-separation iron(II) luminol CL technique for seawater, vanadium(III) and vanadium(IV) were reported to initiate the luminol CL reaction (Hopkinson and Barbeau 2007). They found 10 nM vanadium(III) and vanadium(IV) additions resulted in signal increases equivalent to 0.76 nM and 0.20 nM iron(II), respectively. Although vanadium(V) is the thermodynamically stable oxidation state in seawater, vanadium(III) is rarely found in the natural environment, even in anoxic sediments (Wanty and Goldhaber 1992) and vanadium(IV) is stable under acidic and moderately reducing conditions (Baes and Mesmer 1976). First, to assess the potential interference by vanadium(IV) with our NTA preconcentration method, we added vanadium(IV) to a seawater sample after the sulfite reduction step. A sulfite-reduced 0.50 nM iron seawater sample was run in sequence with an identical sample with 30 nM vanadium added (atomic absorption standard, primarily vanadium(IV), Ultra Scientific) just prior to analyzing the sample, about doubling the natural concentration of vanadium in the seawater sample. The 30 nM vanadium(IV) addition resulted in an increased CL that was below our detection limit for iron (signal of 0.50 nM iron and 30 nM vanadium(IV) was equivalent to ~0.51 nM iron(II)). Second, to test whether a 2 µM sulfite addition would be reducing enough to produce vanadium(III), we added 30 nM vanadium(IV) sulfate (Sigma-Aldrich) to a 0.22 nM iron seawater sample before adding 2 µM sulfite for 12 hrs. After the sulfite reduction step, 30 nM vanadium(IV) addition resulted in an increase in CL signal that was also below our detection limit for iron (signal of 0.22 nM iron and 30 nM vanadium(IV) was equivalent to ~0.23nM iron(II)). We are uncertain of what oxidation state of

vanadium is in our pH 1.8 seawater samples, but even with the assumption that all vanadium is present in the +4 oxidation state after acidification and sulfite reduction, vanadium presents only a minor interference with our iron(II) measurements. Furthermore, vanadium has a relatively conservative oceanic profile and is not likely to vary much within the water column - the mean concentration and standard deviation from three North Pacific profiles by Collier (1984) was 35.1 ± 1.6 nM (n=59, samples taken from between 1-4094 m). The magnitude of interference is within the standard deviation of most seawater sample measurements and also below the detection of the method (0.020 nM). A similar, although substantially smaller, interference was found for cobalt(II). An addition of 1 nM cobalt(II) to a 1 nM iron(II) seawater sample resulted in a signal increase for an 8-HQ preconcentration luminol CL method equivalent to 1.28 nM iron(II) (Bowie et al. 1998). Because cobalt is present at natural concentrations of 0.1-0.3 nM, it was determined not to affect the method by Bowie et al. (1998).

2.4.7. Effect of added iron-binding ligands

We investigated the effect of a strong iron-binding ligand, desferrioxamine B (DFOB), on the recovery of iron(II) on NTA. Although dissolved iron in our samples is in a reduced oxidation state (a result of prolonged storage at low pH and addition of sodium sulfite, see *Sulfite reduction* section above) and probably not associated with ligands (prolonged storage at low pH; Lohan et al. 2006), we wanted to test whether DFOB could possibly complex iron during the step in our method in which pH 1.8 seawater is brought up to pH ~6 with ammonium acetate buffer. The theoretical

DFOB binding could occur if iron(III) was produced due to elevated pH, or through a DFOB-mediated oxidation of iron(II) (Boukhalfa and Crumbliss 2002). Without a reducing agent (such as sulfite), the first order half-life of 250 nM iron(II) in natural seawater at pH 6 was found to be ~2 h (Santana-Casiano et al. 2005). In our method, iron(II) in seawater is buffered in-line, to minimize the length of time the sample is at pH 6. The time that elapses between buffering an acidified seawater sample to pH 6 and loading on it on the NTA column is about 15 seconds. In this time span (again, without the addition of a sulfite reducing agent), in natural seawater at pH 6 with 1 nM iron(II), an estimated 0.002 nM iron(II) would be oxidized to iron(III) (Santana-Casiano et al. 2005). The addition of 1 and 5 nM DFOB (Sigma-Aldrich) to a 0.40 nM iron seawater sample after the sulfite reduction step were undetectable. This indicates that iron(II) remained reduced at pH 6 and was unaffected by the addition of a strong iron-binding ligand.

2.4.8. Oceanic iron measurements

Nearshore and offshore seawater was analyzed from the southern CCS. Samples were processed and stored as described in *Materials and Procedures*. We used this technique to measure seawater iron concentrations ranging 0.05 to 8.2 nM (~60% of samples were below 0.5 nM) with a relative standard deviation of 3.9 ± 4.7% (mean and 1 standard deviation; n=183). Vertical profiles of total dissolved iron concentrations at an offshore station (~700 km southwest of San Diego, CA, July 2007, 29° 51’ N, 123° 36’ W) and a nearshore station (~50 km southwest of Point Conception, CA, April 2007, 34° 19’ N, 120° 48’ W) are shown in Figure 2.4. The

offshore profile is relatively constant at ~0.1-0.2 nM down to ~130 m, where the concentration of iron increased to 0.3 nM at 250 m. This is consistent with dissolved iron profiles characteristic of the North Pacific (Johnson et al. 1997). In contrast, the nearshore profile was sampled following intense wind-driven coastal upwelling near Point Conception. Here, although iron is relatively low in the mixed layer (~0.4 nM), a large subsurface signal (~1.3-2.5 nM from 30-200 m) is present, likely due to upwelling in the vicinity of the continental shelf.

The accuracy of our method was tested using seawater reference standards collected on the SAFe cruise during October/November 2006 in the central Pacific Gyre (30° N, 140° W) from surface waters and at depth (1000 m). Surface and deep SAFe standards were assigned consensus concentrations, representing average values determined by interlaboratory measurements (Johnson et al. 2007). Surface and deep SAFe standards were measured using our method to be: SAFe surface1 bottle #279 = 0.100±0.015 nM and SAFe deep2 bottle #285 = 0.915±0.027 nM. The values were in agreement with interlaboratory consensus measurements: SAFe surface1 = 0.097±0.043 nM and SAFe deep2 = 0.91±0.17 nM). For more information about SAFe and to request standards, email requestsafestandard@ucsc.edu.

2.5. Comments and recommendations

We developed a FI-CL method for determining total dissolved iron via sulfite reduction with luminol, without the need to synthesize 8-HQ, which can be relatively complicated (Landing et al. 1986; Dierssen et al. 2001). As previous studies have found (Lohan et al. 2005, 2006), NTA is a useful resin for FI systems and iron analysis

with preconcentration of iron(III) at pH <2, and we found NTA to be suitable for preconcentration of iron(II) at pH 6. The method is sensitive enough to measure oceanic dissolved iron concentrations in the 0.1 nM range, precise (mean RSD = 3.9%), uses small sample volumes (<2 ml per replicate), and is relatively quick (about 2 min per replicate). We developed this method using components and chemicals that were all commercially available. In particular, the FeLume system (hardware and software) purchased from Waterville Analytical is portable and easy to use, and has been tested by FI analysts and used with various detection methods and configurations. The use of commercially available ultrapure reagents can be costly over time. Inexpensive methods exist for purifying some reagents and can be adapted for the method (e.g. isothermal distillation; Veillon and Reamer 1981). If used shipboard for total dissolved iron measurements, samples would require acidification at pH <2 for at least 9 h (Lohan et al. 2006) before the sulfite reduction step for complete dissociation from organic matter. It should be noted that for freshwater and rainwater applications with samples that might have elevated ligand concentrations (>100 nM), iron(III)-ligand complexes were found to be relatively stable even after 72 h after acidification at pH 2 and reduction with 100 µM sulfite (Ussher et al. 2005).

The determination of dissolved iron via iron(II) sulfite reduction and luminol CL detection gave inconsistent results on the SAFe intercomparison cruise in October/November 2006 (Johnson et al. 2007). The blank correction could result in inaccurate determination of iron with preconcentration of iron(II) on NTA. Because the FI method described in this article (as with many others) is dependent on the pH of working reagents and samples (for example, pH of sample loading for iron recovery

on NTA column), we were unable to use typical methods of double-spiking for assessing the contribution of some reagents, especially the ammonium acetate buffer, to the blank measurement. Therefore, we utilized pH 1.8 Milli-Q water and pH 1.8 UVSW for blank measurements which accounted for both reagent blanks and instrumental blanks. Using this method for blank determination does require access to iron-free water (such as Milli-Q water or UVSW), which may be a challenge for some future users. When using this method for blank correction, it is also convenient to use another method to independently check the blank to assure its low iron concentration.

2.6. Acknowledgements

The authors thank Maeve Lohan, Whitney King, William Landing, Chris Measures, Simon Ussher, Sue Reynolds, Brian Hopkinson and Kristen Buck for valuable input and helpful discussion. Barbeau lab members, the CalCOFI research group, scientists involved in the Standardization and Analysis of Fe (SAFe) cruise, and the crew of the R/V New Horizon, R/V David S. Jordan, R/V Revelle, and R/V Knorr assisted with sample collection. We also thank Ken Johnson for enabling our participation in the SAFe cruise. This work was funded by NASA New Investigator Program (NAG5-12535), the California Current Ecosystem Long-Term Ecological Research program (NSF/OCE-0417616), and OCE-0550302.

This chapter was submitted to Limnology and Oceanography: Methods as: King, Andrew L., and Katherine A. Barbeau. Determination of dissolved iron in seawater using iron(II) sulfite reduction with nitriloacetic acid resin preconcentration and chemiluminescent flow injection analysis.

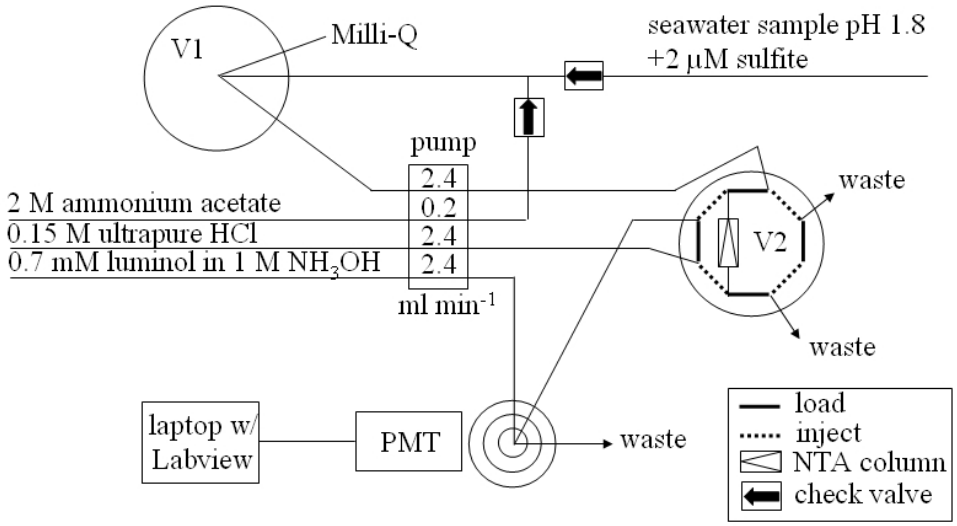

Figure 2.1. A schematic of the flow injection system. Valve 1 (V1) is a 10-port stream select valve and valve 2 (V2) is a 10-port injection valve. The solid lines in the injection valve (V2) indicate flow path during the "load" setting and the dotted-lines indicate flow path during the "inject" setting. The flow rate of each solution is denoted in the rectangle representing the peristaltic pump (ml min^{-1}).

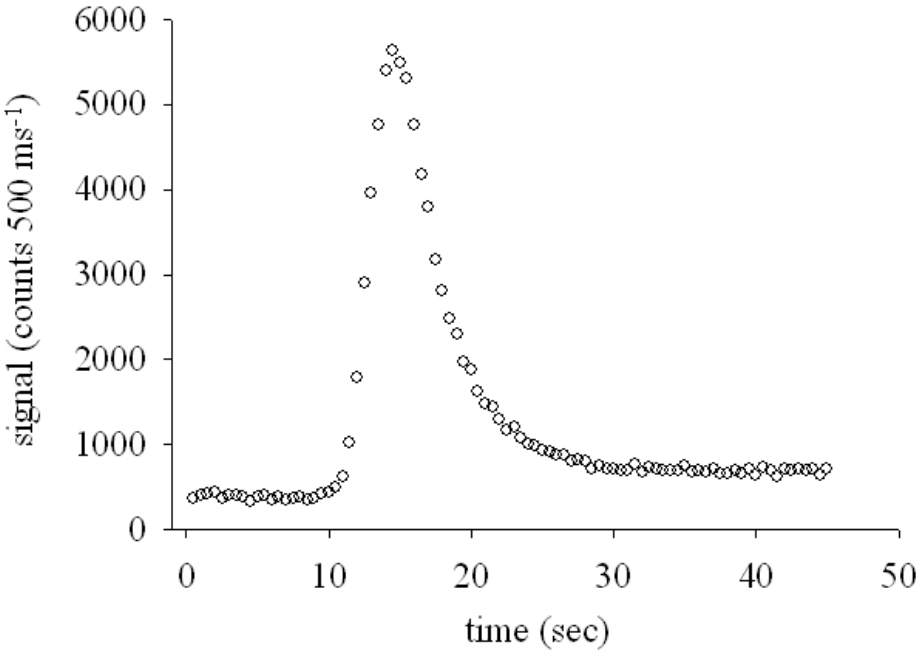

Figure 2.2. An example of chemiluminescence signal response in an elution profile of a 0.2 nM dissolved iron sample.

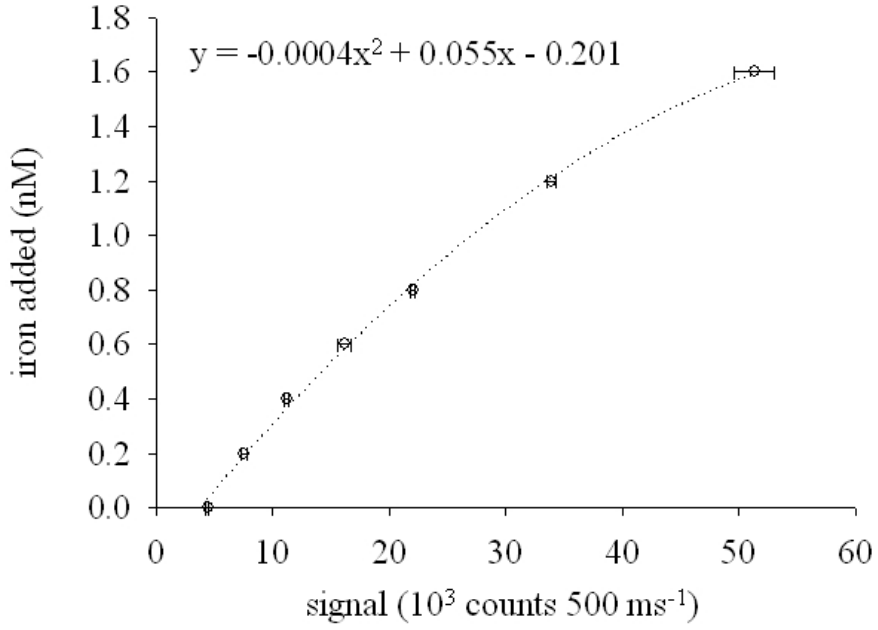

Figure 2.3. Blank-corrected standard addition curve of a 0.2 nM seawater sample with 2 µM sulfite addition and 0.0, 0.2, 0.4, 0.6, 0.8, 1.2 and 1.6 nM iron(III) additions. A quadratic polynomial regression has been fit to the data points ($r^2 = 0.99$). Error bars represent 1 standard deviation of triplicate measurements.

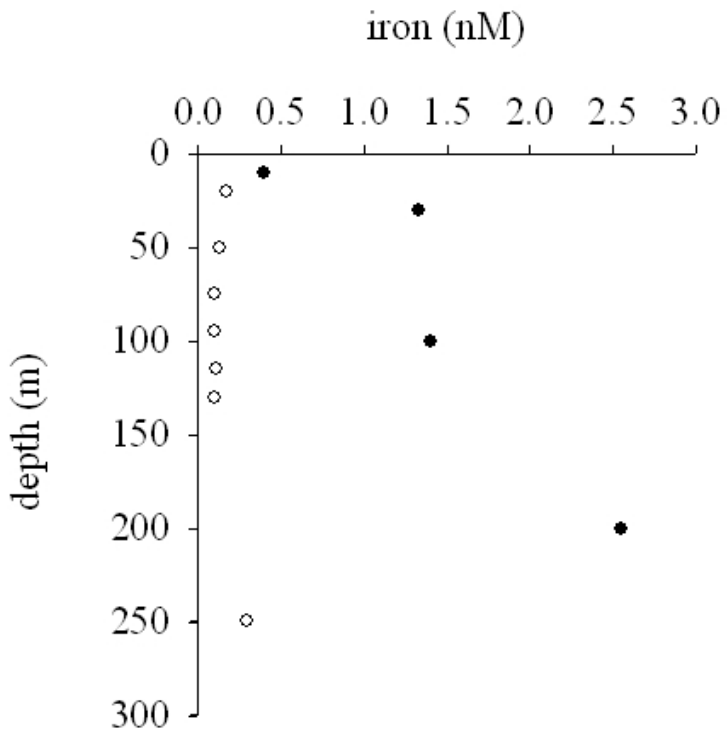

Figure 2.4. Vertical profiles of total dissolved iron concentrations at an offshore station (~700 km offshore San Diego, CA, July 2007, 29° 51’ N, 123° 36’ W) and a nearshore station (~50 km offshore of Point Conception, CA, April 2007, 34° 19’ N, 120° 48’ W). 1 standard deviation of triplicate measurements was smaller than width of symbols.

2.7. Literature cited

Baes, C.I., and R.E. Mesmer. 1976. The hydrolysis of cations. Wiley.

Boukhalfa, H., and A.L. Crumbliss. 2002. Chemical aspects of siderophore mediated iron transport. Biometals 15:325-339.

Bowie, A.R., E.P. Achterberg, R. Fauzi, C. Mantoura, and P.J. Worsfold. 1998. Determination of sub-nanomolar levels of iron in seawater using flow injection with chemiluminescence detection. Anal. Chim. Acta 361:189-200.

Bruland, K.W., and E.L. Rue. 2001. Analytical methods for determination of concentrations and speciation of iron, p. 255-289. *In* D. R. Turner and K. A. Hunter [eds.], The Biogeochemistry of Iron in Seawater. Wiley.

Collier, R.W. 1984. Particulate and dissolved vanadium in the North Pacific Ocean. Nature. 309:441-444.

Dierssen, H., W. Balzer, and W.M. Landing. 2001. Simplified synthesis of an 8-hydroxyquinoline chelating resin and a study of trace metal profiles from Jellyfish Lake, Palau. Mar. Chem. 73:173-192.

Donat, J.R., and K.W. Bruland. 1988. Direct determination of dissolved cobalt and nickel in seawater by differential pulse cathodic stripping voltammetry preceded by adsorptive collection of their nioxime complexes. Anal. Chem. 60:240-244.

Elrod, V., K.S. Johnson, and K.H. Coale. 1991. Determination of subnanomolar levels of iron(II) and total dissolved iron in seawater by flow injection analysis with chemiluminescence detection. Anal. Chem. 63:893-898.

Gledhill, M., and C.M.G. Van den Berg. 1994. Determination of iron(III) with natural organic complexing ligands in seawater using cathodic stripping voltammetry. Mar. Chem.47:41-54.

Hopkinson, B.M., and K.A. Barbeau. 2007. Organic and redox speciation of iron in the eastern tropical North Pacific suboxic zone. Mar. Chem. 106:2-17.

Hutchins, D.A., and K.W. Bruland. 1998. Iron-limited diatom growth and Si:N uptake ratios in a coastal upwelling regime. Nature 393:561-564.

Johnson, K.S., R.M. Gordon, and K.H. Coale. 1997. What controls dissolved iron concentrations in the world ocean? Mar. Chem. 57:137-161.

Johnson, K.S., E. Boyle, K. Bruland, K. Coale, C. Measures, J. Moffett, A. Aguilar-Islas, K. Barbeau, B. Bergquist, A. Bowie, K. Buck, Y. Cai, Z. Chase, J. Cullen, T. Doi, V. Elrod, S. Fitzwater, M. Gordon, A. King, P. Laan, L. Laglera-Baquer, W. Landing, M. Lohan, J. Mendez, A. Milne, H. Obata, L. Ossiander, J. Plant, G. Sarthou, P. Sedwick, G. Smith, B. Sohst, S. Tanner, C. van den Berg, and J. Wu. 2007. Developing standards for dissolved iron in seawater. EOS 88:131-132.

King, D.W., H.A. Lounsbury, and F.J. Millero. 1995. Rates and mechanism of Fe(II) oxidation at nanomolar total iron concentrations. Environ. Sci. Technol. 29: 818–824.

Landing, W.M., and K.W. Bruland. 1987. The contrasting biogeochemistry of iron and manganese in the Pacific Ocean. Geochim. Cosmochim. Acta 51:29–43.

Landing, W.M., C. Haraldsson, and N. Paxeus. 1986. Vinyl polymer agglomerate based transition metal cation chelation ion exchange resin containing the 8-hydroxyquinoline functional groups. Anal. Chem. 58:3031-3035.

Lohan, M.C., A.M. Aguilar-Islas, R.P. Franks, and K.W. Bruland. 2005. Determination of iron and copper in seawater at pH 1.7 with a new commercially available chelating resin, NTA Superflow. Anal. Chim. Acta 530:121-129.

Lohan, M.C., A.M. Aguilar-Islas, and K.W. Bruland. 2006. Direct determination of iron in acidified (pH 1.7) seawater samples by flow injection analysis with catalytic spectrophotometric detection: Application and intercomparison. Limnol. Oceanogr.: Methods 4:164-171.

Martin, J.H., and S.E. Fitzwater. 1988. Iron deficiency limits phytoplankton growth in the north-east Pacific subarctic. Nature 331:341-343.

Measures, C.I., J. Yuan, and J.A. Resing. 1995. Determination of iron in seawater by flow injection analysis using in-line preconcentration and spectrophotometric detection Mar. Chem. 50:3-12.

Millero, F.M., M. Gonzalez-Davila, and J.M. Santana-Casiano. 1995. Reduction of Fe(III) with sulfite in natural waters. J. Geophys. Res. 100:7235-7244.

Obata, H, H. Karatani, and E. Nakayama. 1993. Automated determination of iron in seawater by chelating resin concentration and chemiluminescence detection. Anal. Chem. 65:1524–1528.

Powell, R.T., D.W. King, and W.M. Landing. 1995. Iron distributions in surface waters of the south Atlantic. Mar. Chem. 50:13-20.

Rue, E.L., and K.W. Bruland. 1995. Complexation of iron(III) by natural organic ligands in the Central North Pacific as determined by a new competitive ligand equilibration / adsorptive cathodic stripping voltammetric method. Mar. Chem. 50:117-138.

Rose, A.L., and T.D. Waite. 2001. Chemiluminescence of luminol in the presence of iron(II) and oxygen: oxidation mechanism and implications for its analytical use. Anal. Chem. 73:5909–5920.

Santana-Casiano, J.M., Gonzalez-Davila, M., and F.J. Millero. 2005. Oxidation of nanomolar levels of Fe(II) with oxygen in natural waters. Environ. Sci. Technol. 39:2073-2079.

Ussher, S.J., M. Yaqoob, E.P. Achterberg, A. Nabi, and P.J. Worsfold. 2005. Effect of model ligands on iron redox speciation in natural waters using flow injection with luminol chemiluminescence detection. Anal. Chem. 77:1971-1978.

Veillon, C. and D.C. Reamer. Preparation of high-purity volatile acids and bases by isothermal distillation. Anal. Chem. 53:549-550.

Wanty, R.B., and M.B. Goldhaber. 1992. Thermodynamics and kinetics of reactions involving vanadium in natural systems: accumulation of vanadium in sedimentary rocks. Geochim. Cosmochim. Acta 56:1471–1483.

Wu, J.F., and G.W. Luther. 1995. Complexation of Fe(III) by natural organic-ligands in the northwest Atlantic-Ocean by a competitive ligand equilibration method and a kinetic approach. Mar. Chem. 50:159-177.

Wu, J.F., and E.A. Boyle. 1998. Determination of iron in seawater by high-resolution isotope dilution inductively coupled plasma mass spectrometry afar $Mg(OH)_2$ coprecipitation. Anal. Chim. Acta 367:183-191.

Xiao, C., D.A. Palmer, D.J. Wesolowski, S.B. Lovitz, and D.W. King. 2002. Carbon dioxide effects on luminol and 1,10-phenanthroline chemiluminescence. Anal. Chem. 74:2210-2216.

Chapter 3

Evidence for phytoplankton iron limitation in the southern California Current System

3.1. Abstract

Observations of phytoplankton iron limitation in the world's oceans have primarily been confined to high nutrient, low chlorophyll (HNLC) regimes, found in the western equatorial and subarctic Pacific, Southern Ocean, and coastal upwelling zones off California and Peru. We investigated the potential for phytoplankton iron limitation in coastal transition zones (50-200 km offshore) of the southern California Current System, a weak upwelling regime that is relatively low nutrient (<4 μmol nitrate l^{-1}) and low in chlorophyll (<1 μg chlorophyll *a* l^{-1}). In grow-out incubation experiments conducted during summer, July 2003 and 2004, phytoplankton responded to nanomolar iron-additions, despite the non-HNLC initial conditions. Observed changes in phytoplankton and nutrient parameters upon iron-addition were significant, although markedly lower in amplitude relative to typical grow-out experiments in HNLC regimes. While we cannot disprove alternate explanations for the observed limitation of phytoplankton growth, such as a proximate grazing control, our results indicate that phytoplankton growth in the southern California Current System is at times limited by the supply of iron. Based on our findings and the results of previous studies in this region, we suggest that phytoplankton biomass is generally limited by the supply of nitrate, while iron, directly or indirectly, influences macronutrient utilization, community species composition, and phytoplankton spatial and temporal distribution.

3.2. Introduction

About 30% of the world's oceans are described as high nutrient, low chlorophyll (HNLC) regimes, where phytoplankton standing stock is low and upwelled macronutrients persist in the euphotic zone, typically ~6-25+ μmol nitrate l^{-1} (e.g. Martin et al. 1989, de Baar et al. 1990). The persistence of macronutrients in oceanic HNLC regimes (e.g. equatorial and subarctic Pacific Ocean, and the Southern Ocean) has been explained by the slow net growth of phytoplankton due to limitation by a low supply of iron and proximate control by grazers (Martin et al. 1989, Cullen 1991, Miller et al. 1991, Landry et al. 1997). Similar to oceanic HNLC regimes, iron-limited HNLC conditions in the central and northern California Current System (CCS) and Peru Upwelling eastern boundary current (EBC) systems have been explained by a low supply of iron relative to macronutrients during intense upwelling in summer (Hutchins & Bruland 1998, Bruland et al. 2001, Johnson et al. 2001, Hutchins et al. 2002, Firme et al. 2003, Fitzwater et al. 2003). EBC systems are traditionally thought to be very productive primarily due to the large flux of upwelled macronutrients nitrate, phosphate, and orthosilicic acid to the euphotic zone, but it is now apparent that iron can limit phytoplankton growth in such upwelling systems, to varying degrees (Hutchins et al. 1998).

Phytoplankton iron limitation is thus commonly associated with oceanic and coastal regimes with high macronutrient concentrations. The concept of iron limitation could readily be extended, however, to regions of significantly lower macronutrient concentrations (e.g. <6 μmol nitrate l^{-1}) provided that macronutrients exceed the corresponding iron required for phytoplankton growth. The mesotrophic

southern CCS, extending from the United States-Mexico border to Point Conception, California (Fig. 3.1), might be one such regime. Previous survey cruises in the region have observed the presence of nitrate in surface waters with corresponding low phytoplankton biomass (http://www.calcofi.org). In comparison to the central and northern CCS (central California up to Oregon) and oceanic HNLC regimes, the southern CCS is a weaker upwelling regime (mean nitrate at 10 m between 1985-2005 was only 0.7 μmol l^{-1}; http://www.calcofi.org). The southern CCS spans a range of apparent water masses, from an episodic upwelling nearshore, to a transition zone composed of upwelled and California Current waters, to an oligotrophic offshore (Hayward & Venrick 1998). The region is generally described as being nitrate-limited, as evinced by the general absence of nitrate and presence of phosphate and silicate in the euphotic zone, and the deep water nitrate-phosphate relationship whose slope predicts a depletion in nitrate before phosphate (Ryther & Dunston 1971). Further, observations and experiments conducted over several decades have indicated that phytoplankton standing stock and productivity in southern CCS surface waters is positively correlated to the concentration of nitrate (Eppley et al. 1979, Eppley & Holm-Hansen 1986, Hayward & Venrick 1998).

Recent observations of phytoplankton iron limitation in the central and northern California nearshore (i.e.. within several km's from shore; Johnson et al. 1997, Hutchins et al. 1998) suggest that in addition to nitrate, iron might have a larger role than previously considered in the southern CCS. We investigated the potential influence of iron on phytoplankton growth and community structure in the southern CCS on a large spatial scale, ranging between San Diego and Avila Beach, California,

and spanning from the coastal nearshore to the coastal transition zone, some ~50-200 km offshore. Here we present results from iron-addition grow-out bottle incubation experiments conducted in July 2003 and 2004 in the southern CCS. Experiments were conducted in water masses which were relatively low nutrient (<3.5 μmol nitrate l^{-1}), low chlorophyll *a* (<0.7 μg chl *a* l^{-1}), and low dissolved iron (<0.5 nmol Fe l^{-1}). The addition of iron in grow-out bottle experiments stimulated phytoplankton growth and nitrate depletion, and resulted in a shift in phytoplankton community structure. Our data indicate that in some parts of the southern CCS during summertime, iron was a limiting factor for phytoplankton growth, while the phytoplankton standing stock was limited by nitrate.

3.3. Materials and methods

3.3.1. Study site

The southern CCS (see Fig. 3.1), is the study site of the >50 year California Cooperative Oceanic Fisheries Investigations (CalCOFI; http://www.calcofi.org) continuous time-series and the recently established California Current Ecosystem Long-Term Ecological Research (http://cce.lternet.edu) program. The pelagic ecosystem is mesotrophic on the average: low-nutrient, low phytoplankton biomass, oligotrophic conditions are perturbed by episodic spring and summer wind-driven upwelling events which result in high nutrient concentrations and phytoplankton biomass (Eppley at al. 1979, Jones et al. 1983). In comparison to other EBC systems, wind-driven upwelling in the southern CCS is generally weaker, and exhibits less seasonal variability, because of the physical sheltering of upwelling favorable winds

by Point Conception (Nelson 1977). Generally, upwelling favorable winds occur during spring and summer and force coastal Ekman upwelling (<10 km from shore) and Ekman pumping (wind stress curl upwelling) in the offshore coastal transition zone (Chelton 1982, Winant & Dorman 1997).

The CalCOFI program has focused on the southern CCS in a continuing effort to understand natural biological variability, especially stocks of epipelagic fish such as sardine and anchovy. The study area investigated by the Program since 1984 extends from the United States-Mexico border to Avila Beach, California (just north of Point Conception, California), and consists of six transects which reach ~350 km offshore Point Conception and ~700 km offshore San Diego, California (station plan shown in Fig. 3.1). The stations are evenly spaced ~70 km apart in the offshore regions (>~100-200 km from coast) and <35 km between stations in the nearshore regions. Plots of synoptic conditions during research cruises in July 2003 and 2004 of temperature, salinity, nitrate, and chl *a* were constructed using data provided by the CalCOFI program. The CalCOFI time-series also measures dissolved oxygen, nitrite, phosphate, orthosilicic acid, macrozooplankton biomass, and at select stations, ^{14}C-based primary productivity.

3.3.2. Iron-addition grow-out experiments

Ten shipboard iron-addition grow-out incubation experiments were conducted on two CalCOFI cruises within the southern CCS during 17-31 July 2003 and 15-28 July 2004. Experiments were set up at stations where *in vivo* chl *a* and nitrate concentrations (as determined by spectrophotometry) indicated potential iron

limitation, defined as <1 μg chl *a* l^{-1} and >~1 μmol nitrate l^{-1} in surface waters. Seawater from the mixed layer (5-10 m depth) was collected using trace metal clean techniques with a Teflon diaphragm pumping system and dispensed into 2.7 l polycarbonate bottles. Experimental treatments included either duplicate (July 2004) or triplicate (July 2003) unamended controls and additions of iron to 5 nmol l^{-1} from a stock of $FeCl_3$ in 0.1 mol l^{-1} ultrapure HCl (OmniTrace Ultra, EMD Chemicals). Experiments were placed in deckboard incubators cooled by flow-through seawater at 35% of incident light. The setup and sampling of all experiments was carried out under class 100 laminar flow hoods and in positive-pressure clean areas. Experimental equipment was handled with vinyl gloves and cleaned using HCl and HNO_3 (TraceMetal grade, Fisher Chemicals), with a final ultrapure HCl rinse. Ultrapure Milli-Q water (Millipore) was used for soaking and rinsing of all equipment.

Experiments were sampled daily for chl *a* (0.7 μm Whatman GF/F filters), macronutrients, and microscopy. Periodically, samples were taken for carotenoid pigments and particulate organic carbon (POC) and nitrogen (PON). Chl *a* was analyzed using standard fluorometric methods (Strickland & Parsons 1972). Carotenoid pigments were separated via reverse phase HPLC and detected with an ultraviolet/visible spectrophotometer (Goericke & Montoya 1998). Phytoplankton samples for microscopy were preserved in 1% filtered sodium tetraborate decahydrate-buffered formalin and enumerated with a Zeiss inverted microscope using Utermohl settling chambers (1-30 ml). Samples for macronutrients were frozen and concentrations of nitrate (NO_3^-), phosphate (PO_4^{2-}), and orthosilicic acid ($Si(OH)_4$) were determined colorimetrically by an automated analyzer (Oceanographic Data

Facility, La Jolla, California and Marine Science Institute, Santa Barbara, California). Particulate organic carbon (POC) and nitrogen (PON) were vacuum filtered onto precombusted 0.7 μm Whatman GF/F filters and measured using a carbon, hydrogen, nitrogen (CHN) analyzer (Scripps Institution of Oceanography Analytical Facility, La Jolla, California).

Changes in some experimental parameters from control and iron-added incubations were analyzed as a normalized response – the ratio of a parameter in iron-added replicates and control replicates at the final time point (t_{final}). For example, a 1.0× response indicates that iron-addition had no effect on a parameter. A 1.5× response indicates that after iron-addition, a parameter was 50% greater relative to control replicates. This is similar to the iron limitation indices calculated by Firme et al. (2003).

3.3.3. Analysis of dissolved iron

Dissolved iron was measured in seawater collected for all experiments. Samples for dissolved iron were filtered using 0.4 μm acid-cleaned polycarbonate filters, acidified to pH 1.7-1.8 with ultrapure HCl, and stored in acid-cleaned low density-polyethylene bottles for six months or longer. Dissolved iron concentration was determined using a FeLume flow injection analysis system (Waterville Analytical, Waterville, ME, USA), using a method modified from Bowie et al. (1998). Reagents that were used were ultrapure Milli-Q water (Millipore), sodium sulfite (Sigma Ultra, Sigma-Aldrich), ultrapure HCl, ultrapure NH_3OH (OmniTrace Ultra, EMD Chemicals), ultrapure glacial acetic acid (Optima, Fisher Scientific), and luminol

sodium salt (5-amino-2,3-dihydro-1,4-phthalazinedione, Sigma-Aldrich). A 2 mol l^{-1} ammonium acetate buffer was made by diluting NH_3OH in Milli-Q water and slowly adding glacial acetic acid. An NH_3OH buffer was made by diluting HCl in Milli-Q water and adding NH_3OH (final concentration was 0.5 mol l^{-1} HCl and 1 mol l^{-1} NH_3OH, pH ~9.5). The reagents were not purified further.

Iron in seawater samples was reduced to iron(II) for 12 hours by adding sodium sulfite to a final concentration of 2 μmol l^{-1}, buffered to pH ~5.8 in-line with the addition of ammonium acetate, and preconcentrated on a column (85 μl internal volume, Global FIA, Fox Island, WA, USA) filled with nitriloacetic acid resin (NTA Superflow, Qiagen USA, Valencia, CA, USA; Lohan et al. 2005) at a rate of 1 ml min^{-1} using an eight-channel peristaltic pump (Rainin Instrument, Oakland, CA, USA). Iron(II) was eluted with 0.14 mol l^{-1} HCl carrier solution (at 2 ml min^{-1}) and mixed in a glass reaction coil with the NH_3OH buffer (at 2 ml min^{-1}), the reaction pH of the carrier/luminol-ammonia mixture was ~9.3. Radicals produced by the oxidation of iron(II) to iron(III) catalyzed the oxidation of luminol and produced light at 426 nm, which was detected by a photomultiplier tube (Hamamatsu Photonics, Hamamatsu City, Japan). Iron(II) was determined by measuring peak height with standard addition methodology. The detection limit (3× standard deviation) for this method was as low as 20 pmol l^{-1} and precision (relative standard deviation) was as low as 1.4% (Table 3.1). Using this method, standards from the Sampling and Analysis of Fe (SAFe) intercomparison cruise in October 2004 were measured to be 0.10 ± 0.02 nmol Fe l^{-1} (surface bottle #279, mean ± 1 SD, n = 4) and 0.92 ± 0.03 nmol Fe l^{-1} (deep2 bottle #285, mean ± 1 SD, n = 4). The consensus value of the surface standard is

0.095 ± 0.024 nmol Fe l^{-1} and the deep standard is 0.90 ± 0.09 nmol Fe l^{-1} (K. Johnson, personal communication; SAFe standards and further information available, email: requestsafestandard@ucsc.edu).

3.4. Results

3.4.1. Hydrographic setting

Synoptic surface conditions of the region and the locations of iron-addition incubation experiments conducted in July 2003 and 2004 are shown in Figure 3.2 and Table 3.2. In both 2003 and 2004, upwelling was generally indicated by the presence of nitrate and cooler temperatures at the sea surface. The association of elevated surface nitrate with higher salinity waters was less clear because of the presence of a nearshore pool of warm, ~33.4-33.5 psu water in the southeastern portion of the region, which was approximately the same salinity as upwelled waters (e.g. Lynn & Simpson 1987). Nitrate was generally depleted in surface waters along the coast in the central and southern portion of the study area and well offshore. Nitrate was typically present (~3-8 μmol l^{-1}) near Pt. Conception and in the coastal transition zone between 50-200 km offshore. Time-series wind records obtained from buoys indicated that wind stress fields were equatorward (upwelling-favorable) both preceding and during the cruises (National Oceanic and Atmospheric Administration National Buoy Data Center: http://www.ndbc.noaa.gov). Wind data from the shipboard meteorological system was somewhat biased because of the time lag between stations, but confirmed a similar pattern as reported by buoys in the survey region.

3.4.2. Iron-addition grow-out incubations

The initial conditions (t_o) at 10 stations where seawater for experiments was collected for iron-addition incubations ranged from 0.23-0.65 µg chl *a* l^{-1}, 0.90-3.50 µmol nitrate l^{-1}, and 0.05-0.46 nmol dissolved Fe l^{-1} (Table 3.2). The concentrations of chl *a*, macronutrients, POC, and PON are shown for control and iron-addition experiments at t_{final} in Table 3.2. Nitrate was depleted more rapidly in iron-added replicates relative to controls (up to 2.7×), concomitant with an increase in chl *a* in iron-added replicates by 1.2 to 3.4× relative to controls (Table 3.3). In experiments from July 2003, nitrate depletion and chl *a* increase were significantly greater in iron-added replicates as determined by a paired t-test, $p < 0.001$, $n = 3$. (Paired t-test comparisons of July 2004 experimental results are not possible since experiments were conducted in duplicate, although the differences in means of control and iron-added replicates were always greater than their respective standard deviations). Some iron-added replicates accumulated up to 1.9× more POC and PON relative to controls (Table 3.3). In certain cases (experiments 03-1, 04-1, 04-3, and 04-5), iron-addition resulted in an increase in POC but not PON. Changes in macronutrients phosphate and orthosilicic acid were variable and sometimes difficult to resolve due to large relative standard deviations. Though the general trend for phosphate (except experiments 04-2, 04-3, and 04-6), and in some cases orthosilicic acid, was a greater drawdown in iron-added replicates compared to controls (Table 3.2).

HPLC-determined carotenoid pigments indicated that the initial phytoplankton community was diverse – the largest contributor to total carotenoid pigments was 19'-hexanoyloxyfucoxanthin (38-57% of the total carotenoids by mass), a pigment

characteristic of prymnesiophytes and diatoms. Fucoxanthin (diatoms) accounted for 12-38% of the total carotenoid pigment mass; 19'-butanoyloxyfucoxanthin (pelagophytes and chrysophytes) accounted for 9-23%, chlorophyll c_3 (prymnesiophytes and diatoms) accounted for 9-14%, 9'-*cis*-neoxanthin (chlorophytes) accounted for 0-8%. Iron-addition shifted phytoplankton community structure relative to controls (Table 3.3). The most noted (and consistent) changes in response to iron-addition were in fucoxanthin (up to 4.5× more abundant), 9'-*cis*-neoxanthin (up to 5.9× more abundant), and chlorophyll c_3 (up to 2.6× more abundant). Changes in actual cell numbers, not only chl *a* and carotenoid pigments, were confirmed by microscopy of formalin-preserved samples. Microscopy results for 5 of our 10 experiments are shown in Table 3.4.

Experiments lasted between one and four days, a main factor determining the duration being the rate of nitrate depletion. When nitrate was depleted in bottle incubations, chl *a* typically began to decline and the experiment was terminated (t_{final} parameters recorded). Two general patterns were observed: (1) no or little change in chl *a* in controls, and an increase of chl *a* in iron-added experiments (Fig. 3.3), and more commonly, (2) an increase of chl *a* in controls, but greater increase of chl *a* in iron-added experiments (Fig. 3.4). The normalized response of phytoplankton chl *a* to iron-addition ranged between 1.2 to 3.4× (Table 3.3) and was found to be related to both initial nitrate and dissolved iron concentrations (Fig. 3.5). The phytoplankton response to iron-addition was largest when nitrate was high and iron was low, e.g. >1 μmol nitrate l^{-1} and <0.3 nmol Fe l^{-1} (Fig. .35; Fig. 3.3c). Under these conditions, dissolved iron was low enough that phytoplankton responded to iron-addition, and

nitrate was available long enough to observe the effect of iron-addition. The response to iron-addition was smaller when both nitrate and iron were low, e.g. ≤1 μmol nitrate l^{-1} and ≤0.2 nmol Fe l^{-1} (Fig. 3.5; Fig. 3.4a), or when both nitrate and iron were high, e.g. >1 μmol nitrate l^{-1} and >0.3 nmol Fe l^{-1} (Fig. 3.5; Fig. 3.4c). In the former case (low nitrate and iron; Fig. 3.4a), nitrate in iron-added replicates depleted quickly, before a larger phytoplankton response could occur. In the latter case (high nitrate and iron; Fig. 3.4c), ambient dissolved iron was higher in concentration, nitrate was only depleted slightly faster in iron-added replicates compared to controls, and iron-addition was less important for phytoplankton growth.

3.5. Discussion

3.5.1. Differences between the southern CCS and HNLC regimes

In comparison to reports of similar experiments conducted in oceanic and coastal HNLC regimes, the outcome of our iron-addition grow-out experiments in the southern CCS coastal transition zone had some similarities and differences. The phytoplankton community response to iron-addition varied – the results from some experiments resembled those conducted in oceanic (Martin & Fitzwater 1988) and coastal HNLC regions (Hutchins et al. 1998) where phytoplankton chl *a* in iron-added experiments increased while chl *a* in control experiments changed very little (Fig. 3.3). Also similar to experiments in HNLC regimes, nitrate was depleted in iron-added replicates and to a lesser degree in control replicates, with an accompanying increase in POC and PON. The iron-addition versus control differences in nitrate depletion in these experiments were varied, at times small (e.g. 1.1× more nitrate depleted in iron-

added replicates), but at times relatively high (e.g. 2.9× more nitrate depleted in iron-added replicates, Table 3.3). The patterns (not magnitude) of chl *a* response and nitrate depletion in our studies were somewhat comparable to HNLC central California experiments which were described as being moderately iron-limited and iron-stressed, as opposed to being severely iron-limited (Hutchins et al. 1998).

There were, however, striking differences between our iron-addition experiments in the southern CCS and previously published work from coastal HNLC regimes, in terms of the duration and magnitude of phytoplankton response to iron. The duration of phytoplankton response in our southern CCS grow-out experiments was between 1.1 to 3.0 days with chl *a* response ranging from 1.2 to 3.4× (Table 3.3), while in HNLC central California coastal waters and in the Peru Upwelling the phytoplankton response ranged from 3 to 4 days in duration and was as high as ~3-5× (Hutchins et al. 1998, Hutchins et al. 2002). The relatively shorter duration of phytoplankton response to iron-addition and the relatively low chl *a* response in the southern CCS was likely due to the lower concentration of, and therefore more rapid depletion of, nitrate relative to HNLC regimes. In addition, relatively low concentrations of orthosilicic acid in our experiments might have resulted in co-limitation of diatoms. With respect to a deep water orthosilicic: nitrate acid ratio in the southern CCS region of ~1.25 (mean at 200 m from 1985-2005 CalCOFI database), orthosilicic acid concentrations were initially 11-53% depleted in 9 of our 10 experiments.

The summer-time southern CCS is clearly not a conventional HNLC regime. During our study, the mesotrophic southern CCS coastal transition zone where we

observed iron limitation had <1 μg chl *a* l^{-1} and <~4 μmol nitrate l^{-1}, while oceanic and coastal HNLC regimes typically have <1 μg chl *a* l^{-1} and 6-25+ μmol nitrate l^{-1}. Upon iron-addition in HNLC regimes, chl *a* often exceeds 10 μg chl a l^{-1}, nitrate is depleted 10-20 μmol l^{-1}, POC and PON approach values of 100 and 10 μmol l^{-1}, respectively, and diatom concentrations approach 1000 to >10,000 cells ml^{-1} (e.g. Martin & Fitzwater 1988, Hutchins et al. 1998, Hutchins et al. 2002). In contrast, iron-addition response from our southern CCS incubation experiments were about an order of magnitude lower: yielding <6 μg chl *a* l^{-1}, depletions of 1.0-3.5 μmol nitrate l^{-1}, ~15-20 μmol POC l^{-1}, ~2-5 μmol PON l^{-1}, and diatom concentrations were in the range of 10 to several hundred cells ml^{-1} (Table 3.2 and Table 3.4).

Dissolved iron was relatively low at the locations of our experiments in the southern CCS, but not as low as typically observed in iron-limited HNLC regimes. Dissolved iron (<0.2 μm) in oceanic and coastal HNLC regimes is <0.2 nmol l^{-1}, sometimes approaching 20 pmol l^{-1}, the detection limit of most methods (Johnson et al. 1997). In oceanic regions, it is believed that dissolved iron is low due to the large distance from continental sources of iron (Fung et al. 2000), although whether the primary source of iron to the open ocean is aeolian or upwelling remains a debate (Elrod et al. 2004). Coastal phytoplankton and iron geochemistry studies off the central and northern California coast have observed iron limitation to occur during summer upwelling months when iron was scarce relative to macronutrients (Hutchins et al. 1998). The continental shelf has been identified to be a key variable which influences the concentration of dissolved iron and determines whether iron limitation occurs in coastal wind-driven upwelling water masses, within 10 km of shore. A

broad continental shelf (e.g. Cape Mendocino, 20-50 km wide) is thought to be able to accumulate iron delivered in wintertime fluvial depositions and provide a reservoir of reduced and dissolved iron (Johnson et al. 1999). Upwelled water masses along broad shelves were reported to have 0.3-10 nmol Fe l^{-1} and up to 15 μmol nitrate l^{-1}, and were found to be iron-replete with respect to phytoplankton nutrient requirements (Bruland et al. 2001). In regions of narrower shelf widths (e.g. Big Sur, 2-3 km wide), upwelled water masses had lower dissolved iron concentrations (0.1-0.6 nmol Fe l^{-1}) and up to 15 μmol nitrate l^{-1} (Bruland et al. 2001), and were locations where phytoplankton were observed to be iron-limited (Hutchins et al. 1998).

The continental shelf bordering the southern CCS is relatively broad in comparison to central and northern California, ~50 km wide in the Santa Barbara Basin (northeastern portion of the CalCOFI sampling region) and ~10 km wide elsewhere (as defined by the 200 m isobath, see Fig. 3.1). Along the coastline of the southern CCS, the supply of iron is likely adequate due to the broad continental shelf (nearshore dissolved iron concentrations in the southern CCS were in excess of 1 nmol l^{-1} in July 2003 and 2004, unpubl. data). However, in the case of iron limitation in the southern CCS, the relationship between iron supply and the width of the continental shelf might not be critical. Our observations of iron limitation were not coastal, but primarily within the coastal transition zone of the southern CCS some 50-200 km offshore. In this region of the southern CCS, the supply of iron may be less influenced by benthic sources because the seafloor depth in the coastal transition zone ranges from 570-4000 m. In the coastal transition zone, wind stress curl might force upwelling offshore (Chelton 1982) where a continental shelf source of iron does not

exist. Or alternatively, the coastal transition zone might be composed of coastal upwelling water masses advected offshore from the north or east, which may be relatively depleted in iron relative to nitrate due to biological uptake (e.g. Firme et al. 2004).

3.5.2. Is this iron limitation?

The dissolved iron concentrations at our experimental stations (0.05-0.46 nmol Fe l^{-1}, see Table 3.2) were near estimates of growth half-saturation constants (K_μ, the concentration at which growth rate is at half of the maximum growth rate). Field studies have reported community K_μ to be 0.12 nmol Fe l^{-1} in the equatorial Pacific (Fitzwater et al. 1996), 0.17 nmol Fe l^{-1} in the Humboldt Current, Peru, and 0.26 nmol Fe l^{-1} in the Peru Upwelling (Hutchins et al. 2002). Growth half-saturation constants for iron for an assortment of diatoms recently summarized by Sarthou et al. (2005) were 0.35 ± 0.44 nmol Fe l^{-1} (n = 11, range = 0.59 pmol Fe l^{-1} to 1.14 nmol Fe l^{-1}). Half-saturation constants for iron uptake (K_s) may be a more appropriate metric for our comparison, and have been reported to be 0.034 nmol Fe l^{-1} for the tropical Pacific and 0.22 nmol Fe l^{-1} in the north central Pacific (Price et al. 1994). K_s is the concentration at which nutrient uptake rate is at half of the maximum uptake rate. K_s measurements are typically made over the time scale of hours while K_μ measurements are typically made over the time scale of days, and at steady-state, K_μ begins to approach K_s (Morel 1987). Our measured southern CCS dissolved iron concentrations are within the upper range of the above-referenced K_μ and K_s estimates and could potentially limit phytoplankton from achieving maximum growth rate.

Uptake half-saturation constants of nitrate, phosphate, and orthosilicic acid for an assortment of diatoms were 1.6 ± 1.9 μmol nitrate l^{-1} (n = 35), 0.24 ± 0.29 μmol phosphate l^{-1} (n = 14), and 3.9 ± 5.0 μmol orthosilicic acid l^{-1} (n = 25) (Sarthou et al. 2005). K_s for a variety of cultured oceanic and neritic diatoms, coccolithophores, and flagellates ranged between 0.1 to 10.3 μmol nitrate l^{-1} (Eppley et al. 1969). At our experimental stations, nitrate (0.9-3.5 μmol l^{-1}), phosphate (0.30-0.57 μmol l^{-1}), and orthosilicic acid (0.3-2.2 μmol l^{-1}) concentrations were within the respective K_s ranges and could potentially have been co-limiting nutrients. While these comparisons are suggestive, caution should be exercised in extending results from culture studies to our experiments with natural communities in which diatoms were present, but not dominant (as indicated by HPLC pigment analysis and microscopy).

In the southern CCS, the case for iron limitation is most exemplified by experiments 03-2, 03-3, and 03-4 (Fig. 3.3). In these experiments, chl *a* in control experiments remained low or unchanged, while chl *a* increased in iron-added replicates, as previously documented in HNLC regimes. The phytoplankton community in iron-amended experiments was shifted towards diatoms and chlorophytes (as indicated by pigments fucoxanthin and neoxanthin in Table 3.3). Nitrate was depleted more quickly in iron-added experiments, while nitrate in controls was somewhat depleted. This general pattern was somewhat reflected in larger POC and PON accumulation in iron-added experiments. The type of results described above supports the contention that at those stations, iron was a growth rate-limiting nutrient for the phytoplankton community, or for some segment of the community (e.g. Cullen 1991). The case for iron limitation is less clear in the other experiments

we conducted in the southern CCS (e.g. Fig. 3.4). In these experiments, experiments 03-1 and 04-1 through 04-6, chl *a* increased in control experiments, but, a larger increase was observed and a larger standing stock accumulated with iron-addition (Fig. 3.4c). It is quite evident that in these experiments the addition of iron had some influence on phytoplankton growth and community structure (Table 3.2). The differences in observed chl *a* patterns between experiments in Figure 3.3 versus Figure 3.4 might have been due to differing grazing pressure, and thus control of standing stock. Alternatively, our experiments might have been subject to bottle effects related to grazer exclusion and trace metal contamination (Cullen 1991, Martin & Fitzwater 1988).

Our study and previous studies in the southern CCS (e.g. Eppley et al. 1979) indicate that nitrate is a biomass-limiting nutrient and iron is a growth rate-limiting nutrient for at least some components of the phytoplankton community. The related concept of multiple resource co-limitation has recently been reviewed by Arrigo (2005). In the context of kinetic uptake, the concentration of dissolved iron (0.05-0.46 nmol Fe l^{-1}) at our experimental stations was likely lower than the concentration required for maximum growth, but higher than the concentration at which growth is zero. As a biomass-limiting nutrient, the supply of nitrate in the experiments determines total new production. Once the supply of nitrate is exhausted in our experiments, regardless of how much iron is added, new production is halted and the community relies on recycled N as a nutrient source. Whether a community is growth-rate limited by iron is conceptually and ecologically significant in nitrate-limited upwelling systems like the southern CCS. For example, if iron and nitrate are

replete during upwelling (e.g. 5 μmol nitrate l^{-1} and 2 nmol Fe l^{-1}), the phytoplankton community would presumably be dominated by large cells, net growth would be high and a bloom would occur over a relatively short timescale, until one of the two nutrients is depleted. The onset and fall of the bloom would be determined by a number of factors including temperature, light, recycling rates of N or iron, or micro- or macrozooplankton grazing. If nitrate is replete relative to iron in upwelled waters (e.g. 5 μmol nitrate l^{-1} and 0.05 nmol Fe l^{-1}), the phytoplankton community would be composed of smaller cell-types, growth would be somewhat balanced by grazing, and, in contrast, iron would limit the growth of the larger cells, and subsequently their biomass (Bruland et al. 2001). In this case, it is the concentration of iron which would limit total new production over time. If iron is a growth rate-limiting nutrient, and not a biomass-limiting nutrient, our results suggest that the community would likely consist of diverse taxa, phytoplankton growth would be between the iron-replete and iron-limited systems (not maximal and not zero), and iron availability would limit nitrate utilization (directly or indirectly). Provided that iron remains available, this scenario would continue until nitrate is depleted (this is what is apparently occurring in our incubation experiments). Assuming a given upwelled nitrate concentration in a system that is biomass-limited by nitrate, total new production would be the same regardless of whether iron is growth rate-limiting or replete. A key difference would be that new production under conditions in which iron is growth rate-limiting would occur over a longer period of time (Fig. 3.6), extending surface nitrate residence time, possibly expanding the horizontal distribution of nitrate as a result of mixing or transport. This could also lend to the maintenance of mesotrophic regimes, an

intermediate ecosystem state between low new production oligotrophic systems and high new production, boom-and-bust eutrophic systems. On a global scale, mesotrophic regimes, designated as oceanic regions with between 0.1 and 1 μg chl *a* l^{-1}, account for roughly half of phytoplankton carbon fixation (Behrenfeld & Falkowski 1997).

3.5.3. Historical context and conclusions

CalCOFI time-series measurements made over the last 20 years indicate that the presence of unused nitrate in surface waters is relatively common. Between 1985-2005 (all seasons), from 5803 stations on >80 CalCOFI research cruises in the southern CCS, 989 of the stations had ≥1 μmol l^{-1} nitrate in surface waters, of which 421 stations were in the coastal transition zone (50-250 km offshore). Of these coastal transition zone stations that had >1 μmol l^{-1} nitrate, about two-thirds also had ≤1 μg chl *a* l^{-1} (266 stations); an observation which could possibly be explained by iron limitation. Although macronutrients may not be persisting in surface waters of the southern CCS (i.e. existing unused on the timescale of months as in HNLC regimes), it does appear that macronutrients are often present in surface waters, implying that there may be a relatively consistent supply of macronutrients and a temporal decoupling between this supply and phytoplankton utilization and growth. Based on the relatively low concentration of dissolved iron (<0.45 nmol l^{-1}), the distant proximity of the coastal transition zone to shelf sources of iron, and the results from our iron-addition grow-out experiments, we infer that iron likely plays a role in the discrepancy between unused nitrate and low phytoplankton biomass observed in

the 20-year dataset. However, at this time we cannot rule out alternate factors that may be preventing phytoplankton from utilizing nitrate, separately or in concert with iron limitation, such as (proximate) grazing control or light limitation.

The biogeochemical consequences of iron limitation in the southern CCS may not appear dramatic when compared to iron limitation in HNLC regimes. The amount of unused macronutrients present and the increase in chl *a* after iron-addition were much lower in the southern CCS relative to similar observations from HNLC regimes. Regardless, the degree of iron limitation observed in this study could have significant implications for biogeochemical and ecological processes. During times of upwelling, variability in the supply of iron could influence the type of phytoplankton community which develops and spatial and temporal patterns in phytoplankton distribution. Santa Ana winds, seasonal offshore gusts occurring in the southwestern United States that often transport large amounts of terrestrial material offshore (Hu and Liu 2003), are one such source of variability in supply of iron to the southern CCS. The supply of iron can also modulate phytoplankton nitrate utilization (directly or indirectly), and thus control the residence time and distribution of upwelled nitrate and other micro- and macronutrients. This could create situations in which nitrate may be more or less subject to mixing or transport. The above predictions may result in small, but significant, aberrations in primary production and biogeochemical cycling of nutrients in the southern CCS, which might only be quantified or observed over long time-scales.

3.6. Acknowledgements

We thank B. Hopkinson, J. Nunnery, S. Reynolds, K. Roe, the CalCOFI research group, especially R. Goericke, J. Wilkinson, D. Wolgast, and the officers and crew of the R/V *New Horizon* and *David Starr Jordan*, for assistance in collecting and analyzing data. E. Venrick provided assistance in phytoplankton identification. We also thank two anonymous reviewers for insightful comments and suggestions. This research was funded by NASA NIP grant NAG5-12535 and LTER NSF/OCE-0417616.

This chapter was published previously as: King, Andrew L., and Katherine A. Barbeau. Evidence for phytoplankton iron limitation in the southern California Current System. Marine Ecology Progress Series. 342:91-103.

Table 3.1. Analytical figures of merit for iron analysis. The analytical blank is measured as the sum of reagent iron concentrations (buffers, hydrochloric acid, sulfite). Listed are mean and standard deviation (mean ± SD; nmol Fe l^{-1}), detection limit (DL, defined as three times standard deviation of three replicate measurements; nmol Fe l^{-1}), and relative standard deviation (standard deviation divided by the mean; %RSD).

	blank	seawater
mean±SD	0.13±0.01	-
DL mean	0.04	0.07
DL range	0.02-0.05	0.02-0.12
%RSD mean	7.4%	6.5%
%RSD range	3.6-13.8%	1.4-23.6%

Table 3.2. For iron-addition experiments, the table lists (from top to bottom): experiment name (expt), corresponding CalCOFI station reference (see http://www.calcofi.org for station locations), date and local time (Pacific Standard Time) experiment began, latitude (lat) and longitude (long) of station, bottom depth (m), distance offshore (km). Parameters at t_o are listed for: dissolved iron (dFe; nmol l^{-1}), chlorophyll *a* (chl a; µg l^{-1}), nitrate (nit; µmol l^{-1}), phosphate (phos; µmol l^{-1}), orthosilicic acid (sil; µmol l^{-1}), particulate organic carbon (POC; µmol l^{-1}), and particulate organic nitrogen (PON; µmol l^{-1}). Means and standard deviations (listed below means in italics) for both control and iron-added experiments at t_{final} (days) are listed for: chl a, nitrate, phosphate, orthosilicic acid, POC, and PON (same units as above). nd = no data.

* Because POC and PON samples were not collected daily, t_{final} for POC and PON were on different days than t_{final} for other parameters. t_{final} for POC/PON was 2.1 days for experiment 03-1, 3.8 days for experiment 03-3, 2.9 days for experiment 04-4, and 4.0 days for experiment 04-5.

expt	03-1	03-2	03-3	03-4	04-1	04-2	04-3	04-4	04-5	04-6
CalCOFI station	90.53	80.70	80.80	77.55	90.60	90.53	87.45	83.60	80.70	77.70
date	7/21/03	7/27/03	7/27/03	7/29/03	7/17/04	7/17/04	7/19/04	7/23/04	7/24/04	7/26/04
local time	1700	0500	1400	1330	1600	1720	1700	0100	1900	1300
lat	32.65	33.82	33.48	34.89	32.42	32.65	33.49	33.58	33.82	34.39
long	-119.48	-121.84	-122.53	-121.20	-119.96	-119.48	-119.32	-120.76	-121.84	-122.25
depth (m)	1320	3630	3990	570	895	1320	1641	1400	3630	4020
offshore (km)	155	145	210	50	205	155	75	105	145	155
					t_o					
dFe (nmol l^{-1})	0.05	0.27	0.28	0.20	0.17	0.31	0.46	0.44	0.44	0.19
chl a (µg l^{-1})	0.52	0.41	0.35	0.65	0.36	0.32	0.50	0.48	0.31	0.23
nit (µmol l^{-1})	0.90	1.78	2.20	3.50	2.04	2.12	3.17	1.97	3.35	1.66
phos (µmol l^{-1})	0.43	0.40	0.57	0.54	0.30	0.30	0.40	0.30	0.30	0.30
sil (µmol l^{-1})	0.60	1.10	2.20	1.40	0.40	0.30	1.80	0.40	1.10	1.00
POC (µmol l^{-1})	19.30	10.95	8.76	14.40	6.63	5.40	5.74	nd	3.71	nd
PON (µmol l^{-1})	1.92	1.71	1.25	2.68	1.02	1.16	0.88	nd	0.45	nd
					control t_{final}					
t_{final}	1.1	2.1	2.7	2.9	2.2	1.9	2.1	1.8	3.0	2.0
chl a	0.90	0.50	0.55	0.55	0.94	1.51	3.48	0.57	1.42	0.66
	0.01	*0.02*	*0.03*	*0.03*	*0.07*	*0.01*	*0.22*	*0.19*	*0.14*	*0.02*
nit	0.65	0.77	1.34	1.88	1.22	0.80	0.38	1.33	1.54	1.32
	0.02	*0.01*	*0.13*	*0.07*	*0.19*	*0.12*	*0.12*	*0.08*	*0.13*	nd
phos	0.43	0.44	0.50	0.52	0.23	0.20	0.21	0.25	0.26	0.29
	0.08	*0.06*	*0.03*	*0.04*	*0.00*	*0.00*	*0.01*	*0.01*	*0.00*	nd
sil	0.64	1.06	2.00	0.55	0.30	0.08	0.91	0.34	1.06	0.90
	0.21	*0.16*	*0.26*	*0.00*	*0.34*	*0.03*	*0.09*	*0.06*	*0.06*	nd
POC	19.80*	17.60	10.08*	19.25	10.99	11.57	20.79	10.07*	17.10*	nd
	2.24	*1.22*	*1.50*	*3.32*	*0.37*	*0.20*	*3.60*	*0.53*	*0.11*	nd
PON	2.44*	1.51	1.58*	3.56	1.82	1.66	2.57	1.52*	2.88*	nd
	0.16	*0.04*	*0.22*	*0.67*	*0.08*	*0.00*	*0.53*	*0.04*	*0.26*	nd
					+Fe t_{final}					
t_{final}	1.1	2.1	2.7	2.9	2.2	1.9	2.1	1.8	3.0	2.0
chl a	1.49	1.03	1.46	1.85	2.91	1.97	5.53	1.13	2.13	0.81
	0.03	*0.24*	*0.21*	*0.07*	*0.52*	*0.17*	*0.22*	*0.03*	*0.18*	*0.02*
nit	0.32	0.06	0.37	0.00	0.06	0.56	0.05	0.06	0.72	1.16
	0.04	*0.06*	*0.15*	*0.00*	*0.04*	*0.02*	*0.02*	*0.16*	nd	nd
phos	0.29	0.39	0.32	0.36	0.18	0.19	0.21	0.19	0.22	0.28
	0.05	*0.03*	*0.09*	*0.01*	*0.00*	*0.00*	*0.02*	*0.03*	nd	nd
sil	0.45	1.13	1.20	0.43	0.14	0.14	0.89	0.24	0.43	0.84
	0.18	*0.11*	*0.46*	*0.03*	*0.03*	*0.06*	*0.03*	*0.17*	nd	nd
POC	24.17*	16.05	17.94*	35.07	15.41	15.41	27.52	20.87*	23.17*	nd
	2.57	*0.59*	*1.09*	*1.93*	*3.02*	*3.02*	*1.84*	*3.39*	*2.52*	nd
PON	2.50*	2.94	2.74*	5.29	1.66	1.92	2.57	2.94*	2.90*	nd
	0.08	*0.13*	*0.17*	*0.27*	*0.15*	*0.15*	*0.68*	*0.76*	*0.57*	nd

Table 3.3. Normalized response (the ratio of iron-added at t_{final}:control at t_{final}), for chl *a*, nitrate drawdown, particulate organic carbon (POC), particulate organic nitrogen (PON), and carotenoid pigments for each experiment. For example, a normalized response in chl of 1.5 indicates 50% more chlorophyll in iron-added replicates relative to controls. Carotenoid pigments are reported for the same t_{final} as POC/PON measurements (see Table 3.2); abbreviations and associated taxa for pigments are as follows: 19'butanoyloxyfucoxanthin (19-but; pelagophytes and chrysophytes), fucoxanthin (fuc; diatoms), 19'-hexanoyloxyfucoxanthin (19-hex; prymnesiophytes and diatoms), chl c_3 (c3; prymnesiophytes and diatoms), 9'-*cis*-neoxanthin (neo; chlorophytes), and total carotenoids (car tot) are presented. The last two rows indicate µmol nitrate used per day in control and iron-added experiments. nd = no data.

expt	03-1	03-2	03-3	03-4	04-1	04-2	04-3	04-4	04-5	04-6
	normalized response to +Fe @ t_{final} (+Fe:control)									
chl a	1.7	2.1	2.6	3.4	3.1	1.3	1.6	2.0	1.5	1.2
nitrate drawdown	2.3	1.7	2.1	2.2	2.5	1.2	1.1	2.9	1.2	1.4
POC	1.2	0.9	1.8	1.8	1.4	1.3	1.3	2.1	1.4	nd
PON	1.0	1.9	1.7	1.5	0.9	1.2	1.0	1.9	1.0	nd
19-but	1.0	1.5	1.2	3.4	1.3	0.9	0.6	0.8	1.3	nd
fuc	1.3	2.0	2.6	4.5	2.6	1.3	1.3	1.9	2.0	nd
19-hex	1.0	1.4	1.6	2.9	1.5	0.9	1.0	1.3	1.7	nd
chl c3	1.0	2.1	1.6	2.6	2.2	1.3	1.9	1.5	2.0	nd
neo	2.4	3.5	3.1	5.9	4.9	0.9	1.1	4.9	2.9	nd
car tot	1.4	2.1	2.0	3.8	2.5	1.0	1.2	2.1	2.0	nd
	NO_3 used d^{-1}									
control	0.23	0.48	0.32	0.56	0.37	0.69	1.33	0.36	0.60	0.17
+Fe	0.53	0.82	0.68	1.21	0.90	0.82	1.49	1.06	0.88	0.25

Table 3.4. Estimated phytoplankton cell counts in cells ml^{-1} at t_o and t_x in control and iron-addition experiments from 03-1 through 03-4, and 04-1. t_x is indicated in unit of days for each column. The category "flagellates" includes both heterotrophic and autotrophic flagellates, which could not be discerned under light microscopy.

	expt 03-1			expt 03-2			expt 03-3			expt 03-4			expt 04-1		
	t_o	C $t_{2.1}$	+Fe $t_{2.1}$	t_o	C $t_{2.1}$	+Fe $t_{2.1}$	t_o	C $t_{1.3}$	+Fe $t_{1.3}$	t_o	C $t_{2.2}$	+Fe $t_{2.2}$	t_o	C $t_{1.3}$	+Fe $t_{1.3}$
pennate diatoms	1.2	10	12	0.7	1.9	7.9	0.6	1.5	10	1.2	13	20	120	150	250
centric diatoms	0.5	1.6	16	0.5	1.1	1.6	0.9	0.8	1.4	2	2.6	6.7	25	7.7	160
flagellates	77	690	900	52	150	260	90	100	640	33	220	720	370	230	560
coccolithophores	110	390	420	27	230	160	230	230	310	39	430	560	90	36	160

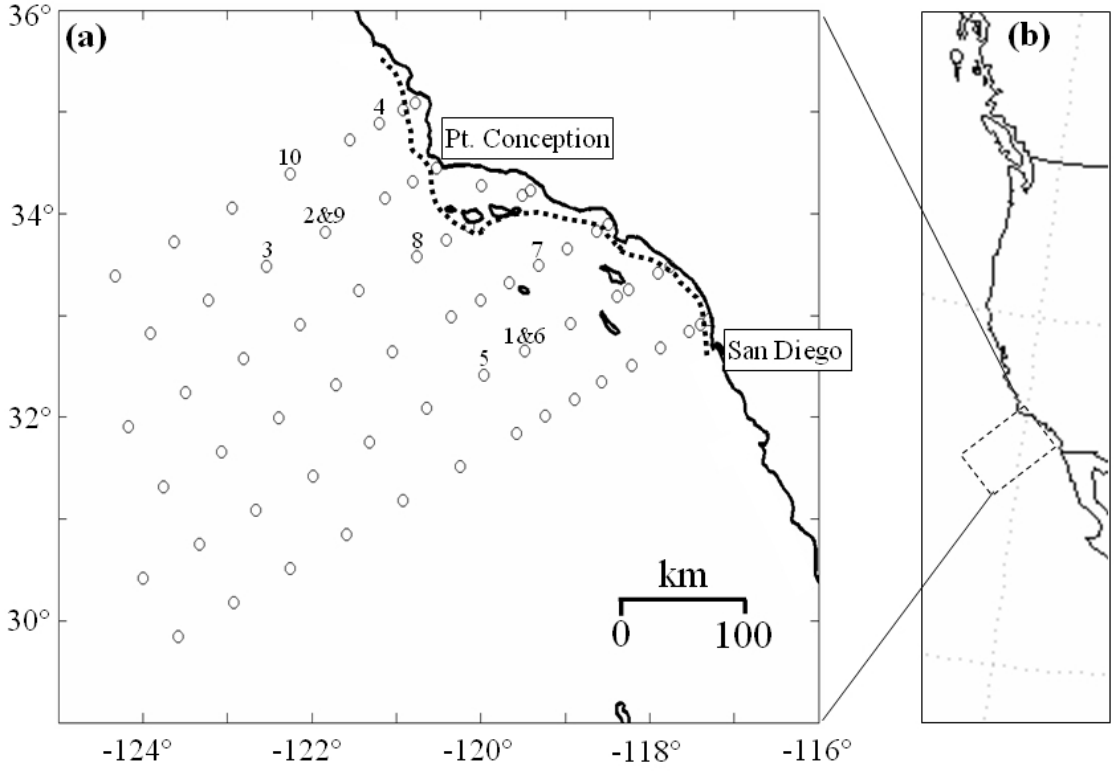

Figure 3.1. (a) The study region of the California Cooperative Fisheries Investigations (CalCOFI) is approximately 175,000 km^2, and includes 66 stations which are marked with open circles. For line and station nomenclature, refer to station map at http://www.calcofi.org. Station locations of iron-addition incubation experiments conducted in July 2003 are marked 1-4, corresponding to experiments 03-1, 03-2, 03-3, and 03-4, respectively (see Table 3.2). Experiments conducted in July 2004 are marked 5-10 and correspond to experiments 04-1, 04-2, 04-3, 04-4, 04-5, and 04-6, respectively (see Table 3.2). The black dashed line marks the 200 m isobath. San Diego and Point Conception, California, USA are labeled for geographic reference. (b) The southern California Current System is in the temperate northeastern Pacific Ocean, off the western coast of North America.

Figure 3.2. (a-d): Synoptic conditions in the southern California Current System (CCS) at 10 m during July 2003: (a) °C temperature, (b) µmol nitrate l^{-1}, (c) practical salinity units (psu), and (d) µg chlorophyll *a* l^{-1}. (e-h): Synoptic conditions in the southern CCS at 10 m during July 2004: (e) °C temperature, (f) µmol nitrate l^{-1}, (g) practical salinity units (psu), and (h) µg chlorophyll *a* l^{-1}. Data in each plot was interpolated between stations marked with black dots. Dissolved iron concentrations are superimposed on (a-g) in nmol l^{-1}. Stations where phytoplankton responded to iron-addition in bottle experiments are indicated with solid red circles and are described in Table 3.2. For geographic reference, Point Conception, California, USA ('PC') and Los Angeles, California, USA ('LA') are labeled in each panel.

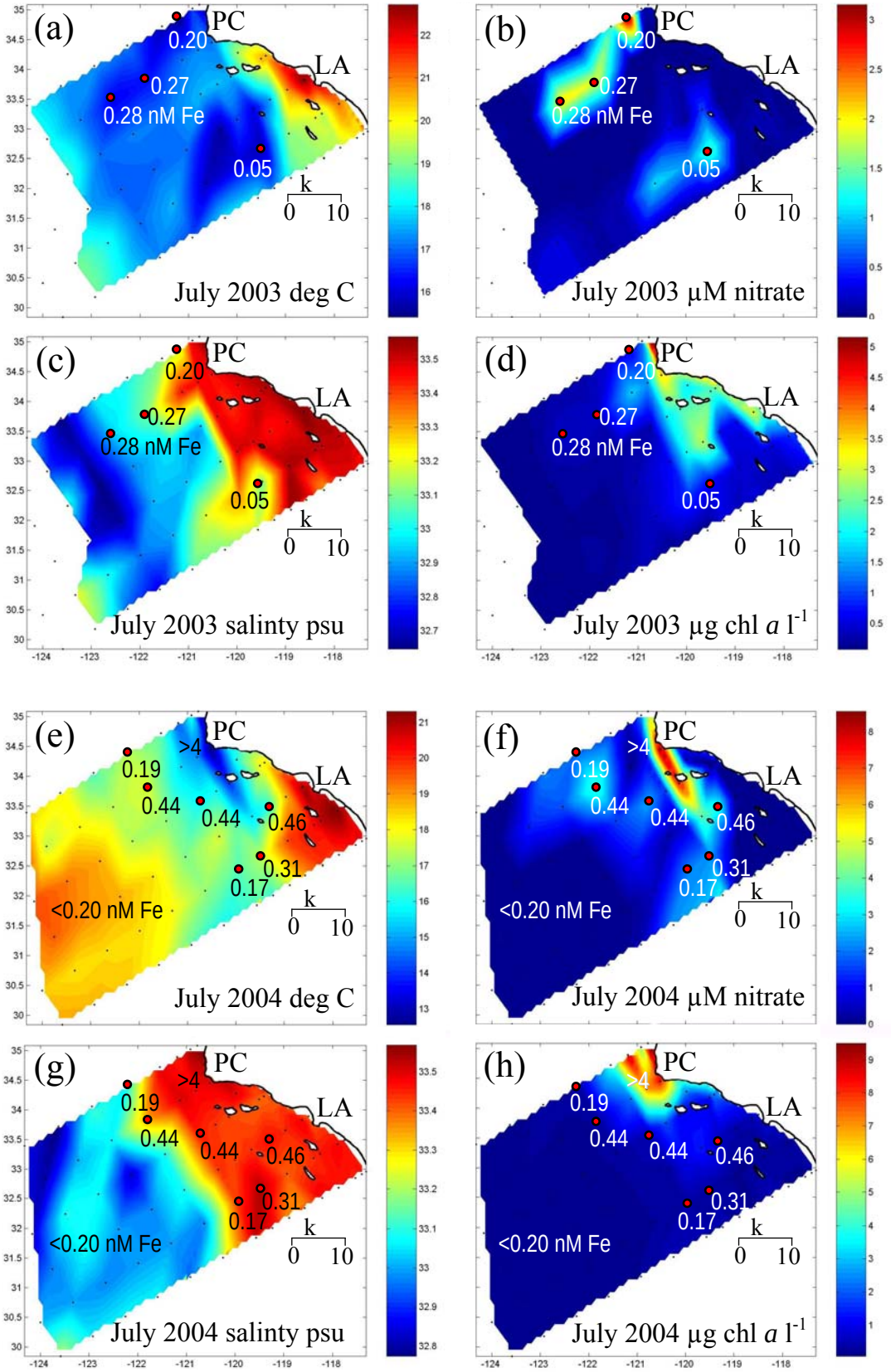
(a)
PC
0.20
LA
0.27
0.28 nM Fe
0.05
k
0 10
July 2003 deg C
(b)
PC
0.20
LA
0.27
0.28 nM Fe
0.05
k
0 10
July 2003 µM nitrate
(c)
PC
0.20
LA
0.27
0.28 nM Fe
0.05
k
0 10
July 2003 salinty psu
(d)
PC
0.20
LA
0.27
0.28 nM Fe
0.05
k
0 10
July 2003 µg chl a l-1
(e)
PC
>4
0.19
LA
0.44
0.44
0.46
0.31
0.17
<0.20 nM Fe
k
0 10
July 2004 deg C
(f)
PC
>4
0.19
LA
0.44
0.44
0.46
0.31
0.17
<0.20 nM Fe
k
0 10
July 2004 µM nitrate
(g)
PC
>4
0.19
LA
0.44
0.44
0.46
0.31
0.17
<0.20 nM Fe
k
0 10
July 2004 salinty psu
(h)
PC
>4
0.19
LA
0.44
0.44
0.46
0.31
0.17
<0.20 nM Fe
k
0 10
July 2004 µg chl a l-1

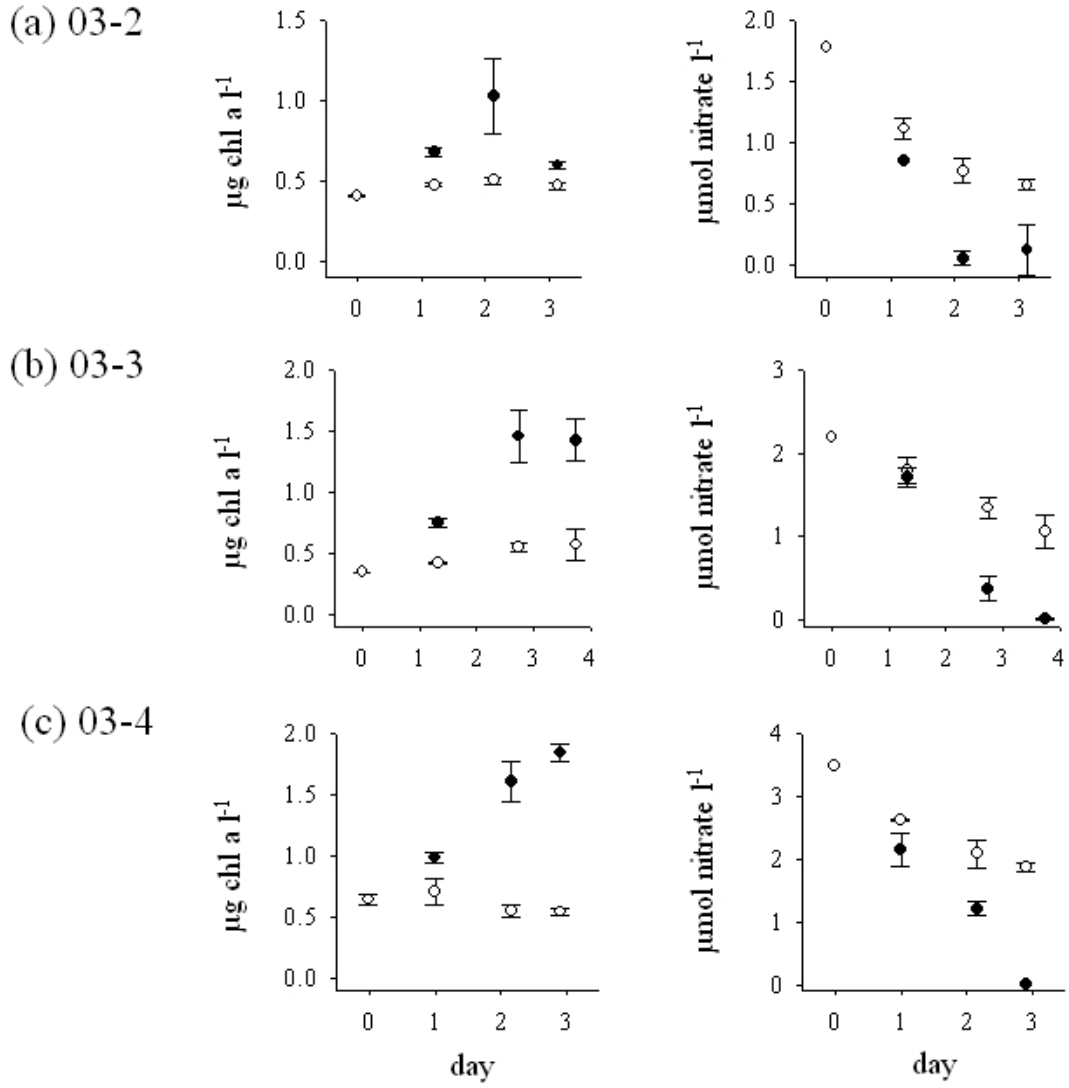

Figure 3.3. Phytoplankton chlorophyll *a* (µg l^{-1}) and nitrate (µmol l^{-1}) from select incubation experiments which exhibited a strong response to iron-addition: (a) experiment 03-2, July 2003, (b) experiment 03-3, July 2003, and (c) experiment 03-4, July 2003. Open circles are values from control experiments and closed circles are values from iron-addition experiments. Error bars represent one standard deviation (n = 3). Note different scales on both x- and y-axes.

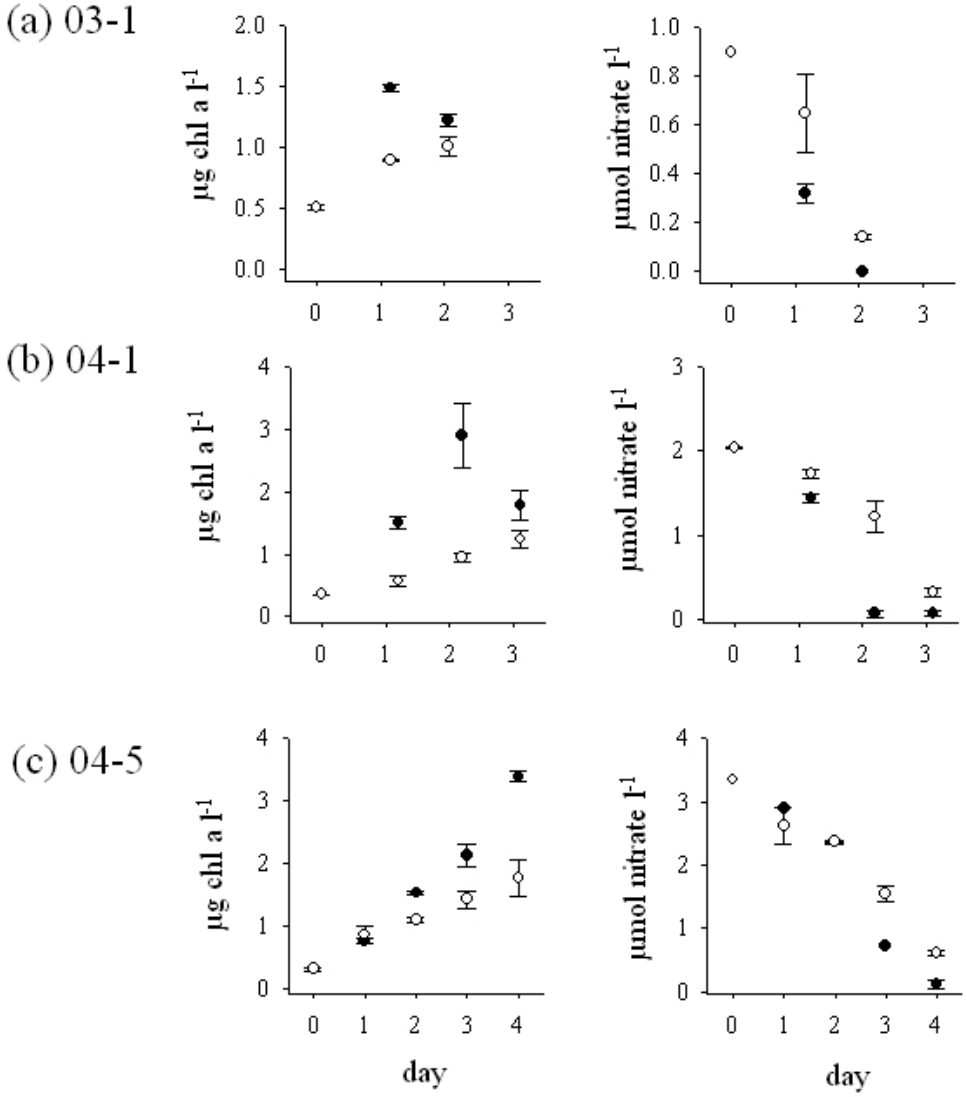

Figure 3.4. Phytoplankton chlorophyll *a* (µg l^{-1}) and nitrate (µmol l^{-1}) from select incubation experiments which exhibited a more subtle response to iron-addition: (a) experiment 03-1, July 2003, (b) experiment 04-1, July 2004, and (c) experiment 04-5, July 2004. Open circles are values from control experiments and closed circles are values from iron-addition experiments. Error bars represent one standard deviation (n = 3 for (a), n = 2 for (b) and (c)). Note different scale on both x- and y-axes.

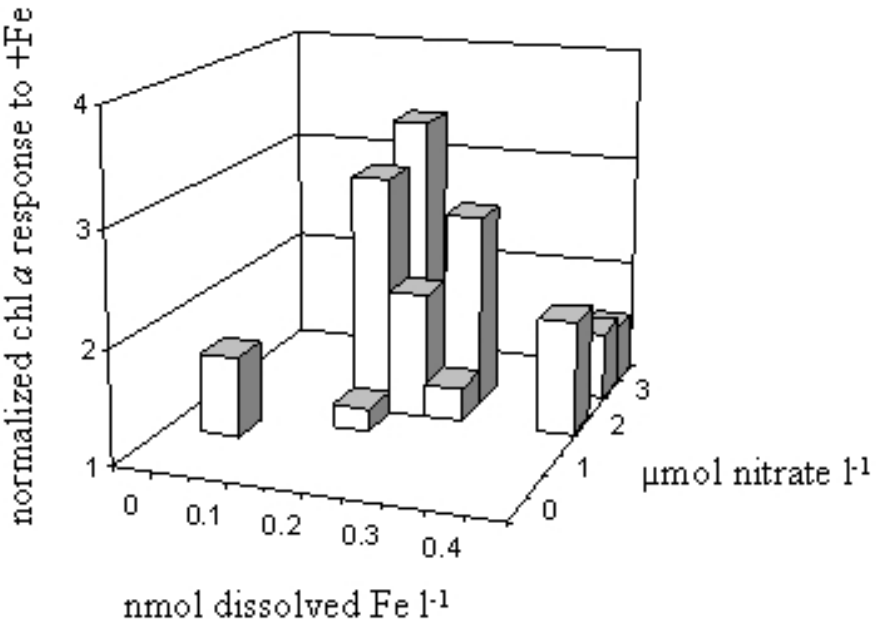

Figure 3.5. The normalized responses of phytoplankton in iron-addition experiments are summarized relative to initial nitrate and dissolved iron concentrations (nitrate binned to 0.5 µmol l^{-1} units, dissolved Fe binned to 0.05 nmol l^{-1} units). Normalized response to iron-addition (y-axis) is the ratio of chlorophyll *a* in iron-addition experiments to chlorophyll *a* in controls at t_{final} (Table 3.3). The effect of iron-addition on phytoplankton growth appears to be strongest under high nitrate, low iron conditions (middle of figure). In contrast, the response to iron-addition was weaker under low nitrate/low iron conditions (left portion of figure) and high nitrate/high iron conditions (right portion of figure).

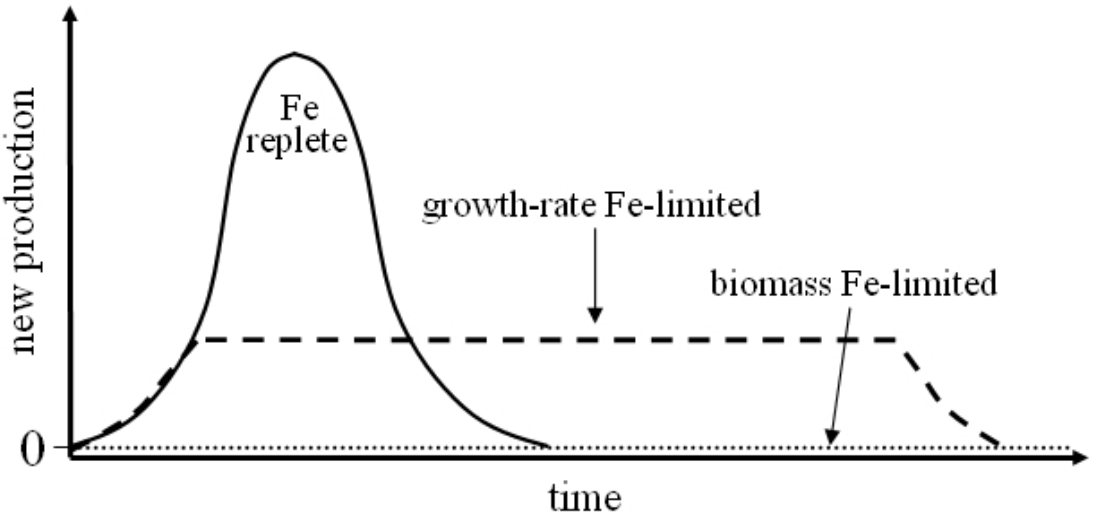

Figure 3.6. A simplified conceptual model of new production over time in three nitrate-limited scenarios in which initial nitrate concentrations are equal. The solid line (—) represents new production in an iron-replete system, the dashed line (- - -) represents new production in a system where iron is a growth-rate limiting nutrient, and the dotted line (···) represents new production in a system where iron is a biomass-limiting nutrient (e.g. high nutrient, low chlorophyll regime). New production is higher and occurs over a relatively short period of time in the iron-replete scenario, while new production is lower and occurs over a longer time period in the growth-rate iron limitation. Note that total new production in both iron-replete and iron growth-rate limited situations is equivalent because nitrate is the biomass-limiting nutrient. Units on the x- and y-axes are arbitrary.

3.7. Literature cited

Arrigo, K.R. 2005. Marine microorganisms and global nutrient cycles. Nature 437:doi:10.1038/nature04158.

Behrenfeld, M.J., and P.G. Falkowski. 1997. Photosynthetic rates derived from satellite based chlorophyll concentration. Limnol. Oceanogr. 42:1-20.

Bowie, A.R., E.P. Achterberg, R. Fauzi, C. Mantoura, and P.J. Worsfold. 1998. Determination of sub-nanomolar levels of iron in seawater using flow injection with chemiluminescence detection. Anal. Chim. Acta 361:189-200.

Bruland, K.W., E.L. Rue, and G.J. Smith. 2001. Iron and macronutrients in California coastal upwelling regimes: Implications for diatom blooms. Limnol. Oceangr. 46:1661-1674.

Chelton, D.B. 1982. Large-scale response of the California Current to forcing by the wind stress curl. Calif. Coop. Ocean. Fish. Invest. Rep. 23:130-148.

Cullen, J.J. 1991. Hypotheses to explain high-nutrient conditions in the open sea. Limnol. Oceangr. 36:1578-1599.

de Baar, H.J.W., and A.G.J. Buma, R.F. Nolting, G.C. Cadee, G. Jacques, and P.J. Treguer. 1990. On iron limitation of the Southern Ocean: experimental observations in the Weddell and Scotia Seas. Mar. Ecol. Prog. Ser. 65:105-122.

Elrod, V.A., W.M. Berelson, K.H. Coale, K.S. Johnson. 2004. The flux of iron from continental shelf sediments: A missing source for global budgets. Geophys. Res. Lett. 31, L12307, doi:10.1029/2004GL020216.

Eppley, R.W., J.N. Rangers, and J.J. McCarthy. 1969. Half-saturation constants for uptake of nitrate and ammonium by marine phytoplankton. Limnol. Oceangr. 14:912-920.

Eppley, R.W., and O. Holm-Hansen. 1986. Primary production in the Southern California Bight, pp. 176-215. In: Eppley RW (ed) Plankton Dynamics of the Southern California Bight. Lecture Notes on Coastal and Estuarine Studies, 15. Springer-Verlag.

Eppley, R.W., E.H. Renger, and W.G. Harrison. 1979. Nitrate and phytoplankton production in Southern California coastal waters. Limnol. Oceangr. 24:483-494.

Firme, G.F., E.L. Rue, D.A. Weeks, K.W. Bruland, and D.A. Hutchins. 2003. Spatial and temporal variability in phytoplankton iron limitation along the California

coast and consequences for Si, N, and C biogeochemistry. Global Biogeochem. Cycles 17:10.1029/2001GB001824.

Fitzwater, S.E., K.H. Coale, M. Gordon, K.S. Johnson, and M.E. Ondrusek. 1996. Iron deficiency and phytoplankton growth in the equatorial Pacific. Deep-Sea Res. Part II 43:995-1015.

Fitzwater, S.E., K.S. Johnson, V.A. Elrod, J.P. Ryan, L.J. Coletti, S.J. Tanner, R.M. Gordon, and F.P. Chavez. 2003. Iron, nutrient and phytoplankton biomass relationships in upwelled waters of the California coastal system. Cont. Shelf Res. 23:1523-1544.

Fung, I.Y., A.K. Meyn, I. Tegen, S.C. Doney, J.G. John, and J.K.B. Bishop. 2000. Iron supply and demand in the upper ocean. Global Biogeochem. Cycles 14:281-295.

Goericke, R., and J.P. Montoya. 1998. Estimating the contribution of microalgal taxa to total chl a in the field - variations of pigment ratios under nutrient- and light-limited growth. Mar. Ecol. Prog. Ser. 169:97-112.

Hayward, T.L., and E.L. Venrick. 1998. Nearsurface pattern in the California Current: coupling between physical and biological structure. Deep-Sea Res. Part II 45:1617-1638.

Hu, H., and W.T. Liu. 2003. Oceanic thermal and biological responses to Santa Ana winds. Geophys. Res. Lett. 30:1596, doi:10.1029/2003GL017208.

Hutchins, D.A., and K.W. Bruland. 1998. Iron-limited diatom growth and Si:N uptake ratios in a coastal upwelling regime. Nature 393:561-564.

Hutchins, D.A., G.R. DiTullio, Y. Zhang, and K.W. Bruland. 1998. An iron limitation mosaic in the California upwelling regime. Limnol. Oceangr. 43:1037-1054.

Hutchins, D.A., C.E. Hare, R.S. Weaver, Y. Zhang, G.F. Firme, G.R. DiTullio, M.B. Alm, S.F. Riseman, J.M. Maucher, M.E. Geesey, C.G. Trick, G.J. Smith, E.L. Rue, J. Conn, and K.W. Bruland. 2002. Phytoplankton iron limitation in the Humboldt Current and Peru Upwelling. Limnol. Oceangr. 47:997-1011.

Johnson, K.S., R.M. Gordon, and K.H. Coale. 1997. What controls dissolved iron concentrations in the world ocean? Mar. Chem. 57:137-161.

Johnson, K.S., F.P. Chavez, and G.E. Friederich GE. 1999. Continental-shelf sediment as a primary source of iron for coastal phytoplankton. Nature 398:697-700.

Johnson, K.S., F.P. Chavez, V.A. Elrod, S.E. Fitzwater, J.T. Pennington, K.R. Buck, P.M. Waltz. 2001. The annual cycle of iron and the biological response in the central California coastal waters. Geophys. Res. Lett. 28:1247-1250.

Jones, B.H., K.H. Brink, R.C. Dugdale, D.W. Stuart, J.C. Vanleer, D. Blasco, and J.C. Kelley. 1983. Observations of a persistent upwelling center off Point Conception, California, Part A, pp. 37-60. In: Suess E, Thiede J (eds), Coastal Upwelling, Its Sediment Record. Plenum.

Landry, M.R., R.T. Barber, R.R. Bidigare, F. Chai, K.H. Coale, H.G. Dam, M.R. Lewis, S.T. Lindley, J.J. McCarthy, M.R. Roman, D.K. Stoecker, P.G. Verity, and J.R. White. 1997. Iron and grazing constraints on primary production in the central equatorial Pacific: An EqPac synthesis. Limnol. Oceangr. 42:405-418.

Lohan, M.C., A.M. Aguilar-Islas, R.P. Franks, and K.W. Bruland. 2005. Determination of iron and copper in seawater at pH 1.7 with a new commercially available chelating resin, NTA Superflow. Anal. Chim. Acta 530:121-129.

Lynn, R.J., J.J. Simpson. 1987. The California Current System: the seasonal variability of its physical characteristics. J. Geophys. Res. 92 C12:12947-12966.

Martin, J.H., and S.E. Fitzwater. 1988. Iron deficiency limits phytoplankton growth in the north-east Pacific subarctic. Nature 331:341-343.

Martin, J.H., M.R. Gordon, S. Fitzwater, and W.W. Broenkow. 1989. VERTEX: phytoplankton/iron studies in the Gulf of Alaska. Deep-Sea Res. 36:649-680.

Miller, C.B., B.W. Frost, P.A. Wheeler, M.R. Landry, N. Welschmeyer, and T.M. Powell. 1991. Ecological dynamics in the subarctic Pacific, a possibly iron-limited ecosystem. Limnol. Oceangr. 36:1600-1615.

Morel, F.M.M. 1987. Kinetics of nutrient uptake and growth in phytoplnankton. J. Phycol. 23:137-150.

Nelson, C.S. 1977. Wind stress and wind stress curl over the California Current. NOAA Tech. Rep. NMFS-SSRF-714.

Price, N.M., B.A. Ahner, and F.M.M. Morel. 1994. The equatorial Pacific Ocean: grazer controlled phytoplankton populations in an iron-limited ecosystem. Limnol. Oceangr. 39:520-534.

Ryther, J.H., and W.M. Dunston. 1971. Nitrogen, phosphorus and eutrophication in the coastal marine environment. Science 171:1008-1112.

Sarthou, G., K.R. Timmermans, S. Blain, and P. Treguer. 2005. Growth physiology and fate of diatoms in the ocean: a review. J. Sea. Res. 53:25-42.

Strickland, J.D.H., and T.R. Parsons. 1972. A practical handbook of sea-water analysis, 2nd ed. Bull. Fish. Res. Bd. Canada 167.

Winant, C.D., and C.E. Dorman. 1997. Seasonal patterns of surface wind stress and heat flux over the Southern California Bight. J. Geophys. Res. C 102:5641-5653.

Chapter 4

Iron distribution in the southern California Current System and relation to macronutrients and phytoplankton

4.1. Abstract

The distribution of dissolved iron in the southern California Current System (sCCS) is presented from ten research cruises from 2002-2007. While dissolved iron was generally low in most of the study area (<0.5 nM), maximum mixed layer and water column dissolved iron concentrations (up to 8 nM) were found to be associated with coastal upwelling along the continental shelf, both along the continental margin and some island platforms. A significant supply of iron was probably not from a deep remineralized source, but rather from the continental shelf and bottom boundary layer, as identified in previous studies along the central and northern California coast. Moving offshore, dissolved iron decreased more rapidly than nitrate due to biological utilization and resulting in a transition zone (10-250 km offshore) in spring and summer that had relatively high ratios of nitrate:dissolved iron and phytoplankton iron limitation. Also likely due to biological utilization, a decoupling between the depth of the ferricline and nitracline was observed at three stations in July 2007. The data suggest that the decoupling between nitrate and dissolved iron (both spatially and at depth) has significant interactive consequences for sCCS biogeochemical patterns.

4.2. Introduction

The southern California Current System (sCCS) has been intensely studied for the last 50+ years in research programs such as the California Cooperative Fisheries Investigations (CalCOFI) (1949 to the present) and the Southern California Bight Studies (1974-1983). These research programs have provided extraordinary templates for understanding processes and variability in physical and biogeochemical processes, and arguably most notable, explanations for spatial and temporal patterns of phytoplankton and macronutrients. Evidence from observations and experiments indicate that new production in the sCCS region is dependent on the supply of upwelled macronutrient nitrate - phytoplankton biomass and productivity are closely related to nitrate availability (Eppley and Holm-Hansen 1986; Hayward and Venrick 1998). In the 1980's, oceanographers began to use trace metal clean techniques which led to the confirmation that iron was an important micronutrient controlling phytoplankton growth in high nutrient, low chlorophyll regimes in the open ocean (Martin et al. 1989). Although close to continental sources of iron, low iron concentrations and phytoplankton iron limitation was also found in coastal upwelling regimes of central California and Peru (Hutchins et al. 1998; Hutchins et al. 2002; Firme et al. 2003). The distribution of dissolved iron, particularly in relation to coastal upwelling, has recently been the subject of studies off central California (Bruland et al. 2001; Fitzwater et al. 2003) and Oregon (Chase et al. 2002).

In this chapter, we present the mixed layer distribution of dissolved iron between 2002 and 2007, primarily from seven CalCOFI cruises, but include mixed layer and water column data from two California Current Ecosystem Long Term

Ecological Research (CCE-LTER) program cruises and a Deep Chlorophyll Maximum (DCM) study cruise. The objectives of this study was to document horizontal and vertical dissolved iron distributions in the context of physical, biological and chemical data collected on these cruises. We examine the potential biogeochemical consequences of dissolved iron variability with respect to coastal upwelling and wind stress curl upwelling, and the consequences of decoupling between nitrate and dissolved iron observed in the mixed layer and water column in spring and summer.

4.3. Methods

4.3.1. Cruises and sampling protocol

Samples for dissolved iron analysis were collected on seven CalCOFI cruises, two CCE-LTER Process cruises, and one DCM cruise. Mixed layer samples were collected on six of the seven CalCOFI cruises, herein referred to as CalCOFI survey cruises. CalCOFI survey cruises were in November 2002 (10 to 26 November 2002 on R/V New Horizon), February 2003 (30 January to 18 February 2003 on R/V Jordan), April 2003 (4 to 25 April 2003 on R/V Revelle), July 2003 (17 to 31 July 2003 on R/V New Horizon), April 2004 (12 to 24 April 2004 on R/V New Horizon), and July 2004 (12 to 28 July 2004 on R/V Jordan). Both mixed layer and water column samples (13 profiles total) were collected during the October 2006 CalCOFI cruise (only along line 83; 27 October to 1 November 2006 on R/V Revelle), CCE-LTER process cruises in May 2006 (8 May to 7 June 2006 on R/V Knorr) and April 2007 (2 to 21 April 2007 on R/V Thompson), and July 2007 DCM cruise (17 July to 3 August 2007 on R/V New Horizon).

Non-trace metal clean sampling on these cruises was conducted with Niskin bottles and a rosette sampling system. The rosette had sensors for measuring depth, temperature, salinity, density (sigma-theta), fluorescence, light transmission, and dissolved oxygen. An ISUS nitrate sensor was also attached to the rosette sampling system on May 2006 and April 2007 CCE-LTER cruises and July 2007 DCM cruise. Discrete samples were collected from Niskin bottles for analysis of chlorophyll a (chl) via fluorometer and macronutrients (nitrate, silicic acid, and phosphate) via autoanalyzer. Particulate organic carbon and nitrogen were also measured on CCE-LTER cruises. The CalCOFI time series also samples for macrozooplankton biomass and, at select stations, ^{14}C-based primary productivity measurements. Recent additions to the CalCOFI time series include CCE-LTER-augmented measurements of pico- and nanoplankton analysis at select stations, POC/PON, HPLC, etc.

CalCOFI survey cruises - Since 1984, the CalCOFI sampling plan has consisted of 66 stations in the sCCS (Fig. 4.1). On CalCOFI cruises between November 2002 and July 2004, samples for dissolved iron were collected at a subset of stations depending on time availability and weather conditions. Because of these limitations, the sampling scheme for dissolved iron was based on higher intensity sampling at nearshore stations where gradients were expected to be larger and lower intensity sampling at offshore stations where gradients were expected to be lower. Samples were collected from 181 of 396 stations occupied, and on average about half of the 66 stations were sampled during each CalCOFI cruise.

CCE-LTER process cruises - Both CCE-LTER process cruises were based on four-day Lagrangian experimental cycles using drogued drift arrays to track and study

water masses. Dissolved iron data presented in this article are from the mixed-layer during one experimental cycle in May 2006 (herein referred to as drifter study 1), and from four-bottle profiles during two experimental cycles in April 2007 (herein referred to as drifter study 2 and 3). Drifter study 1 (May 2006) originated near CalCOFI station 80.55 and ended about 35 km southwest over four days. Drifter study 2 (April 2007) originated near CalCOFI station 80.55, initially began to move northwest, and then southwest ending about 40 km west of station 80.55 after four days. Drifter study 3 (April 2007) began just southwest of CalCOFI station 80.60, drifted south-southeast and then east ending about 50 km southeast of station 80.60.

Station locations can be referred to in Fig. 4.1.

October 2006 CalCOFI cruise and July 2007 DCM cruise - On the October 2006 CalCOFI cruise, dissolved iron samples from four-bottle profiles were collected at five stations along line 83: stations 83.42, 83.51, 83.60, 83.70, and 83.90. On the July 2007 DCM cruise, dissolved iron was collected from eight-bottle profiles at five stations on CalCOFI line 93: stations 93.40, 93.60, 93.80, 93.110, 93.120.

4.3.2. Cleaning protocols

Low density polyethylene, high density polyethylene, and fluorinated high density polyethylene bottles (LDPE, HDPE, FLPE; Nalgene) for seawater collection and sample storage were cleaned with acidic soap (Citranox), 2 M Trace Metal grade HCl (Fisher Chemical), and 2 M Trace Metal grade HNO_3 (Fisher Chemical), with several rinses with Milli-Q water between steps. Each acid cleaning step was at either 25 °C for weeks, or 60 °C for one day. Bottles were then stored in 0.01 M ultrapure

HCl (~1-6 months) until rinsed and filled with seawater samples. All equipment with Teflon pieces were cleaned with 6 M Trace Metal grade HCl and 6 M Trace Metal grade HNO_3 at 60 °C for several days. Polycarbonate membrane filters were soaked in 1 M ultrapure HCl for 1 week and stored in Milli-Q water. Trace metal free pipette tips used for sample acidification were cleaned in 1 M Trace Metal grade HCl for one week followed by several rinses with Milli-Q water.

4.3.4. Methods for trace metal clean sample collection

The majority of seawater samples from the mixed layer were collected using a custom-made ~7 m trace metal clean fiberglass pole sampler (similar to Boyle et al. 1981). Two 1 L FLPE bottles were mounted to the end of the pole using an assembly constructed with acrylic and tygon tubing. The pole sampler was extended ~3-4 m from the ship's railing and FLPE bottles were filled and emptied with seawater at least twice before sample collection. About 15 mixed layer seawater samples were collected using a trace metal clean Teflon pump system. Seawater from 5-10 m depth was collected via Teflon tubing (Cole-Parmer) connected to an air-driven diaphragm pump (Cole-Parmer; all wetted parts were Teflon).

Profiles for dissolved iron analysis were collected using GO Flo bottles (General Oceanics) attached to a synthetic line (New England Ropes) with a coated lead ballast and lowered using a hydraulic winch. GO Flo bottle depths were determined using a line-out counter attached to a trace metal clean metering block (University of Washington and InterOcean Systems) and correcting for estimated wire angle. Coated GO Devil messengers (General Oceanic) and custom-made Teflon

messengers were used to trip GO Flo bottles in series. Seawater was sampled from GO Flo bottles using filtered N_2 overpressure.

After collection, all seawater samples were processed under Class 100 laminar flow hoods and in positive pressure clean areas. Operationally-defined dissolved fractions were collected by either vacuum filtering or in-line filtering samples through acid-cleaned 0.4 μm polycarbonate membrane filters. The wetted parts of both vacuum filtering and in-line filtering apparatuses were constructed of Teflon (Savillex). An LDPE bottle was rinsed with the filtrate, filled, and acidified to pH ~1.8 by adding 2 ml 6 M ultrapure HCl to 500 ml sample.

4.3.5. Dissolved iron analysis

Dissolved iron was measured using an FeLume flow injection analysis system (Waterville Analytical) with an iron(II) sulfite reduction chemiluminescent flow injection analysis method (based on Powell et al. (1995) and Bowie et al. (1998)). Dissolved iron in acidified seawater samples is reduced to iron(II) with 2 μM sulfite for 12 hours, buffered in-line with 2 M ammonium acetate (~90% sample/10% buffer) to pH ~6 and iron(II) is preconcentrated on a column filled with nitriloacetic acid (NTA) resin (NTA Superflow, Qiagen). Iron(II) is then eluted and oxidized when mixed with a pH >9.5 luminol-ammonia buffer. Luminol is subsequently oxidized by radical intermediates and the resulting chemiluminescence production (425 nm) is measured with a photomultiplier tube. Dissolved iron is determined using standard addition methodology. The apparatus and procedure are described in detail in King and Barbeau (submitted). The average relative standard deviation of the method is 3.9

± 4.7% (mean and 1 standard deviation; n=183) and the detection limit (three times standard deviation of blank measurement) for this method is 0.02 nM (n=27). Using this method, seawater reference samples from the Sampling and Analysis of Fe (SAFe) intercomparison cruise in October 2004 were measured to be 0.10 ± 0.02 nM Fe (Surface bottle 279, mean ± 1 SD, n = 4) and 0.92 ± 0.03 nM Fe (Deep2 bottle 285, mean ± 1 SD, n = 4). The consensus value of the surface reference sample is 0.097 ± 0.043 (n = 140) nM Fe and the deep2 reference sample is 0.91 ± 0.17 (n = 168) nM Fe (Johnson et al. 2007; SAFe standards and further information available by email from requestsafestandard@ucsc.edu).

4.4. Results

4.4.1. October 2002 to July 2004 CalCOFI survey cruises

The distribution of mixed-layer density (sigma-theta) are shown for six CalCOFI survey cruises in November 2002, February 2003, April 2003, July 2003, April 2004 and July 2004 in Fig. 4.2 through 4.7. Based on long-term means (1984-2006, n=80?) and results of previous studies (e.g. Lynn and Simpson 1987; Hayward and Venrick 1998), the study region can be divided into four biogeochemical domains (Table 4.1): northern coastal (cold, salty, and high density), transition zone (cool, medium salinity, and medium density), southern coastal (hot, salty, and low density), and offshore (warm, fresh, and low density). Macronutrients and chlorophyll in the majority of the study were generally low - the mean mixed layer values for the six CalCOFI surveys in Fig. 4.2-4.7 were 0.4 µM phosphate, 0.8 µM nitrate, 1.9 µM silicic acid, and 1.3 µg a L^{-1} chl (n=396). The sCCS can be characterized as a

mesotrophic regime (defined as chl ranging between 0.1 to 1 μg L^{-1}; Behrenfeld and Falkowski 1997) with episodic upwelling events occurring in the spring and summer that supply macronutrients to surface waters via upwelling. In comparison to the CCS off central and northern California and Oregon, the sCCS is a region of weak upwelling (Eppley et al. 1979; Jones et al. 1983). For example, nitrate concentrations reported during upwelling off central California and Oregon exceeded 15-20 μM (Hutchins et al. 1998; Johnson et al. 1999; Chase et al. 2002). During the six surveys, the concentration of nitrate in the mixed layer reached 16 μM at only one station in the most northeastern corner of the study area (April 2004 station 77.49). In some instances, there was low spatial coherence between dissolved iron, macronutrients, and chl in the mixed layer. For example, in April 2003 at station 82.47 chl was high and both macronutrients and dissolved iron were low, and in July 2003 at station 80.51 dissolved iron was high and both macronutrients and chl were low. This was likely due to the synoptic nature of CalCOFI surveys and temporally-discrete sampling, and should be taken into consideration when evaluating interpretations of the data.

Northern coastal domain - The northern coastal domain was generally cool (~10.5-15 °C), saline (~33.3-33.7 psu) and dense (~24.6-25.7 sigma-theta). Equatorward wind stress along the coast is at a maximum during spring and somewhat during summer (Nelson 1977), which results in the upwelling of nutrient-rich waters in the vicinity of Pt. Conception. The largest coastal upwelling signal was in April 2003 and 2004 with waters that were as cool as ~11.0 °C, as high as 33.6-33.7 psu, and >25.4 sigma-theta. Macronutrients, dissolved iron, and chl were elevated during all six surveys in the northern coastal domain, especially in April 2003, April 2004

and July 2004 when mixed layer waters maximum concentrations were ~3-8 nM dissolved iron, ~0.9-1.4 μM phosphate, ~9-16 μM nitrate, ~8-16 μM silicic acid, and ~12-30 μg L^{-1} chl. Presumably due to less upwelling favorable winds, macronutrients and chl in the northern coastal domain in November 2002, March 2003, and July 2003 were closer to the regional mean values, but were still substantially higher when compared to surrounding waters (except for November 2002 station 77.49 which resembled springtime values). Although maximum wind stress and subsequent Ekman transport that drive coastal upwelling should be physically restricted to a region within ~10 km from the continental shelf, hydrographic and biogeochemical signatures from upwelling are often present up to 50 km offshore (e.g. in April 2003 and April 2004, waters with 25.0 sigma-theta extend ~50 km off Point Conception). Regional wind models suggest that wind stress curl is also at a maximum in the northern coastal regime during spring (Di Lorenzo 2003).

. In April 2003, July 2003, April 2004, and July 2004 (Fig. 4.4-4.7), dissolved iron at Point Conception (station 80.51) was consistently high, ranging between 2.8-8.0 nM (dissolved iron was ~1 nM in November 2002 and not sampled in March 2003). There were also instances of high dissolved iron at stations that were situated near island platforms that were at times associated with elevated macronutrients and chl. For example, at station 83.51, on the southern edge of Santa Rosa Island, dissolved iron ranged from ~1-3 nM in April 2003, July 2003, and April 2004 (station not sampled in July 2004). In April 2003, a station on the northwestern edge of San Nicolas Island (87.50) had ~2 nM dissolved iron. Dissolved iron at stations ~50 km offshore of these island platforms dropped to concentrations <0.5 nM.

Transition zone domain - The transition zone is a domain that is a continuum bridging coastal upwelling in the northern coastal regime to other lower nutrient regimes, typically 50-150 km offshore and bounded by the eastern edge of the California Current (CC) jet system (Lynn and Simpson 1987). During our study, the transition zone domain was particularly pronounced in summertime between 50-250 km offshore with waters that were ~15-17 °C, ~33.0-34.0 psu and ~24.0-24.4 sigma-theta. During spring, it was narrower and closer to shore (~10-100 km from the coast) with waters that were ~12.5-14.5 °C, ~33.0-33.4 psu, and ~24.6-25.2 sigma-theta. The water mass has intermediate temperature and salinity values as a consequence of waters transported via the CC from the subarctic Pacific, possible advection of northern coastal domain waters, and due to isopycnal shoaling due to wind stress curl upwelling and processes associated with high eddy kinetic energy. During times of upwelling favorable winds, especially summer, the wind stress field is arranged in an onshore-offshore gradient of increasing wind stress, primarily due to the eastward cut in the coastal topography of the California coastline south of Pt. Conception, resulting in a divergence of Ekman transport (Nelson 1977; Chelton 1982; Bakun and Nelson 1991). Although wind stress curl upwelling (~1-2 m d^{-1}) is not as vigorous as coastal upwelling (~6-12 m d^{-1}), due to its large areal extent wind stress curl upwelling can account for about twice as much vertical transport as coastal upwelling (~3 Sv v. ~6 Sv) in the central and southern CC region (Rykaczewski and Checkley 2008).

During spring and summer 2003 and 2004, macronutrients in the transition zone domain were intermediate (~0.3-0.5 µM phosphate, ~1-4 µM nitrate, ~0.5-2.0 µM silicic acid) with generally low dissolved iron (<0.5 nM dissolved iron) and chl (1

μg L^{-1}. An exception was dissolved iron at station 90.53 (~175 km offshore) in April 2003 and April 2004 was somewhat higher (~0.5 nM) in comparison to surrounding stations, likely due to the proximity of Cortez and Tanner Banks that reach <20 m from the sea surface (Fig. 4.8).

In the transition zone domain, there was a conspicuous decoupling between the offshore gradients in dissolved iron and nitrate in which dissolved iron concentrations declined more rapidly relative to nitrate. Nitrate:dissolved iron (N:Fe) ratios in summer (July 2003 and 2004) were as high as 16 (Fig. 4.9). In comparison, N:Fe ratios in the northern coastal regime were generally less than 1 (either due to water masses with high dissolved iron and either low or high nitrate). In April 2003 and 2004, N:Fe ratios were also elevated (as high as 40), but confined to a narrower transition zone that was much closer to shore (~10-100 km). In April 2003 and 2004 at stations 77.49, 77.51, and 77.55 over a distance of ~45 km, a increase in N:Fe ratio was accompanied by a decrease in silicic acid:nitrate ratios (Si:N) (Table 4.2). At station 77.49, nitrate (11-15 μM), silicic acid (9-16 μM), dissolved iron (1.9-2.5 nM), and chl (6-9 μg L^{-1}) were initially high in the northern coastal domain with nitrate:silicic acid ratios 0.9-1. About 15 km southeast, at station 77.51, the decline in dissolved iron was much greater than that of nitrate or silicic acid and Si:N ratios began to drop while chl remained high (~9 μg L^{-1}). At station 77.55, 30 km further southeast, dissolved iron concentrations were near-oceanic (0.2-0.3 nM), nitrate was still 6.4-7.5 μM, and Si:N ratios dropped to 0.6-0.7. This equated to a substantially larger decrease in dissolved iron (-83-95%) in comparison to phosphate (-31-41%),

nitrate (-40-51%), and silicic acid (-60-68%) (Table 4.2). N:Fe ratios were 3-8 at station 77.49 and increased to between 23-40 at stations 77.51 and 77.55.

Southern coastal and offshore domain - As mentioned in the description of the transition zone domain, the southern California coastline south of Point Conception veers southeast and effectively shelters the southern coastal domain from upwelling-favorable winds, and coastal upwelling is therefore weak (Nelson 1977). This southern coastal water mass was generally warm (16-23 °C), salty (33.2-33.6) and low density (23-24.8 sigma-theta). The hydrography of the region is quite variable between seasons because of the shift between generally equatorward flow during the spring and poleward flow during summer and early fall (Lynn and Simpson 1987; Di Lorenzo 2003). During summer, poleward flow of central North Pacific waters in the southern coastal domain with characteristic spiciness (warm and salty) has been observed (Lynn and Simpson 1987). Macronutrients, dissolved iron, and chl were generally low through out the southern coastal domain (<1 μM nitrate, <0.5 nM dissolved iron, <1 μg L^{-1} chl). An exception was in the nearshore (<~20 km from the coast) where dissolved iron (0.5-4.5 nM) and chl (1-5 μg L^{-1}) were elevated.

The offshore domain accounted for up to 50% of the study region and was typically situated >150-250 km offshore. Mixed layer waters were typically 16-19 °C, 32.7-33.1 psu, and sigma-theta as low as 23. The boundary between the transition zone and the offshore domains is dependent on the intensity and location of the CC jet, which has been documented to shift onshore during spring and further offshore in fall and winter (Lynn and Simpson 1987; Strub and James 2000). This region was generally low in dissolved iron (<0.5 nM, and <0.2 nM in the far offshore reaches of

the domain), low in macronutrients (<0.4 μM phosphate, <0.2 μM nitrate, <2 μM silicic acid), and low in chlorophyll (<0.3 μg L^{-1}). In July 2003, there was station in the offshore domain with anomalously high silicic acid (~5 μM) with low phosphate and nitrate concentrations.

4.4.2. CCE-LTER Lagrangian drifter studies

In May 2005 and April 2007, three water masses were followed with a drogued drift array (drifter studies 1, 2, and 3). Initial (t = 1 d) and final (t = 4 or 4.5 d) observations are presented in Table 4.3. Drifter studies 1 and 2 began ~35 km southwest of Point Conception near CalCOFI station 80.55 and drifter study 3 began ~70 km southwest of Point Conception near CalCOFI station 80.60. Initial observations of cool (11.3-12.2 °C), saline (33.6-33.7), and dense (25.5-25.7 sigma-theta) waters in the mixed layer indicate that all three drifter studies were in the northern coastal domain and near coastal upwelling. In the May 2005 drifter study 1, dissolved iron and macronutrients declined at roughly the same rate in the mixed layer over time (Table 4.3). But during April 2007 drifter studies 2 and 3, dissolved iron was removed up to twice as fast as macronutrients (Table 4.3). Dissolved iron concentrations dropped from 1.47 nM to 0.33 nM (-78%) in drifter study 2 and from 1.28 nM to 0.17 nM (-87%) in drifter study 3. Dissolved iron removal was 1.9-2.8x faster than phosphate, 1.4-1.8x faster than silicic acid, and 1.4-2.0x faster than nitrate. While N:Fe ratios in drifter study 1 dropped from 7 to 6, they increased in drifter study 2 from 5 to 14, and from 9 to 25 in drifter study 3. Si:N ratios did not drop appreciably in drifter studies 2 and 3 (as was observed in the April 2003 and 2004 line

77 mesoscale example), potentially due to the relatively low abundance of diatoms in these studies (M. Landry, R. Goericke, pers. comm.).

4.4.3. Profiles from October 2006, April 2007, and July 2007

Below the mixed layer, dissolved iron concentration increased with depth in profiles from the CalCOFI October 2006, CCE-LTER April 2007, and DCM July 2007 cruises (Fig. 4.10). The highest subsurface dissolved iron concentrations were at stations that were situated on the continental shelf where dissolved iron at 70 m was between 2-4 nM (e.g. Fig. 4.10a, October 2006 stations 83.42 and 83.51; both stations were ~20 km offshore and on the continental shelf with the seafloor at ~100 m). At nearshore stations that were close to the continental shelf (but not on the continental shelf), dissolved iron was generally greater than 1 nM between 100-250 m (e.g. Fig. 4.10a, October 2006 station 83.60 (85 km offshore, seafloor at 2200 m); Fig. 4.10b, April 2007 drifter study 2 t = 1 d (~35 km offshore, seafloor at 800 m) and t = 4.5 d (~75 km offshore, seafloor depth 2264 m); Fig. 4.10b, April 2007 drifter study 3 t = 3.5 d (~80 km offshore, seafloor ~2200 m); Fig. 4.10c, July 2007 station 93.40 (~100 km offshore, seafloor 1600 m). In profiles further than 100 km offshore, dissolved iron concentrations were generally lower at depth. For example, dissolved iron was less than ~1 nM at depths >200 m in profiles at October 2006 stations 83.70 and 83.90 (Fig. 4.10a), and July 2007 stations 93.60, 93.80, 93.110, and 93.120 (Fig. 4.10c).

At three stations in July 2007, there was a vertical decoupling between the depth of the nitracline (as defined by the presence of 1 μM nitrate) and ferricline (as defined by the presence of ~0.2 nM dissolved iron). The distance between the

nitracline and ferricline ranged between 10-60 m at stations 93.40, 93.60 and 93.80 in July 2007, resulting in elevated N:Fe ratios at depth relative to the mixed layer (Fig. 4.11, Table 4.4).

4.5. Discussion

4.5.1. Remineralized source of iron to surface waters

The highest concentrations of dissolved iron were found near the coast, particularly in the northern coastal regime where coastal upwelling occurs. With a dissolved iron:phosphate ratio ($R_{Fe:PO4}$) from estimated source waters for coastal upwelling (along 25.3-25.7 isopycnal, typically as deep as 100 m, and out to ~100 km offshore based on observations and a passive tracer simulations by Chhak and Di Lorenzo (2007)), we estimated expected remineralized iron from upwelling source waters (Fe_{remin}) using observed mixed layer phosphate concentrations ($phosphate_{ML}$):

$$Fe_{remin} = phosphate_{ML} \times R_{Fe:PO4} \quad (1)$$

where $R_{Fe:PO4} = 0.2$ to 0.4

$$Fe_{remin/ML} = Fe_{remin} / Fe_{ML} \quad (2)$$

Fe_{remin} represents the concentration of dissolved iron that is expected to accompany a given concentration of phosphate in the source waters for coastal upwelling. $Fe_{remin/ML}$ is the proportion of observed dissolved iron in the mixed layer (Fe_{ML}) that was contributed from Fe_{remin}. By plotting $Fe_{remin/ML}$ versus Fe_{ML} (Fig. 4.12), we estimate that <10% of Fe_{ML} >~1 nM was supplied by a remineralized dissolved iron source.

About 50% of Fe_{ML} in the 0.2-0.3 nM range was supplied by a remineralized dissolved iron source. At concentrations <~0.1-0.2 nM, Fe_{remin} was in excess of Fe_{ML}, possibly due to biological iron depletion in the mixed layer. This estimate does not account for any $phosphate_{ML}$ that was biologically removed prior to the time of sampling. An upper bound estimate indicates that as much as 50% of observed dissolved iron >1 nM could have been from a remineralized source (Fe_{remin} calculated assuming that all $phosphate_{ML}$ was equal to 1.3 μM in eq. 1, the maximum mixed layer concentration of phosphate observed during the six CalCOFI surveys). In the northern coastal domain, dissolved iron was often >1 nM and therefore a source of iron besides remineralized iron must exist.

4.5.2. Shelf source of iron and upwelling

Based on the association between high dissolved iron, coastal upwelling, and the continental shelf (Fig. 4.2-4.8), the continental shelf and bottom boundary layer (BBL) could be a significant source of dissolved iron to upwelled water masses. In central and northern California, the continental shelf and BBL has been identified as an important source of dissolved iron to upwelled water masses (Johnson et al. 1999; Bruland et al. 2001; Elrod et al. 2004). It was found that the width of the continental shelf was an important criterion determining the amount of fluvially-delivered, fine-grained, iron-rich sediments that could be deposited during wintertime storms. Dissolved iron directly scavenged from rivers has also been hypothesized to be deposited onto the continental shelf (Chase et al. 2007). Upwelling in the subsequent spring and summer then entrains reduced iron from the continental shelf and BBL.

Along broad shelves, such as off Monterey and Point Reyes (~20-30 km wide), dissolved iron in the water column was found to be high (0.3-10 nM dissolved iron); and along narrow continental shelves, such as Big Sur (<1 km wide), dissolved iron was much lower (<0.2-1 nM) (Bruland et al. 2001). It was also noted that there was a large fluvial input of iron to the broad shelves of Monterey and Point Reyes, while there was little fluvial input to the narrow shelf off Big Sur. Although the supply of dissolved iron differed markedly between the different shelf-width conditions, the supply of macronutrients via upwelling along these shelves did not. Therefore, wide shelf locations were macronutrient and iron-replete and dominated by diatoms and narrow shelf locations were low in iron and diatoms despite high concentrations of macronutrients (Bruland et al. 2001).

In the sCCS, the continental shelf is between ~2-7 km wide in the southern coastal domain and ~10-20 km wide along the northern coastal domain, between Pt. Conception and Ventura, CA (200 m isobath is approximately defined by yellow contour in Fig. 4.8). In the northern coastal domain, the northern Channel Islands extend the edge of the continental shelf to about 50 km from shore (Fig. 4.8). Although, the continental shelf is not continuous here due to the presence of the Santa Barbara Basin (~515 m deep) between the islands and shore. Major fluvial inputs include the Santa Ynez River (just north of Point Conception, CA) and Santa Clara River (eastern edge of Santa Barbara Basin), both marked in Fig. 4.1, that account for about 50% of total suspended sediment load amongst 18 rivers flowing into the region between 1944-1995, equivalent to a mean annual suspended sediment flux of 2×10^6 tons (Inman and Jenkins 1999). Suspended sediment discharge is typically limited to

1-3 d following wintertime precipitation. For example, on average, the Santa Clara River discharges half of its annual sediment load in the span of ~3 days and has negligible discharge for 70% of the year (Warrick 2002). Variability in suspended sediment load to the sCCS is influenced by a combination of factors including climate-related rainfall patterns linked to the Pacific/North America climate pattern (PNA) and El Nino-Southern Oscillation (ENSO), the geological composition the Transverse Ranges watershed (watershed for both the Santa Ynez and Santa Ana rivers) which is composed of easily eroded, geologically-overturned Cenozoic sediments, and anthropogenic impacts such as agricultural run-off, building of dams, and other water retention and diversion structures (Inman and Jenkins 1999).

It is plausible that a scenario similar to central and northern California is occurring in the sCCS. Fluvially-delivered iron is deposited on the continental shelf during wintertime storms and coastal upwelling entrains this iron-rich benthic boundary layer during spring and summer. The Santa Ynez River and Santa Clara River had at least one high flow event (>500 m^3 s^{-1}) during the winter between 2002/2003 and 2005/2006 (Table 4.5). In 2007, because of low precipitation and drought conditions throughout California, there were no major flow events in the 2006/2007 winter. The continental shelf in the sCCS coastal upwelling (northern coastal) domain and near the Santa Ynez River and Santa Clara River outlets is relatively wide (10-20 km). We think that this explains why northern coastal water masses in the sCCS are generally rich in dissolved iron (>1 nM) and exceed the estimated upwelling source water iron concentrations (Fe_{remin}). The shelf source of iron is further supported by observations of high dissolved iron in subsurface waters at

stations near the continental shelf (Fig. 4.10). Theoretically, the flux of iron via coastal upwelling can be qualitatively predicted by the wintertime fluvial deposition and the intensity and duration of spring and summertime upwelling (Johnson et al. 1999).

In comparison to coastal upwelling, wind stress curl upwelling can occur in the transition zone regime, some 50-250 km offshore, and is not expected to interact with the continental shelf (Bakun and Nelson 1991; Rykaczewski and Checkley 2008). By comparing isopycnal sections from line 90 in summer CalCOFI cruises (2002-2005), we estimate the maximum vertical displacement of wind stress curl upwelling to be ~50 m. This relatively shallow shoaling (in comparison to coastal upwelling) is consistent with slow vertical velocities (1-2 m d^{-1}) induced by wind stress curl upwelling. Without a shelf source of iron, wind stress curl upwelling is expected to supply surface waters dissolved iron close to Fe_{remin} from Eq. 1. It is important to note that coastal upwelling water masses can potentially advect offshore and mix with wind stress curl upwelling water masses. This is especially true in the transition zone domain west of the northern coastal domain during summer when coastal upwelled water masses tend to propagate westward (offshore) into the wind stress curl upwelling zone (Di Lorenzo 2003). Because of the large distance between coastal upwelling and the southern transition zone domain (e.g. lines 90 and 93 are ~150-200 km from the northern coastal domain), advected coastal upwelling water masses probably remain separate from wind stress curl upwelling water masses in this region.

4.5.3. Other sources of iron to the sCCS

Other than upwelling of a remineralized deep source or from the continental shelf and BBL, potential sources of dissolved iron to the sCCS include the allochthonous input of iron directly from rivers, atmospheric deposition, and equatorward transport of water masses from central California by the CC jet system. Although dissolved iron is likely at very high concentrations in river waters, nearly all iron is lost upon mixing with ocean water, both in estuaries and over the continental shelf (Boyle 1977; Chase et al. 2007). The dissolution of suspended sediment input by rivers, however, could increase dissolved iron concentrations in the surrounding ocean. Sediment plumes following discharge events in the sCCS have been observed to extend 10's of km in either the offshore or alongshore direction (e.g. Warrick et al. 2007). However, as discussed above, fluvial sediment input to the region is very episodic and patchy with the majority occurring after brief, intense winter storms (Table 4.5). The February 2003 CalCOFI and May 2006 CCE-LTER studies lagged about 1 month after high flow events. A potential signal from the Santa Clara River could have been at station 83.40.6 (station nearest the Santa Clara River outflow) during the February 2003 CalCOFI survey cruise where dissolved iron was ~5 nM. In comparison, station 83.40.6 was also sampled in July 2004 and had ~0.5 nM dissolved iron.

The transport and deposition of dust to this area from eolian sources have been documented to originate from western North America via Santa Ana winds (Muhs et al. 2007) and as far away as Asia (Tratt et al. 2001). Santa Ana winds occur when a high pressure cell develops over the Great Basin region (Nevada, Utah, Oregon, and

Idaho) and a relatively low pressure cell develops off southern California. The pressure gradient between the two regions results in strong north and northeast winds (up to 10 m/s, gusts to 35 m/s) over the Mojave Desert (central California), coastal southern California, and Baja California, Mexico. Santa Ana wind events typically occur several times per year, generally between fall and spring and peaking during winter (Raphael 2003). Wind events have been documented with remote-sensing satellites to transport large amounts of eolian material (and iron) up to 1000 km offshore (past the western edge of the study region) (Hu and Liu 2003). Like fluvial input, Santa Ana wind events are very episodic with few events per year and generally occur over timescales of days. As a side note, Santa Ana winds have also been shown to be coupled with transporting large amounts of wild fire-generated ash offshore (Westerling et al. 2004), which could also serve as a significant source of iron to the sCCS. A list of notable sustained offshore wind events from National Buoy Data Center station 46025 (Santa Monica Basin, near CalCOFI station 87.40) that occurred between January 2002 and December 2007 are listed in Table 4.5. Two wind events characteristic of Santa Ana winds occurred over a period between 5-13 February 2003, about a month prior to the March 2003 CalCOFI cruise, possibly explaining elevated dissolved iron concentrations along line 93 out to station 93.40 (~100 km offshore) where dissolved iron was >1.5 nM.

The equatorward transport of the CC jet system has been observed to range between 0.25 to 0.5 m s^{-1}, which could possibly result in advection of iron-rich waters from central or northern California. Source waters for the CC originate in the subarctic Pacific as a southeastward continuation of the subarctic frontal zone (Lynn

and Simpson 1987), and are generally found to be relatively low iron (Martin et al. 1989). The CC jet system could potentially be enriched by waters containing shelf-derived iron in coastal central and northern California by meanders of the CC close to the shelf or the offshore transport of shelf waters in eddies or filaments into the CC. The subsequent equatorward transport of these water masses might serve as a source of iron to the sCCS. There were, however, no indications of elevated dissolved iron concentrations in waters associated with the core of flow of the CC, reported to be 200-300 km offshore (Fig. 4.9; Lynn and Simpson 1987).

We are unable to quantitatively assess the relative contribution of fluvial input and atmospheric deposition to dissolved iron distributions between November 2002 and July 2004. Although episodic in nature, both fluvial input and atmospheric deposition could still serve as important sources of iron to the sCCS. Because both processes are temporally decoupled from coastal upwelling that occurs in the spring and summer, it appears that the major source of iron during this time period is from the continental shelf and BBL. Eolian deposition might be an important source of iron to the transition zone domain where wind stress curl upwelling has been found to occur year-round (Bakun and Nelson 1991).

4.5.4. Removal of iron by biological uptake: Lagrangian drifter studies

During Lagrangian drifter studies (1-3) in May 2006 and April 2007, dissolved iron concentrations decreased ~1 nM over 4 d (Table 4.3). Scavenging and biological uptake are the primary processes that could remove dissolved iron from seawater. In general, over 99.9% of dissolved iron in oceanic seawater is thought to be complexed

by organic ligands (Gledhill and Van de Berg 1994; Rue and Bruland 1995), counteracting the short lifetime of iron(II), low solubility of iron(III), and subsequent scavenging into the colloidal and particulate phases. The strong complexation of dissolved iron by organic ligands has been found to be consistent with dissolved iron concentrations as high as ~20 nM (K. Buck, pers. comm.). In the April 2007 Lagrangian drifter study 2, the concentration of iron-binding ligands was determined using competitive ligand exchange with cathodic stripping voltammetry. During the 4 d study, it was found that a strong ligand (L1 class) exceeded the concentration of dissolved iron at all depths (K. Buck, pers. comm.). In the same study, dissolved iron concentrations declined from 1.47 nM (t = 1 d) to 0.40 nM (t = 3.5 d) and finally 0.33 nM (t= 4.5 d) (Table 4.3). The excess of L1-class ligands at all depths suggests that the decline in dissolved iron was due to biological uptake.

The uptake of dissolved iron by phytoplankton has been found to vary based on species-specific iron requirement, ambient concentration of dissolved iron, and relative cell health status (Sunda and Huntsman 1995; Quigg et al. 2003). In what is termed luxury uptake, some phytoplankton maintain high iron uptake rates despite already achieving maximum growth rates (Sunda and Huntsman 1995). Using chl-based intrinsic growth rates (grazing-corrected with dilution experiments, M. Landry, pers. comm.), *in situ* POC:chl ratios, and a range of iron:carbon ratios (2-40; Sunda and Huntsman 1995), we calculated that with iron:carbon ratios ranging 15-40, it was plausible that phytoplankton accounted for the observed drawdown in dissolved iron in May 2006 and April 2007 drifter studies (Table 4.6). Rates of phytoplankton growth, zooplankton grazing, and carbon export at depth were found to be relatively

coupled (M. Landry, pers. comm.), indicating that grazing and subsequent sinking of fecal pellets might be a significant process for exporting iron out of the euphotic zone (also see Firme et al. 2003).

4.5.5. Decoupling between dissolved iron and nitrate in the mixed layer and phytoplankton iron limitation: CalCOFI surveys and drifter studies

In the mixed layer, on both regional and meso- scales, the decreasing gradient observed in nitrate was smaller relative to the decreasing gradient in dissolved iron (Fig. 4.9, Tables 4.2 and 4.3). That is, dissolved iron was presumably utilized by phytoplankton at a rate faster than nitrate. In Lagrangian drifter study 1 (May 2006), dissolved iron and nitrate were depleted at roughly the same rate (Table 4.3). However, in April 2007, dissolved iron was depleted faster than nitrate over distances of ~50 km on ~4 d timescales (Table 4.3). Dissolved iron was also observed to decrease faster than nitrate between stations 77.49 and 77.55 (~45 km) during April 2003 and 2004 CalCOFI. N:Fe ratios from drifter studies and CalCOFI April 2003 and 2004 line 77 ranged between ~14-40. Using shipboard iron addition bottle experiments in July 2003 and July 2004, phytoplankton were found to be iron stressed in the regions of nitrate:iron ratios ~6-12 (King and Barbeau 2007). Also, using iron addition bottle experiments in May 2006 and April 2007 drifter studies, phytoplankton were less iron-limited when N:Fe ratios were 5-9 (t=1d) and more severe iron limitation was observed in bottle experiments started at the end of the drifter studies when nitrate:iron ratios reached 14-26 (t=3.5-4.5 d) (Table 4.3). Nitrogen:iron quotas for a variety of phytoplankton at maximum growth rates have been estimated to range

from ~3-19 nM iron:16 μM nitrate (Bruland et al. 1991; Sunda and Huntsman 1995; Quigg et al. 2003), equivalent to a requirement of N:Fe at ratios of ~1-5.

Plasticity in community iron and nitrate requirements, such as luxury uptake of iron, could have resulted in a decoupling of iron and nitrate uptake. Also, low iron availability has been shown to indirectly rate-limit nitrate utilization (at the nitrite reduction step) due to the decreased supply of ferrdoxin/flavodoxin from the photosynthetic electron transport chain (Milligan and Harrison 2000). While it is reasonable to attribute the decrease in dissolved iron to biological uptake (see section 4.5.5), without experimentally-derived uptake rates we can only speculate as to why the rates of nitrate and dissolved iron removal were decoupled.

4.5.6. Iron limitation and decoupling between silicic acid and nitrate

There is evidence of enhanced silicic acid uptake relative to nitrate in spring and summer CalCOFI cruises. This can be demonstrated by calculating excess silicic acid with a formula modified from Gruber and Sarmiento (1997) using an estimated Si:N ratio from source waters of coastal upwelling and wind stress curl upwelling ($R_{Si:NO3}$):

$$Si_{ex} = \text{silicic acid}_{ML} - (\text{nitrate}_{ML} \times R_{Si:NO3}) \qquad (3)$$

where $R_{Si:NO3} = \sim 1.0$

For an estimate, we use a $R_{Si:NO3}$ value of 1, which is the approximate silicic acid:nitrate ratio from upwelling source waters. However, depending on the depth of

upwelling, $R_{Si:NO3}$ may been have been as low as 0.8 if upwelling was relatively shallow and as high as 1.2 if upwelling was relatively deep. Negative Si_{ex} values indicate preferential uptake by phytoplankton of silicic acid relative to nitrate (Fig. 4.13). During spring and summer and using $R_{Si:NO3} = 1$, excess silicic acid values ranged from -1 to -2.5 in the coastal upwelling and wind stress curl upwelling domains, indicating a 1 to 2.5 μM depletion in silicic acid relative to nitrate. With a sufficient supply of macronutrients and dissolved iron, the phytoplankton community in the coastal upwelling domain is typically dominated by diatoms (Venrick 1998, 2002). When healthy and under nutrient replete conditions, diatoms are expected to utilize silicic acid and nitrate in a 1:1 ratio (Brzezinski 1985). Upon iron stress, due to reduced nitrate utilization, diatoms tend to accumulate silicic acid at a much faster rate than nitrate (Hutchins and Bruland 1994). There was evidence of decreasing Si:N ratios in the sCCS in April 2003 and April 2004 at stations 77.49 to 77.55 (Table 4.2). Over-silicification by diatoms could also explain silicic acid concentrations <2 μM in the mixed layer at the border between the northern coastal and transition zone regimes in April 2003, April 2004 and July 2004 (Fig. 4.4, 4.5 and 4.7). The net result of iron limitation - both low dissolved iron and silicic acid - would further limit diatoms. Si_{ex} values were positive in the offshore and southern coastal domains in April 2003, July 2003, April 2004 and July 2004, and positive throughout the study area in November 2002 and February 2003 (data not shown).

A cursory analysis of archived CalCOFI data from 1985-2005 revealed Si_{ex} values <-1 were only found in 71 of >7000 stations sampled. About 28 of the 71 observations (~39%) were from April 2003 and 2004 and July 2003 and 2004.

Virtually all of the remaining observations were at nearshore stations in the northern coastal domain during spring and summer cruises. This observation is relatively consistent with the general lack of diatoms present outside of the northern coastal domain of the sCCS (Venrick 2002). A decrease in silicic acid relative to nitrate would require an appreciable abundance of diatoms. In contrast, there were over twice as many stations (~200) in which mixed layer silicic acid concentrations were > 4 μM (maximum was 11.4 μM) associated with low nitrate and low phosphate concentrations. These observations were similar to a station in the southern offshore domain during July 2003 (Fig. 4.5d), where silicic acid was high (~5 μM) yet both phosphate and nitrate were low. While some stations with high silicic acid from the archive analysis were in the offshore domain, many stations were nearshore in the coastal upwelling domain. In the relatively high silicic acid, low nitrate water masses identified above, it appears that diatoms were probably never present at high numbers. If diatoms were present with a sufficient supply of iron, both silicic acid and nitrate would be drawn down and Si_{ex} would be near zero. If diatoms were present and iron stressed, then silicic acid would be drawn down, a residual nitrate signal would remain, and Si_{ex} would be negative. In the relatively high silicic acid, low nitrate water masses identified above (positive Si_{ex}), it appears that diatoms were probably never present in high numbers. An explanation consistent with this observation is that iron could have been deficient enough in these upwelled water masses to prevent diatom growth, leaving other non-siliceous phytoplankton with low iron requirement to use phosphate and nitrate and leave silicic acid unused.

4.5.7. Decoupling between the ferricline and nitracline

Profiles in October 2006 and April 2007 showed a general agreement between the depth of the nitracline and the ferricline (data not shown; not conclusive at some stations with low sampling resolution). However, at some stations in July 2007, there was a decoupling of dissolved iron and nitrate gradients. Similar to the case for the mixed layer, phytoplankton were found to be iron-limited (data not shown) at the depth where N:Fe ratios were high, ranging 10-100 (Fig. 4.11). At various locations in the eastern North Pacific including the sCCS, Hopkinson and Barbeau (in press) found instances of iron-light co-limitation of phytoplankton in the SCM with nitrate:iron ratios as high as 35.

The vertical distributions of dissolved iron and nitrate are generally expected to both have a nutrient-type profile, with depletion in the euphotic zone due to biological utilization (and somewhat due to scavenging for iron) and concentrations increasing with depth due to remineralization below the euphotic zone. In July 2007, there were three stations in which the ferricline was found to be deeper than the nitracline (Fig. 4.11). Similar instances of decoupling between the nitracline and ferricline have been observed in the north equatorial Pacific (between 60-120 m), the south equatorial Pacific (100-250 m) (Johnson et al. 1997) and the southeastern subtropical Pacific (100-400+ m) in (Blain et al. 2008). Johnson et al. (1997) attribute the decoupling between the ferricline and nitracline to the subduction of high nitrate, low iron waters at high latitudes, lateral transport at depth, and subsequent upwelling in lower latitudes (meridional overturning). In addition to lateral transport of iron deficient waters,

Blain et al. (2008) attributes the decoupling to low biological utilization and remineralization and low atmospheric iron input.

Our observations were much closer to the coast and relatively shallower in comparison to the open ocean observations cited above. We do not think that the ferricline-nitracline decoupling we observed was the result of a laterally advected and upwelled high nitrate, low iron water mass in the sCCS. Contrary to the reduced biological utilization case of the ultra-oligotrophic subtropical Pacific, we hypothesize that the ferricline/nitracline decoupling we observed was the result of higher biological depletion of dissolved iron relative to nitrate, analogous to the offshore decoupling observed in the mixed layer. The biological depletion could be supported by the observation that the SCM's found at stations 93.40, 93.60 and 93.80 were maxima in phytoplankton biomass maxima, as opposed to fluorescence-only maxima as observed in the open ocean. Higher requirements for iron at SCM's with lower light availability may have also contributed to the ferricline/nitracline decoupling (Sunda and Huntsman 1997). Nitracline depths were near SCM peaks while ferricline depths were much closer to the depth of remineralization (as defined as <100% oxygen saturation) and the bottom of the euphotic zone (as indicated by chl) (Fig. 4.11). The presence of the nitracline above the depth of remineralization can be explained by the observation that phytoplankton were iron-limited and were unable to efficiently use nitrate as a source of nitrogen.

The following scenario could be an explanation for our observed decoupling of the ferricline and nitracline:

1) Assuming that the nitracline and ferricline were once coupled at depth, a mechanism for shoaling (such as wind stress curl upwelling) raises the nitracline and ferricline to a depth of higher light availability (whether into the euphotic zone or higher into the euphotic zone). Wind stress curl determined from a blended observation/satellite model (Zhang et al. 2006) from June 2007 and July 2007 indicated relatively large positive curl ranging 0.005-0.015 N m^{-2} (Rykaczewski and King, unpubl.).

2) Phytoplankton begin to grow and utilize both dissolved iron and nitrate and form a (larger) SCM.

3) Initially, both dissolved iron and nitrate are not limiting in the SCM, but relative removal (uptake) rate of iron is greater than nitrate (similar to nearshore-offshore observation of mixed layer iron and nitrate).

4) N:Fe ratios in the euphotic zone begin to climb, the ferricline begins to deepen relative to the nitracline, and iron stress reduces ambient Si:N ratios. (At the depth of decoupling, Si:N ratios were ~0.8 at stations 93.40 and 93.60).

5) The decoupling is at its maximum when dissolved iron is reduced to limiting concentrations (<0.2 nM) in the euphotic zone and increases below the depth of remineralization, while nitrate remains in the euphotic zone and is slowly utilized by iron-limited phytoplankton.

4.6. Conclusions

Dissolved iron distributions in the mixed layer were spatially coherent with the continental shelf. Maximum dissolved iron concentrations in the mixed layer were

spatially and temporally associated with coastal upwelling in spring and summer 2003 and 2004. While fluvial input and atmospheric deposition could provide for an episodic and patchy supply of iron, these events typically occur during winter time, out of phase with coastal upwelling. We believe that the continental shelf and BBL must account for a large portion of dissolved iron supplied to coastal upwelling water masses. In addition to coastal upwelling, nutrients are supplied to the offshore sCCS via wind stress curl, a dominant processes accounting for about two times more vertical transport that that of coastal upwelling. However, wind stress curl upwelling is far from a shelf source of dissolved iron (~50-250 km offshore) with small vertical velocities (1-2 m d^{-1}). Source waters are from a shallower depth where dissolved iron is already low.

In coastal upwelling and wind stress curl upwelling waters, the relative removal of nitrate, silicic acid, and dissolved iron by phytoplankton appears to vary. Both regional and mesoscale observations support that the decreasing offshore gradient in dissolved iron is greater than that of nitrate. Spatially-lagging the decreasing N:Fe pattern is the depletion of silicic acid relative to nitrate. There was also evidence of similar decoupling between nitrate, silicic acid, and iron at the depth, near the SCM. The decoupling between nitrate and iron in both the mixed layer and the SCM resulted in some instances of phytoplankton iron limitation. Our study supports conclusions from previous work that the availability of dissolved iron plays a critical role in regulating and varying offshore gradients in nitrate and silicic acid (Bruland et al. 2001; Firme et al. 2003). The resulting alteration to the ambient

nutrient field subsequently influences the succession of phytoplankton community structure.

For the most part, the sCCS is a mesotrophic regime - an intermediate between low new production and high new production (Behrenfeld and Falkowski 1997). Our study indicates that this is the result of moderate supply nitrate to surface waters via upwelling (coastal upwelling nearshore and wind stress curl upwelling offshore) and, in part, the apparent extension of the distribution of nitrate, both horizontally and vertically, due low iron availability. This is especially relevant to the expansive transition zone domain where both aged coastal upwelling waters and wind stress curl upwelling waters are high in macronutrients relative to dissolved iron. In comparison to short-lived, boom-and-bust coastal phytoplankton blooms in the northern nearshore sCCS, phytoplankton new production in the offshore sCCS would continue at moderate rates over longer periods of time with potentially important bottom-up effects on the pelagic ecosystem.

4.7. Acknowledgements

We thank B. Hopkinson, J. Nunnery, S. Reynolds, K. Roe, K. Buck, J. Leblond, the CalCOFI and LTER research groups, especially R. Goericke, J. Wilkinson, D. Wolgast, M. Landry and the officers and crew of the R/V New Horizon, David Starr Jordan, Revelle, Thompson, and Knorr, for assistance in collecting and analyzing data. This research was funded by NASA NIP grant NAG5-12535 and LTER NSF/OCE-0417616.

This chapter is in preparation for publication as: King, Andrew L., and Katherine A. Barbeau. Iron distribution in the southern California Current System and relation to macronutrients and phytoplankton.

Table 4.1. Hydrographic domains based on mixed-layer observations during October 2002, February 2003, April 2003, July 2003, April 2004, and July 2004 CalCOFI cruises, 1984-2005 CalCOFI mixed-layer means, and previous work by Lynn and Simpson (1987) and Hayward and Venrick (1998). Parameters include temperature (temp), salinity (sal), density, macronutrients (nuts), iron and phytoplankton (chl).

domain	temp	sal	density	nuts	chl	iron
northern coastal	cold	salty	high	high	high	high
transition zone	cool	mid	mid	med	low	low
southern coastal	hot	salty	low	low	low	med
offshore	warm	fresh	low	low	low	low

Table 4.2. Temperature (temp, °C), salinity (sal, psu), density (sigma-theta), chlorophyll a (chl, µg L^{-1}), phosphate (phos, µM), nitrate (µM), silicic acid (sil, µM), dissolved iron (dFe, nM), nitrate:dissolved iron ratio (N:Fe), and excess silicic acid (Si_{ex}) as calculated by eq. 3 for stations 77.49, 77.51, and 77.55 in April 2003 and April 2004 CalCOFI survey cruises. Percent decrease in phosphate, nitrate, silicic acid, and dissolved iron area also shown.

April 2003	temp	sal	density	chl	phos	nitrate	sil	dFe	N:Fe	Si_{ex}
77.49	11.25	33.73	25.75	6.18	1.15	10.7	9.2	3.47	3.1	-0.4
77.51	11.39	33.54	25.57	9.06	0.92	9.3	7.4	0.28	33.2	-1.0
77.55	11.99	33.16	25.17	3.43	0.79	6.4	3.7	0.16	40.0	-2.1
				% change	-31%	-40%	-60%	-95%		

April 2004	temp	sal	density	chl	phos	nitrate	sil	dFe	N:Fe	Si_{ex}
77.49	10.62	33.63	25.77	9.17	1.33	15.3	15.7	1.90	8.1	0.4
77.51	10.78	33.49	25.64	9.01	1.22	14	12.8	0.38	36.8	-1.2
77.55	11.95	33.24	25.23	0.15	0.79	7.5	5.1	0.32	23.4	-2.4
				% change	-41%	-51%	-68%	-83%		

Table 4.3. Temperature (temp, °C), salinity (sal, psu), density (sigma-theta), chlorophyll a (chl, µg L^{-1}), phosphate (phos, µM), nitrate (µM), silicic acid (sil, µM), dissolved iron (dFe, nM), nitrate:dissolved iron ratio (N:Fe), and excess silicic acid (Si_{ex}) as calculated by eq. 3 for Lagrangian drifter studies 1, 2, and 3 during May 2006 and April 2007 CCE-LTER process cruises. Percent decrease in phosphate, nitrate, silicic acid, and dissolved iron area also shown.

May 2005 drifter 1	temp	sal	density	chl	phos	nitrate	sil	dFe	N:Fe	Si_{ex}
t=1 d	11.31	33.64	25.69	2.76	1.1	13.6	15.8	2.00	6.8	3.5
t=4 d	12.30	33.59	25.46	6.24	0.6	6.5	10.2	1.10	5.9	4.4
				% change	-46%	-52%	-35%	-45%		

April 2007 drifter 2	temp	sal	density	chl	phos	nitrate	sil	dFe	N:Fe	Si_{ex}
t=1 d	12.19	33.60	25.49	2.18	0.7	7.6	10.2	1.47	5.2	3.4
t=4.5 d	12.49	33.47	25.34	1.21	0.5	4.7	5.9	0.33	14.2	1.7
				% change	-28%	-38%	-42%	-78%		

April 2007 drifter 3	temp	sal	density	chl	phos	nitrate	sil	dFe	N:Fe	Si_{ex}
t=1 d	11.80	33.70	25.64	1.04	0.9	11.12	14.3	1.28	8.7	4.3
t=4 d	12.50	33.44	25.32	0.68	0.5	4.4	5.4	0.17	25.9	1.4
				% change	-46%	-60%	-62%	-87%		

Table 4.4. Depth in meters of ferricline, nitracline, chlorophyll maximum (chl max), depth of furthest extent of chlorophyll (chl deep), and depth of remineralization as indicate by <100% O_2 saturation (remin) from July 2007 DCM cruise stations 93.40, 93.60, and 93.80.

station	ferricline	nitracline	chl max	chl deep	remin
93.40	70-100	30	36	72	53
93.60	75-100	20	18	100	81
93.80	75-100	65	67	124	118

Table 4.5. Dates of high flow events (>500 m^3 s^{-1}) from upstream gauges for the Santa Ynez River (United States Geological Survey station 11133000, near Lompoc, CA) and Santa Clara River (United States Geological Survey station 11109000, near Piru, CA). Also listed are dates of >5 m s^{-1} winds sustained for 2 days or more at National Data Buoy Center station 46025, Santa Monica Basin, ~60 km west southwest of Santa Monica, CA.

* denotes Santa Clara River flow event and Santa Ana wind events preceded March 2003 CalCOFI cruise by ~1 month. ** denotes Santa Clara River flow event preceded May 2006 CCE-LTER cruise by ~1 month.

Santa Ynez River	Santa Clara River	Santa Ana winds
	from August 2002	
20 December	none	none
	2003	
15 March	12 February*	6-7 January
		5-8 February*
		11-13 February*
	2004	
25 February	26 February	4-5 January
28-31 December	8-29 December	20-21 November
		3-4 December
	2005	
25 January	7-13 January	11-12 February
16 February-22 March	18 February-8 March	
	2006	
2 January	2 January	23-24 January
4-7 April	27-28 February	29-30 November
	28 March	18-19 December
	4-5 April**	
	through August 2007	
none	none	13-18 January
		21-22 September

Table 4.6. Estimated biological uptake of dissolved iron from May 2006 and April 2007 drifter studies. The following parameters are listed: initial dissolved iron (Fe_{init}) and after t = 4 or 4.5 d (Fe_{final}), chl mean specific growth rate (μ) over the 4 day study as determined by dilution experiments (M. Landry, pers. comm.), initial chl (chl_{init}) and expected chl (chl_{exp}) based on a natural log growth equation with μ, mean μg C:μg chl ratio over the 4 day study based on POC, expected μg C based on C:chl ratio (C_{exp}), and nM iron drawdown based on nM Fe:μM C (Fe:C) ratios from 10-40 (Sunda and Huntsman 1995; Quigg et al. 2003). Values in bold indicate the closest match to observed drawdown (Fe_{init} - Fe_{final}). Calculations predict phytoplankton Fe:C ratios to range between 15-40.

								Fe:C				
								10	15	20	30	40
	Fe_{init}	Fe_{final}	μ	chl_{init}	chl_{exp}	C:chl	C_{exp}	nM Fe drawdown				
May 2006 drifter 1	2	1.1	0.51	3.1	11.0	64	702	0.5	0.8	**1.1**	1.6	2.2
April 2007 drifter 2	1.47	0.33	0.65	2.2	13.0	82	1061	0.9	**1.2**	1.6	2.5	3.3
April 2007 drifter 3	1.28	0.17	0.5	1.1	3.7	93	347	0.3	0.4	0.5	0.8	**1.1**

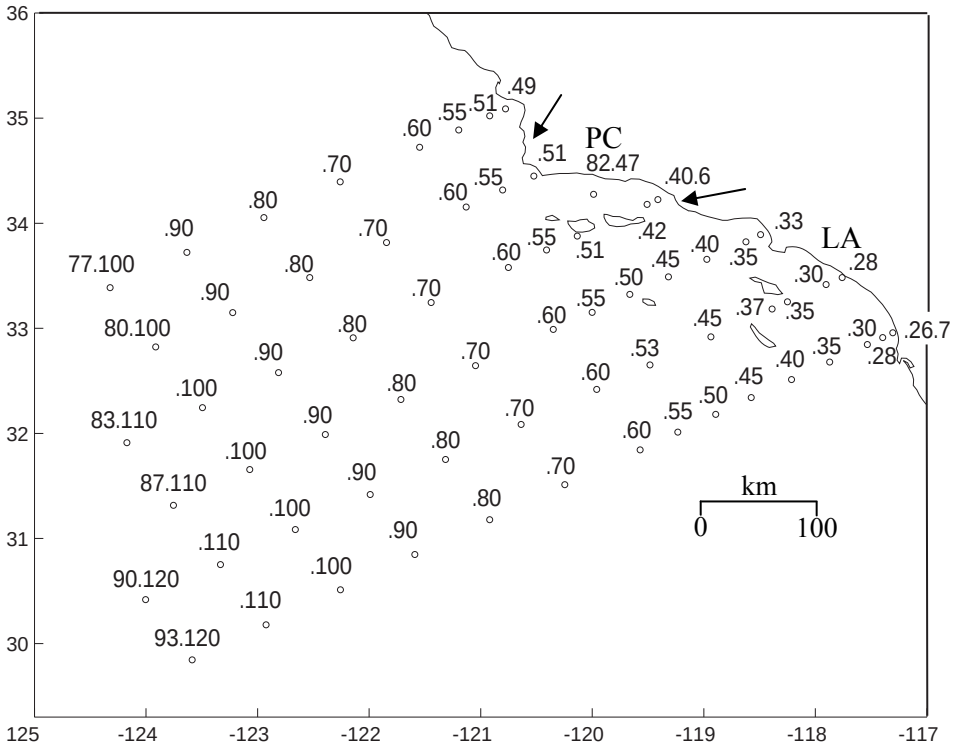

Figure 4.1. A map of the sCCS with 66 standard CalCOFI stations. For geographic reference, Point Conception (PC) and Los Angeles (LA), CA are labeled. Line numbers are designated to the left of decimal point and station numbers are to the right, i.e. 90.53 = line 90, station 53. The locations the Santa Ynez River (arrow north of Point Conception) and Santa Clara River (arrow between Point Conception and Los Angeles) are marked.

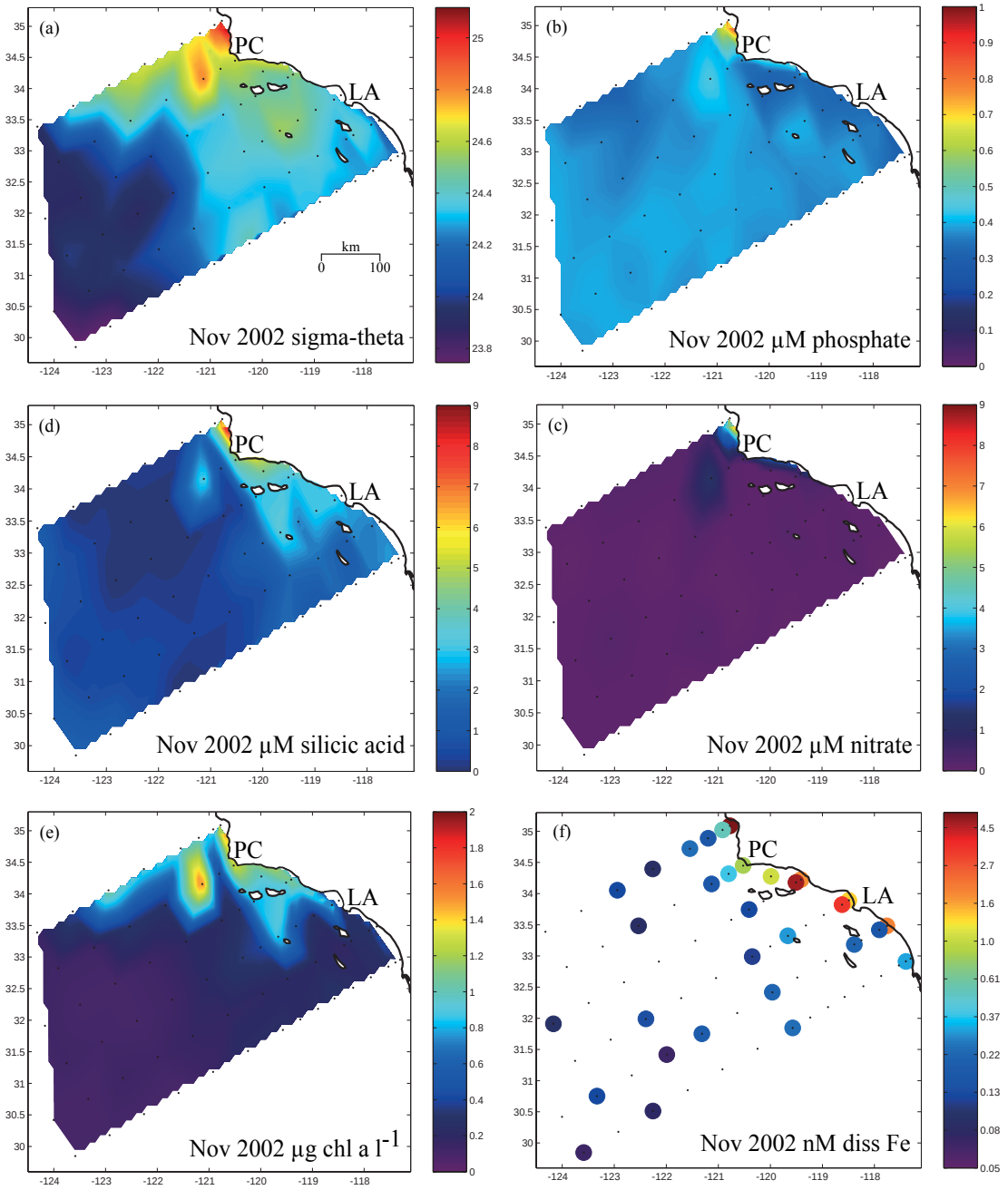

Figure 4.2. (a-e) Synoptic views of density (sigma-theta), phosphate (µM), nitrate (µM), silicic acid (µM), chlorophyll a (µg L^{-1}), and dissolved iron (nM) from surface waters during November 2002 CalCOFI cruise. Data were interpolated between stations marked with black dots. For geographic reference, Point Conception (PC) and Los Angeles (LA), CA are labeled in each panel.

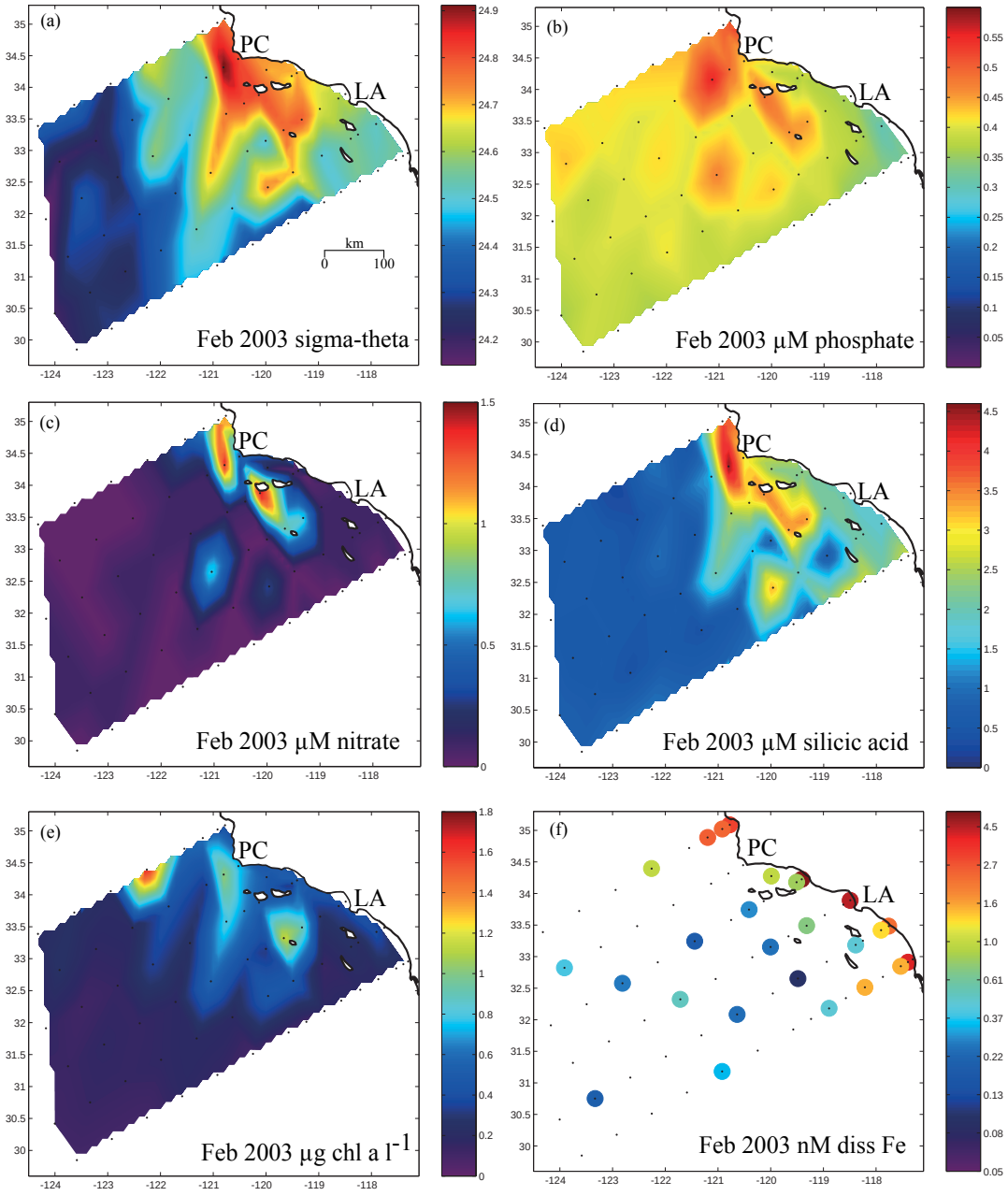

Figure 4.3. (a-e) Synoptic views of density (sigma-theta), phosphate (µM), nitrate (µM), silicic acid (µM), chlorophyll a (µg L^{-1}), and dissolved iron (nM) from surface waters during February 2003 CalCOFI cruise. Data were interpolated between stations marked with black dots. For geographic reference, Point Conception (PC) and Los Angeles (LA), CA are labeled in each panel.

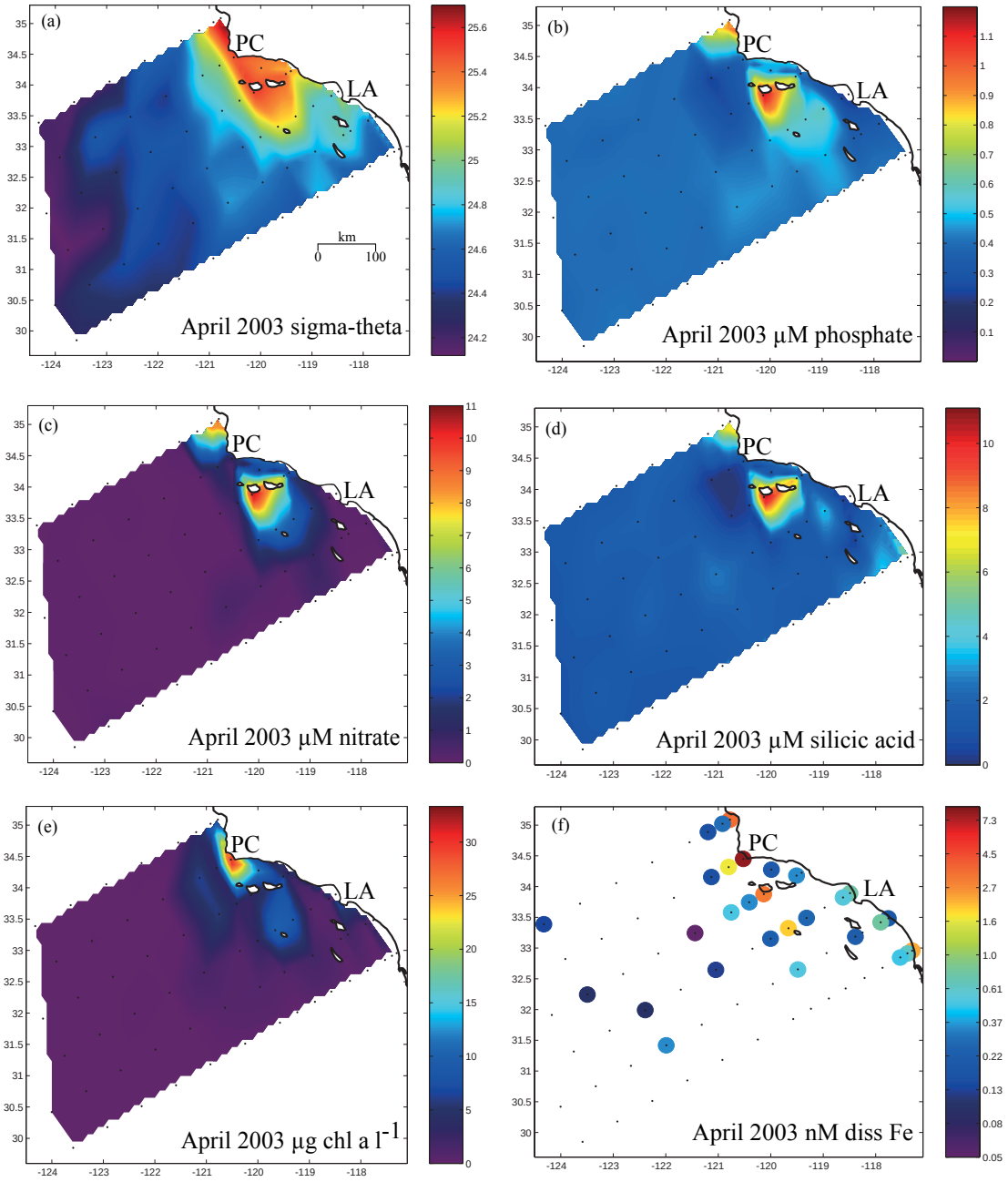

Figure 4.4. (a-e) Synoptic views of density (sigma-theta), phosphate (µM), nitrate (µM), silicic acid (µM), chlorophyll a (µg L^{-1}), and dissolved iron (nM) from surface waters during April 2003 CalCOFI cruise. Data were interpolated between stations marked with black dots. For geographic reference, Point Conception (PC) and Los Angeles (LA), CA are labeled in each panel.

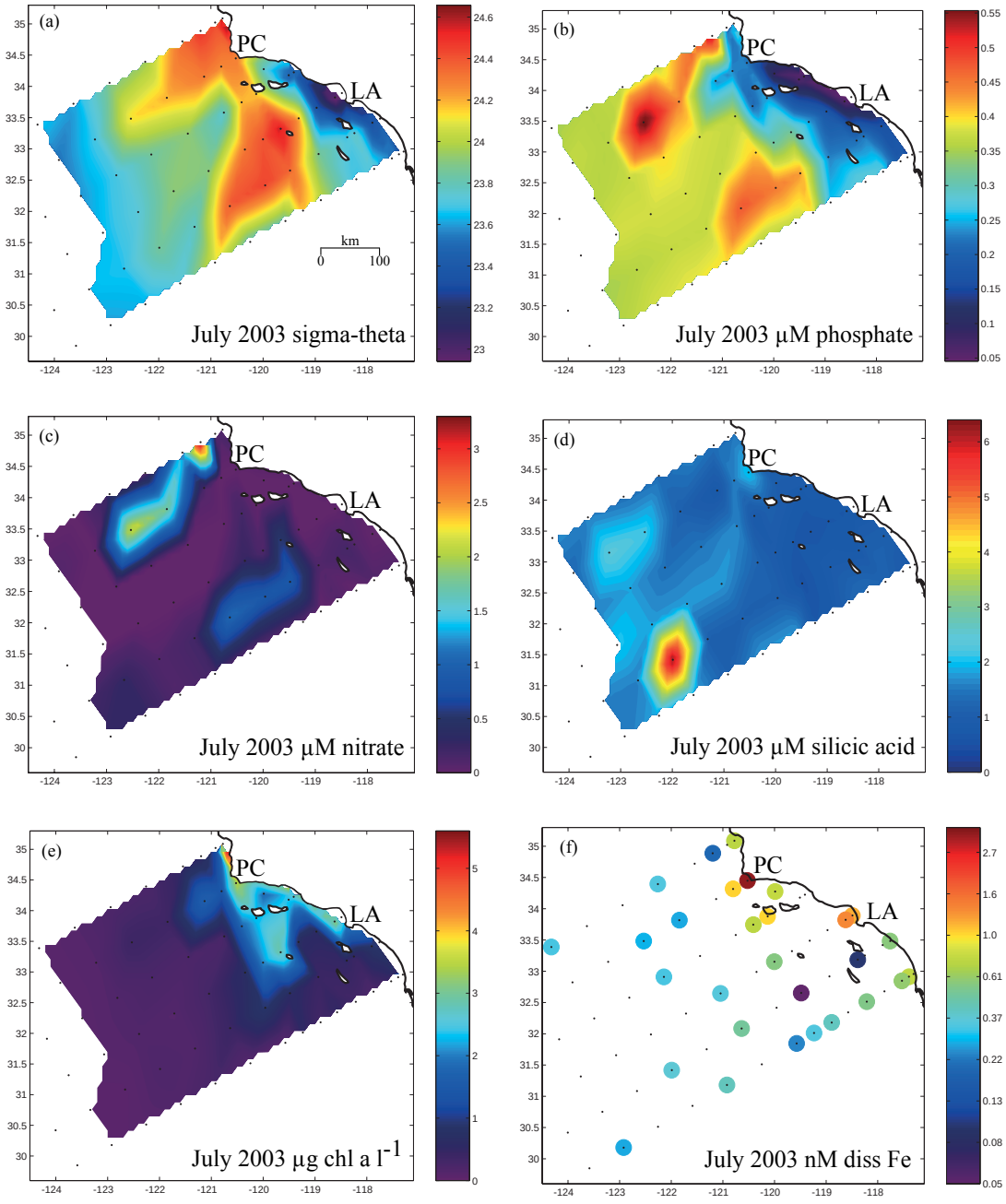

Figure 4.5. (a-e) Synoptic views of density (sigma-theta), phosphate (µM), nitrate (µM), silicic acid (µM), chlorophyll a (µg L^{-1}), and dissolved iron (nM) from surface waters during July 2003 CalCOFI cruise. Data were interpolated between stations marked with black dots. For geographic reference, Point Conception (PC) and Los Angeles (LA), CA are labeled in each panel.

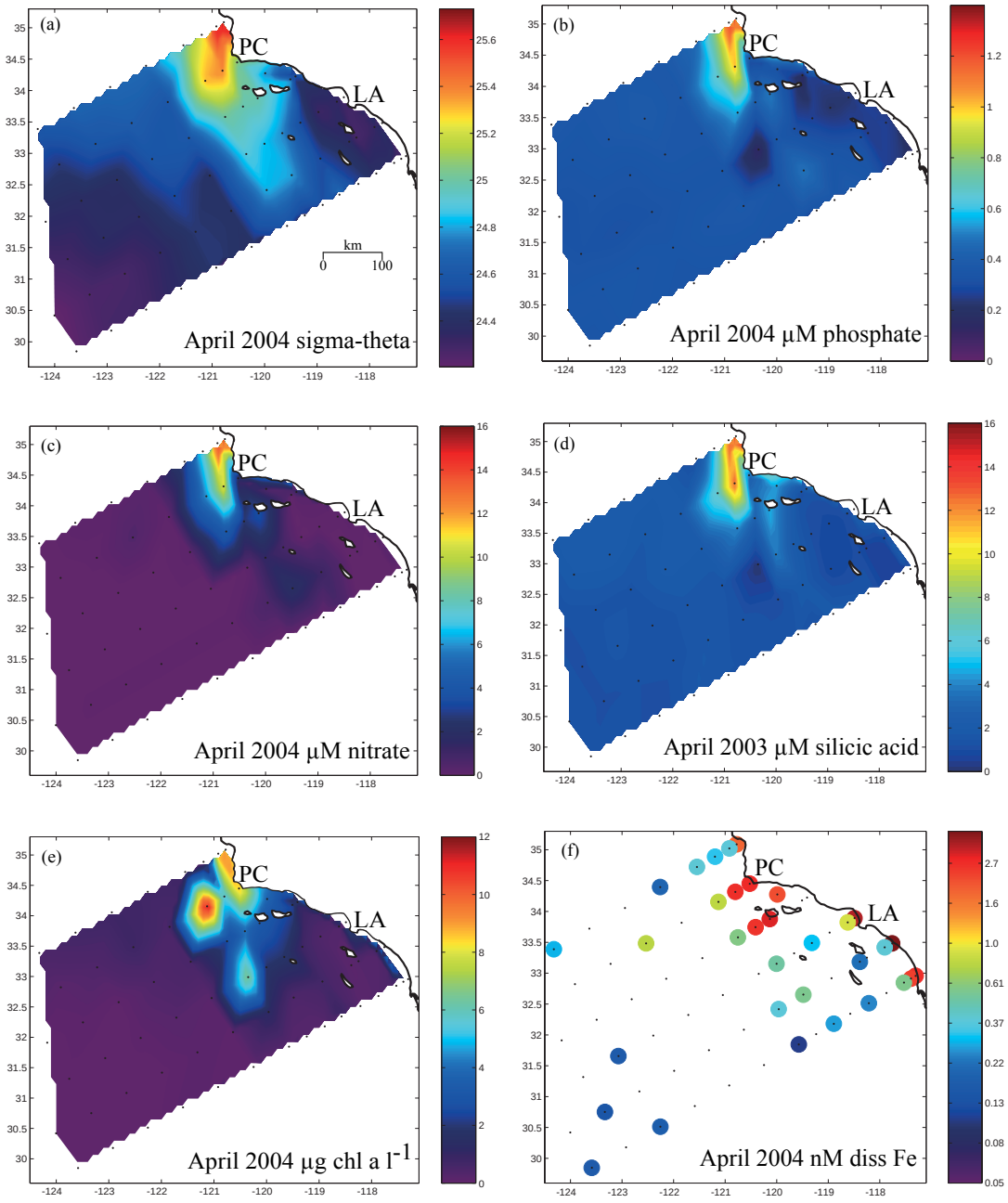

Figure 4.6. (a-e) Synoptic views of density (sigma-theta), phosphate (µM), nitrate (µM), silicic acid (µM), chlorophyll a (µg L^{-1}), and dissolved iron (nM) from surface waters during April 2004 CalCOFI cruise. Data were interpolated between stations marked with black dots. For geographic reference, Point Conception (PC) and Los Angeles (LA), CA are labeled in each panel.

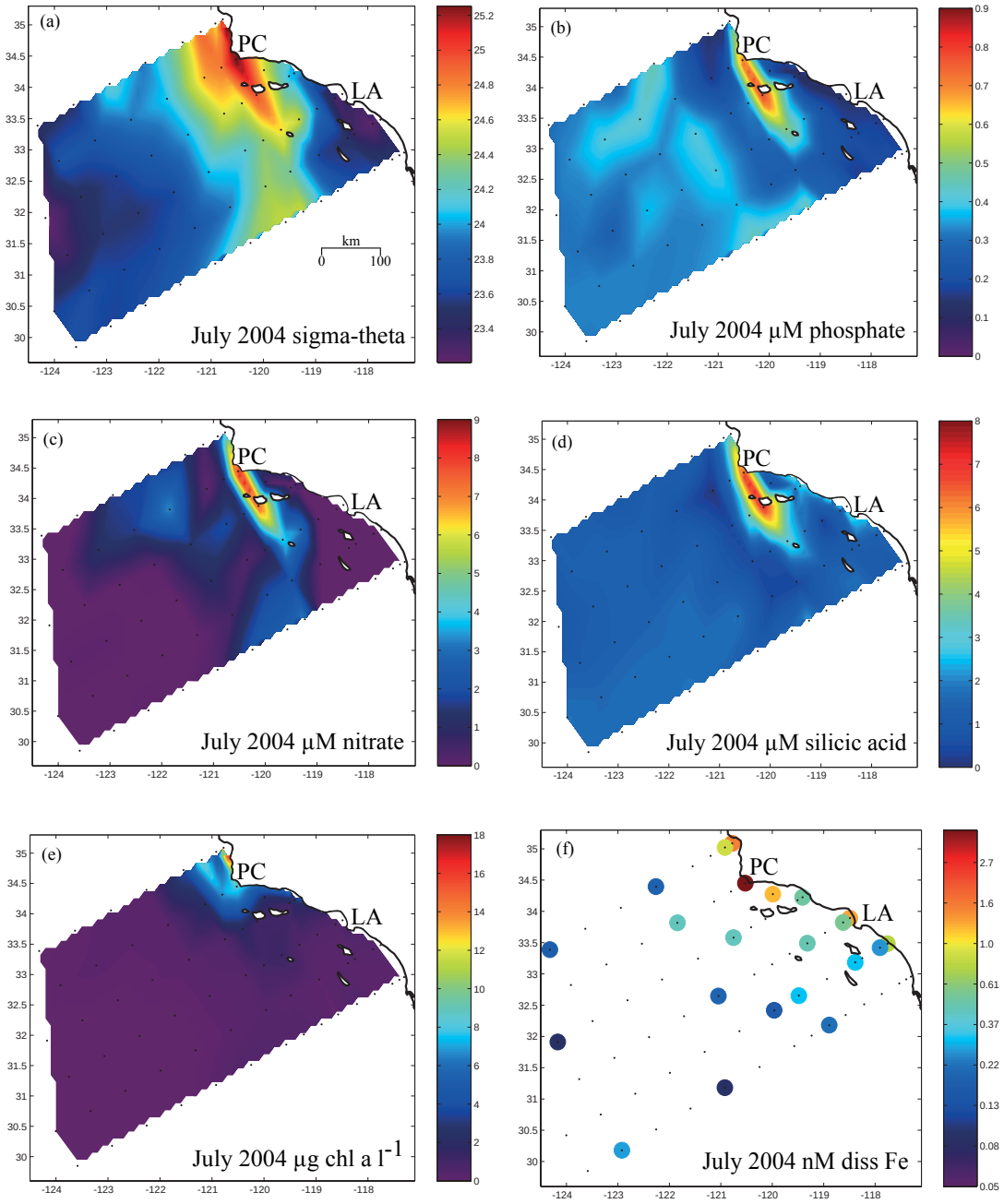

Figure 4.7. (a-e) Synoptic views of density (sigma-theta), phosphate (µM), nitrate (µM), silicic acid (µM), chlorophyll a (µg L^{-1}), and dissolved iron (nM) from surface waters during July 2004 CalCOFI cruise. Data were interpolated between stations marked with black dots. For geographic reference, Point Conception (PC) and Los Angeles (LA), CA are labeled in each panel.

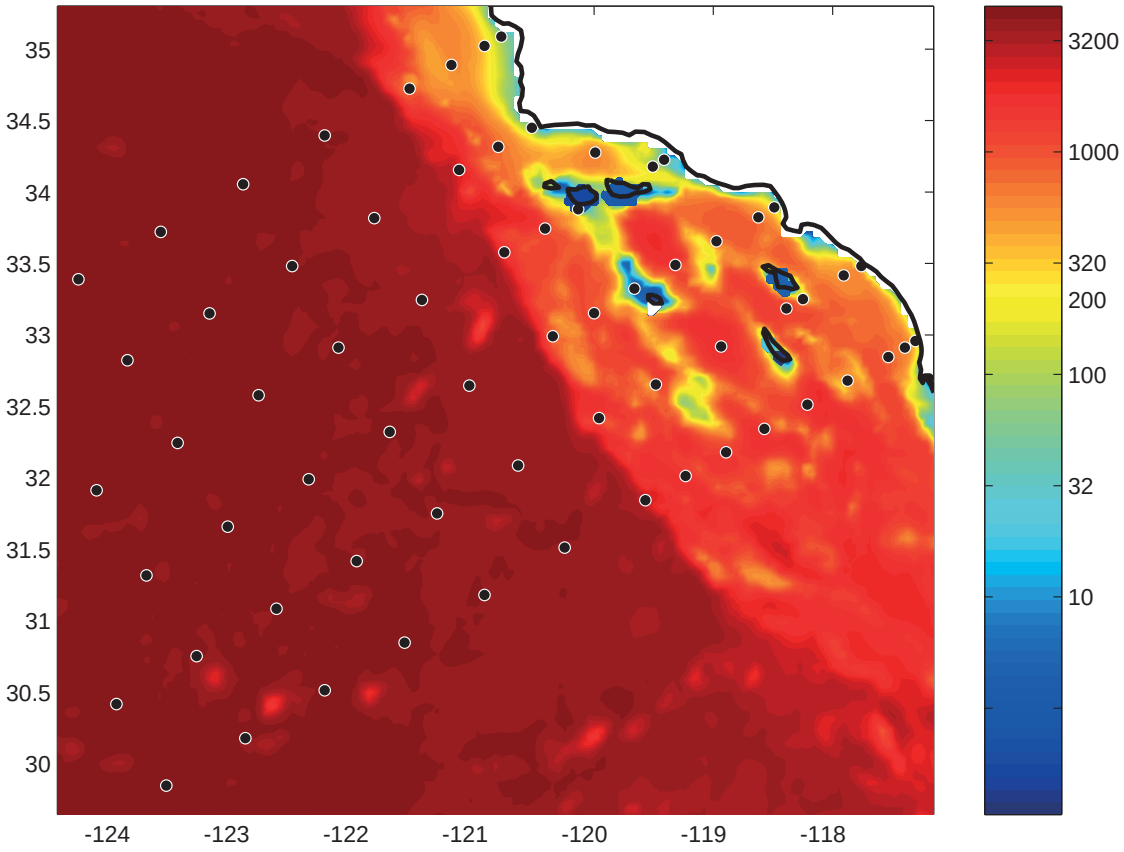

Figure 4.8. sCCS bathymetry in meters (ln scale). The continental shelf (as defined by the ~200m isobath) is bounded by the yellow contour. The locations of CalCOFI stations are overlaid. Cortez and Tanner Banks are at approximately 32.5 °N, 119 °W.

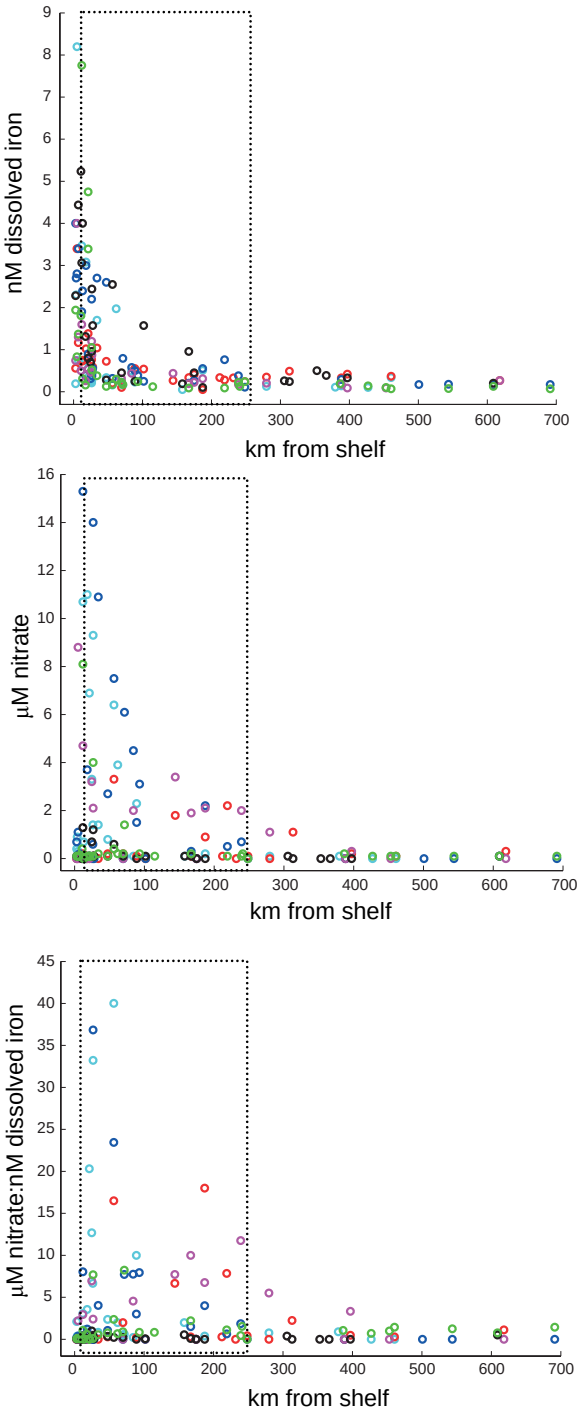

Figure 4.9. Dissolved iron, nitrate, and nitrate:dissolved iron ratio versus km offshore and for November 2002 (green), February 2003 (black), April 2003 (cyan), July 2003 (red), April 2004 (blue), and July 2004 (magenta). Dotted black box denotes the range of the transition zone for spring (~10-50 km) and summer (~50-250 km).

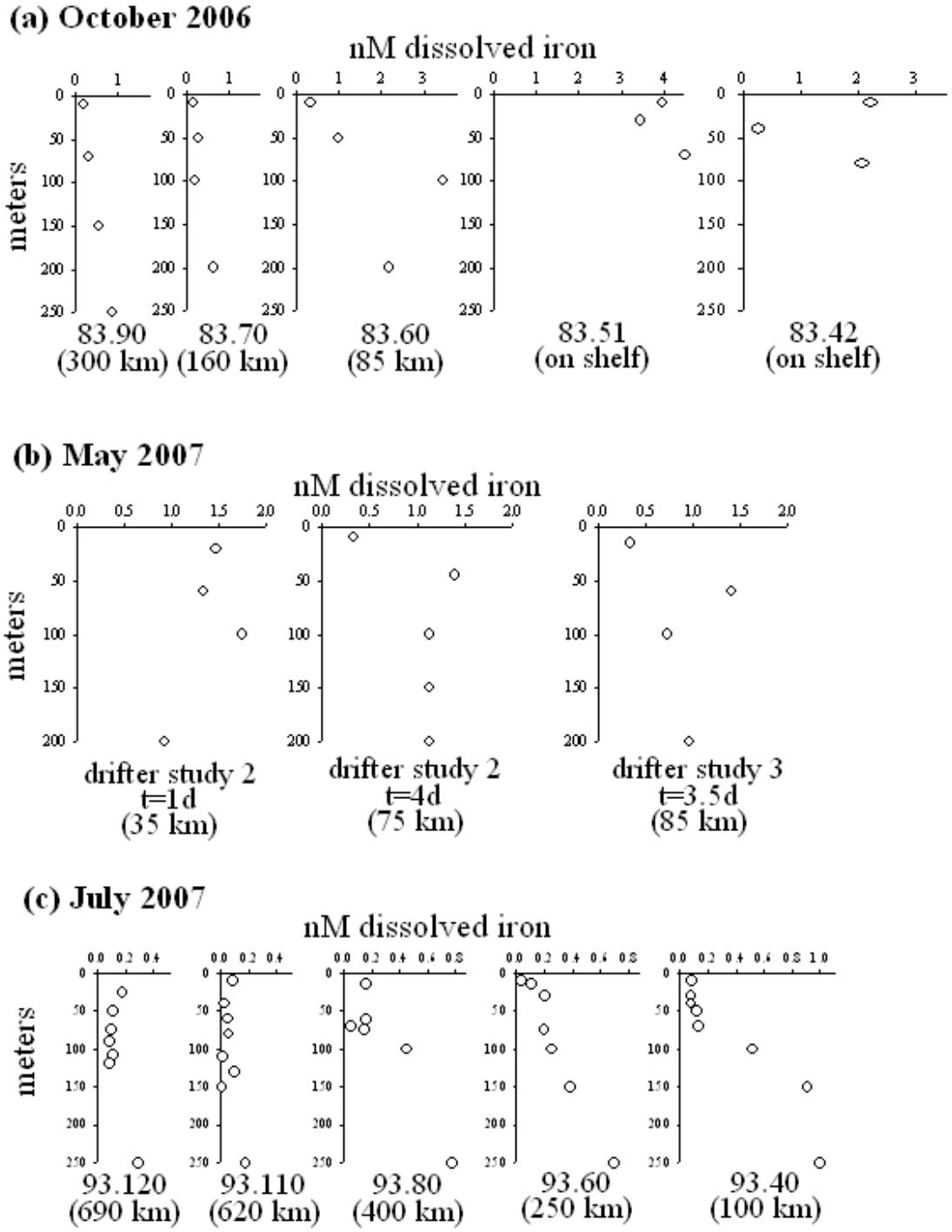

Figure 4.10. Dissolved iron profiles from (a) October 2006 CalCOFI cruise, (b) April 07 CCE-LTER cruise, and (c) July 2007 DCM cruise. Each profile is labeled with corresponding study/station number and approximate distance from the continental shelf.

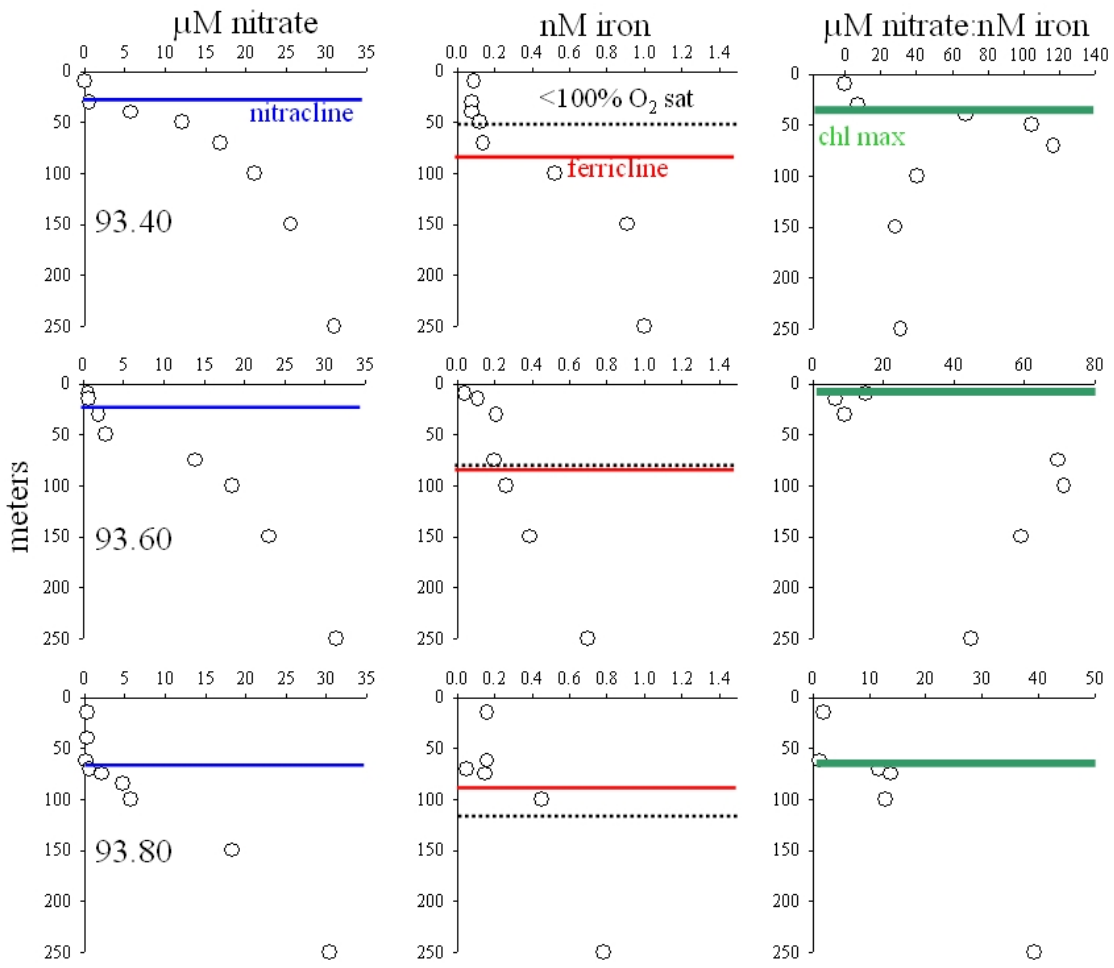

Figure 4.11. Dissolved iron, nitrate, and nitrate:dissolved iron ratio profiles from July 2007 DCM cruise stations 93.40 (top 3 panels), 93.60 (middle 3 panels), and 93.80 (bottom 3 panels). The approximate depth of the nitracline (>1 µM nitrate) is labeled with a blue line, the depth of the ferricline (>0.2 nM) is labeled with a red line, the depth of <100 O_2 saturation is labeled with a dotted black line, and the chlorophyll maximum is labeled with a green line.

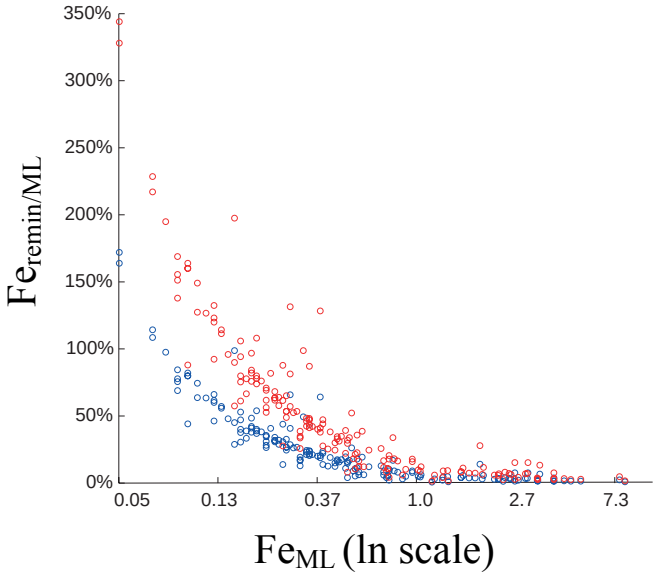

Figure 4.12. Observed dissolved iron (ln scale) in the mixed layer during November 2002-July 2004 CalCOFI cruises (Fe_{ML}) versus % contributed from remineralized deep source ($Fe_{remin/ML}$) as calculated by eq. 2. Blue circles represent $R_{Fe:PO4} = 0.2$ and red circles represent $R_{Fe:PO4} = 0.4$.

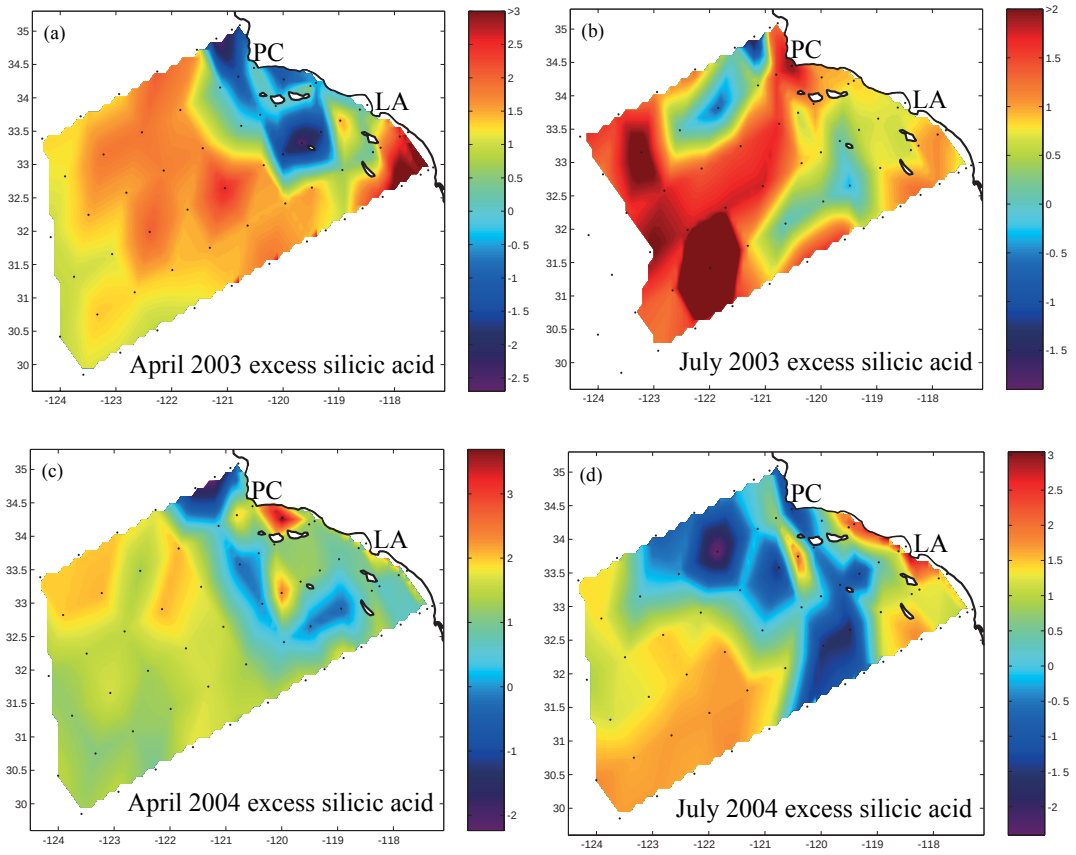

Figure 4.13. (a-d) Synoptic views Si_{ex} calculated using eq. 3 and $R_{Si:NO3} = 1$ in April 2003, July 2003, April 2004, and July 2004 CalCOFI cruises. Data were interpolated between stations marked with black dots. For geographic reference, Point Conception (PC) and Los Angeles (LA), CA are labeled in each panel. For viewing clarity, Si_{ex} values 3-6 for April 2003 and 2-6.3 for July 2003 were binned into the magenta contour and listed as >3 and >2, respectively.

4.8. Literature cited

Bakun, A., and C.S. Nelson. 1991. The seasonal cycle of wind-stress curl in subtropical eastern boundary current regions. J. Phys. Oceanogr. 21:1815-1834.

Behrenfeld, M.J., and P.G. Falkowski. 1997. Photosynthetic rates derived from satellite based chlorophyll concentration. Limnol. Oceanogr. 42:1-20.

Blain, S., S. Bonnet, and C. Guieu. 2008. Dissolved iron distribution in the tropical and sub tropical South Eastern Pacific. Biogeosciences 5:269-280.

Bowie, A.R., E.P. Achterberg, R. Fauzi, C. Mantoura, and P.J. Worsfold. 1998. Determination of sub-nanomolar levels of iron in seawater using flow injection with chemiluminescence detection. Anal. Chim. Acta 361:189-200.

Boyle, E.A., J.M. Edmond, and E.R. Sholkovitz. 1977. Mechanism of iron removal in estuaries. Geochim. Cosmochim. Acta 41:1313-1324.

Boyle, E.A., A.S. Huested, and S.P. Jones.1981. On the distribution of copper, nickel, and cadmium in the surface waters of the North Atlantic and North Pacific Ocean. J. Geophys. Res. 86:8084-8066.

Bruland, K.W., J.R. Donat, and D.A. Hutchins. 1991. Interactive influences of bioactive trace metals on biological production in oceanic waters. Limnol. Oceanogr. 36:155-1577.

Bruland, K.W., E.L. Rue, and G.J. Smith. 2001. Iron and macronutrients in California coastal upwelling regimes: Implications for diatom blooms. Limnol. Oceangr. 46:1661-1674.

Brzezinski, M.A. 1985. The Si:C:N ratio of marine diatoms: interspecific variability and the effect of some environmental variables. J. Phycol. 21:347–357.

Chase, Z., A. van Geen, P.M. Kosro, J. Marra, and P.A. Wheeler. 2002. Iron, nutrient, and phytoplankton distributions in Oregon coastal waters. J. Geophys. Res. 107, doi:10.1029/2001JC000987.

Chase, Z., P.G. Strutton, and B. Hales. 2007. Iron links river runoff and shelf width to phytoplankton biomass along the U.S. West Coast. Geophys. Res. Lett. 34, L04607, doi:10.1029/2006GL028069.

Chhak, K., and E. Di Lorenzo. 2007. Decadal variations in California Current upwelling cells. Geophys. Res. Lett. 34, L14604, doi:10.1029/2007GL030203.

Chelton, D.B. 1982. Large-scale response of the California Current to forcing by the wind stress curl. Calif. Coop. Ocean. Fish. Invest. Rep. 23:130-148.

Di Lorenzo, E. 2003. Seasonal dynamics of the surface circulation in the Southern California Current System. Deep Sea Res., Part II 50:2371-2388.

Elrod, V.A., W.M. Berelson, K.H. Coale, K.S. Johnson. 2004. The flux of iron from continental shelf sediments: A missing source for global budgets. Geophys. Res. Lett. 31, L12307, doi:10.1029/2004GL020216.

Eppley, R.W., and O. Holm-Hansen. 1986. Primary production in the Southern California Bight, pp. 176-215. In: Eppley RW (ed) Plankton Dynamics of the Southern California Bight. Lecture Notes on Coastal and Estuarine Studies, 15. Springer-Verlag.

Eppley, R.W., E.H. Renger, and W.G. Harrison. 1979. Nitrate and phytoplankton production in Southern California coastal waters. Limnol. Oceangr. 24:483-494.

Firme, G.F., E.L. Rue, D.A. Weeks, K.W. Bruland, and D.A. Hutchins. 2003. Spatial and temporal variability in phytoplankton iron limitation along the California coast and consequences for Si, N, and C biogeochemistry. Global Biogeochem. Cycles 17:10.1029/2001GB001824.

Fitzwater, S.E., K.S. Johnson, V.A. Elrod, J.P. Ryan, L.J. Coletti, S.J. Tanner, R.M. Gordon, and F.P. Chavez. 2003. Iron, nutrient and phytoplankton biomass relationships in upwelled waters of the California coastal system. Cont. Shelf Res. 23:1523-1544.

Gledhill, M., and C.M.G. Van den Berg. 1994. Determination of iron(III) with natural organic complexing ligands in seawater using cathodic stripping voltammetry. Mar. Chem.47:41-54.

Gruber, N., and J.L. Sarmiento. 1997. Global patterns of marine nitrogen fixation and denitrification. Global Biogeochem. Cycles 11:235-266.

Hu, H., and W.T. Liu. 2003. Oceanic thermal and biological responses to Santa Ana winds. Geophys. Res. Lett. 30:1596, doi:10.1029/2003GL017208.

Hutchins, D.A., and K.W. Bruland. 1998. Iron-limited diatom growth and Si:N uptake ratios in a coastal upwelling regime. Nature 393:561-564.

Hutchins, D.A., G.R. DiTullio, Y. Zhang, and K.W. Bruland. 1998. An iron limitation mosaic in the California upwelling regime. Limnol. Oceangr. 43:1037-1054.

Hutchins, D.A., C.E. Hare, R.S. Weaver, Y. Zhang, G.F. Firme, G.R. DiTullio, M.B. Alm, S.F. Riseman, J.M. Maucher, M.E. Geesey, C.G. Trick, G.J. Smith, E.L. Rue, J. Conn, and K.W. Bruland. 2002. Phytoplankton iron limitation in the Humboldt Current and Peru Upwelling. Limnol. Oceangr. 47:997-1011.

Inman, D.L., and S.A. Jenkins. 1999. Climate change and the episodicity of sediment flux of small California rivers. J. Geol. 107:251-270.

Johnson, K.S., R.M. Gordon, and K.H. Coale. 1997. What controls dissolved iron concentrations in the world ocean? Authors' closing comments. Mar. Chem. 57:181-186.

Johnson, K.S., F.P. Chavez, and G.E. Friederich GE. 1999. Continental-shelf sediment as a primary source of iron for coastal phytoplankton. Nature 398:697-700.

Johnson, K.S., F.P. Chavez, V.A. Elrod, S.E. Fitzwater, J.T. Pennington, K.R. Buck, P.M. Waltz. 2001. The annual cycle of iron and the biological response in the central California coastal waters. Geophys. Res. Lett. 28:1247-1250.

Jones, B.H., K.H. Brink, R.C. Dugdale, D.W. Stuart, J.C. Vanleer, D. Blasco, and J.C. Kelley. 1983. Observations of a persistent upwelling center off Point Conception, California, Part A, pp. 37-60. In: Suess E, Thiede J (eds), Coastal Upwelling, Its Sediment Record. Plenum.

King, A.L., and K.A. Barbeau. 2007. Evidence for phytoplankton iron limitation in the southern California Current System. Mar. Ecol. Prog. Ser. 342:91-103.

Lynn, R.J., J.J. Simpson. 1987. The California Current System: the seasonal variability of its physical characteristics. J. Geophys. Res. 92 C12:12947-12966.

Martin, J.H., M.R. Gordon, S. Fitzwater, and W.W. Broenkow. 1989. VERTEX: phytoplankton/iron studies in the Gulf of Alaska. Deep-Sea Res. 36:649-680.

Milligan, A.J., and P.J. Harrison. 2000. Effects of non-steady-state iron limitation on nitrogen assimilatory enzymes in the marine diatom Thalassiosira weissflogii (Bacillariophyceae). J. Phycol. 36:78-86.

Muhs, D.R., J. Budahn, M. Reheis, J. Beann, G. Skipp, and E. Fisher. 2007. Airborne dust transport to the eastern Pacific Ocean off southern California: Evidence from San Clemente Island. J. Geophys. Res.112:D13202, doi:10.1029/2006JD007577

Nelson, C.S. 1977. Wind stress and wind stress curl over the California Current. NOAA Tech. Rep. NMFS-SSRF-714.

Powell, R.T., D.W. King, and W.M. Landing. 1995. Iron distributions in surface waters of the south Atlantic. Mar. Chem. 50:13-20.

Quigg, A., Z.V. Finkel, A.J. Irvin, Y. Rosenthal, T.Y. Ho, J.R. Reinfeler, O. Schofield, F.M.M. Morel, and P.G. Falkowski. The evolutionary inheritance of elemental stoichiometry in marine phytoplankton. Nature 425:291-294.

Raphael, M.N. 2003. The Santa Ana winds of California. Earth Interact. 7:1-13.

Rue, E.L., and K.W. Bruland. 1995. Complexation of iron(III) by natural organic ligands in the Central North Pacific as determined by a new competitive ligand equilibration / adsorptive cathodic stripping voltammetric method. Mar. Chem. 50:117-138.

Rykaczewski, R.R., and D.M. Checkley. 2008. Influence of ocean winds on the pelagic ecosystem in upwelling regions. Proc. Natl. Acad. Sci. U.S.A. 105:1965-1970.

Sunda, W.G. and S.A. Huntsman. 1995. Iron uptake and growth limitation in oceanic and coastal phytoplankton. Mar. Chem. 50:189-206.

Sunda, W.G., and S.A. Huntsman. 1997. Interrelated influence of iron, light and cell size on marine phytoplankton growth. Nature 390:389–392.

Tratt, D.M., R.J. Frouin, and D.L. Westphal. 2001. April 1998 Asian dust event: a southern California perspective. J. Geophys. Res. 106:18371-18379.

Venrick, E.L. 1998. The phytoplankton of the Santa Barbara Basin: patterns of chlorophyll and species structure and their relationships with those of surrounding stations. CalCOFI Rep. 39:124-132.

Venrick, E.L. 2002. Floral patterns in the California Current System off southern California: 1990-1996. J. Mar. Res. 60:171-189.

Warrick JA. 2002. Short-term (1997–2000) and long-term (1928–2000) observations of river water and sediment discharge to the Santa Barbara Channel, California. PhD Dissertation. University of California, Santa Barbara.

Warrick, J.A., P.M. DiGiacomo, S.B. Weisbery, N.P. Nezlin, M. Mengel, B.H. Jones, J.C. Ohlmann, L. Washburn, E.J. Terrill, and K.L. Farnsworth. 2007. River plume patterns and dynamics within the Southern California Bight. Cont. Shelf Res. 27:2427-2448.

Westerling, A.L., D.R. Cayan, T.J. Brown, B.L. Hall, and L.G. Riddle. 2004. Climate, Santa Ana winds and autumn wildfires in Southern California. Eos 85:289-300.

Zhang, H., J.J. Bates, and R.W. Reynolds. 2006. Assessment of composite global sampling: Sea surface wind speed. Geophys. Res. Lett. 33:doi:10.1029/2006GL027086.

Chapter 5

Conclusions and future directions

5.1. Conclusions and future directions

Iron is an important micronutrient for phytoplankton productivity and in many parts of the world's oceans, termed high nutrient, low chlorophyll (HNLC) regimes, dissolved iron concentrations are low enough to limit both what kind of phytoplankton grow and how well they grow. The research presented in this dissertation has helped to elucidate the role of iron in a non-HNLC regime: the mesotrophic southern California Current System (sCCS). Relative to HNLC regimes, the sCCS is a low nutrient regime with moderate wind-driven upwelling near the coast and wind stress curl upwelling occurring offshore. The biogeochemical characterization of iron in the sCCS involved developing a high-throughput, sensitive method for measuring dissolved iron in seawater, collecting and measuring samples for dissolved iron concentration, and experimentally testing the influence of iron availability on phytoplankton growth.

In Chapter 2, a detailed description and assessment is presented for a new method for determining iron(II) with nitriloacetic acid (NTA) preconcentration and chemiluminescence detection. The method is sensitive enough to measure low oceanic dissolved iron concentrations (detection limit of 0.02 nM), uses small sample volumes (~2 ml per replicate), and is relatively quick (~2 min per replicate). Surface and deep seawater reference samples were analyzed and results were contributed to the Standardization and Analysis of Fe (SAFe) international intercalibration program. In addition to measuring dissolved iron in a filtered acidified seawater sample (<0.4 µm filter), a similar procedure can likely be applied for measuring total dissolvable iron (acidified unfiltered seawater). Total dissolvable iron concentrations (when

subtracted from dissolved iron concentrations) would provide an estimate of particulate iron concentration, which would be useful for assessing recycling and residence time of iron. Sensitivity and detection limit of the method can be improved by increasing the sample loading time and thus preconcentration. Another potential modification that might be more convenient is the production of trace metal-free synthetic seawater as a substitute for acidified Milli-Q water and trace metal-free ultraviolet irradiated seawater.

The results from shipboard iron addition bottle experiments for assessing phytoplankton iron limitation in the sCCS are described in Chapter 3. These were simple manipulation experiments comparing changes in biological and chemical parameters in iron-added bottle incubations to unamended controls. At ten transition zone stations in July 2003 and 2004, phytoplankton were found to be iron-limited to varying degrees. Overall, iron availability modulated nitrate utilization by phytoplankton. When more iron was available, phytoplankton net growth rates increased and nitrate utilization also increased. When less iron was available, both phytoplankton net growth rates and nitrate utilization were low. This is a novel finding in a region where phytoplankton productivity was previously described as being primarily dependent on nitrate availability. A resulting hypothesis of this work was that the control of nitrate utilization by iron availability regulates, in combination with other factors, the spatial distribution of nitrate in the sCCS. Results indicated that with ambient iron availability, nitrate (1-4 μM) can persist in bottle experiments for several days, but it remains to be seen how long nitrate naturally persists in the sCCS transition zone. Conducting a Lagrangian drifter study of a relatively high nitrate, low

chlorophyll, and low dissolved iron water mass in the offshore transition zone could lend insight to this issue. In some iron addition bottle experiments, silicic acid concentrations may have been low enough to limit some diatoms. It would be of interest to explore whether low concentrations of silicic acid (<2 μM) and dissolved iron could both limit *in situ* diatom growth. Lastly, a virtually open venue exists for studying the role of grazers in both suppressing phytoplankton net growth in iron addition bottle experiments and the rate at which grazers are recycling iron. Does nitrate exist unused in the sCCS transition zone during summer due to iron limitation, or efficient grazing and ammonia production, or a combination of both? It would be informative to assess uptake flux by phytoplankton from the dissolved iron pool and biologically-recycled sources, essentially providing quantifiable evidence for an iron f-ratio.

Chapter 4 summarizes the distribution of dissolved iron in the mixed layer from six CalCOFI cruises between 2002 and 2004, in addition to Lagrangian drifter studies and vertical profiles from cruises in 2006 and 2007. The highest dissolved iron concentrations were found in the northeastern region of the CalCOFI study area, the northern coastal domain. Here, coastal upwelling during spring and summer brings macronutrient and iron rich waters to the euphotic zone. The temporal coherence between elevated iron and upwelling, and the association between elevated iron and the continental shelf suggests that the supply of iron is from the continental shelf and/or its associated bottom boundary layer. Moving away from the region of coastal upwelling, biological uptake in aging upwelled waters preferentially removes dissolved iron, followed by silicic acid, and finally nitrate. The ratio of

nitrate:dissolved iron increases moving offshore and thus increases the severity of phytoplankton iron limitation. In the transition zone domain, without a continental source of iron, wind stress curl upwelling supplies the euphotic zone with relatively low iron and high macronutrient concentrations, thus reinforcing the high nitrate:dissolved iron ratio in aging upwelled waters advected offshore. At some stations in July 2007, there was a vertical decoupling between the depth of the ferricline and nitracline, much like the offshore spatial decoupling pattern observed in the mixed layer. We hypothesize that the ferricline-nitracline decoupling is a product of wind stress curl upwelling of an initially-coupled ferricline and nitracline into the euphotic zone. After shoaling, decoupling occurs due to the faster removal of dissolved iron via biological uptake in comparison to nitrate. This is a feature previously observed in the open ocean where there is a low supply of iron (Johnson et al. 1997; Blaine et al. 2005), and has not been previously observed in regions near continental margins. This is an interesting phenomenon in a productive continental margin where the source of iron is expected to be relatively higher and subsurface cholorophyll maxima (SCM) are biomass maxima. Further investigation of ferricline-nitracline decoupling could be facilitated by a trace metal-clean Rosette sampling system for high-resolution dissolved iron profiles to more clearly define the depth of the ferricline. Iron and nitrate uptake experiments with natural assemblages at the subsurface chlorophyll maximum (SCM) could corroborate the hypothesized higher biological removal rates of iron relative to nitrate (Hopkinson and Barbeau, in press).

Wind stress curl upwelling is a unique and dominant regional-scale forcing in the sCCS and future efforts should be focused on its biogeochemical consequences,

especially nutrient flux estimates into the euphotic zone and the biological response. To distinguish between advected coastal upwelling waters and wind stress curl upwelling waters, future studies will need to incorporate physical-wind models with geochemical tracers indicative of shelf interactions, such as dissolved manganese or radium isotopes. It would also be useful to substantiate the hypothesis that the continental shelf is the primary source of iron to surface waters by quantifying the flux of iron from the shelf and bottom boundary layer and quantifying the flux and subsequent dissolution rates of other potential sources of iron to the study area such as fluvial sediment discharge and eolian deposition via Santa Ana wind events.

This thesis provides a previously-unavailable biogeochemical assessment of iron in the sCCS, in the context of biological, chemical, and physical data collected by the CalCOFI and CCE-LTER time series studies. Dissolved iron, as it has become apparent in recent years, is a key micronutrient for phytoplankton productivity. Close to the continental shelf, high iron availability and elevated concentrations of macronutrients results in high phytoplankton productivity and blooms of large cells such as diatoms. Offshore (50-250 km from the coast), low iron availability results in low macronutrient utilization and thus low phytoplankton net production. While the supply of macronutrients (with relatively constant phosphate:nitrate:silicic acid ratio) is primarily dependent on a remineralized deep ocean source (either via coastal or wind stress curl upwelling), the supply of iron to the sCCS appears to be primarily dependent on a non-deep ocean source including fluvial deposition on the continental shelf and into adjacent surface waters and atmospheric deposition. The waxing and waning of these sources of iron are largely dependent on climate variability (rainfall

and wind patterns) and would be expected to significantly affect biological and geochemical processes in the CCS.

5.2. Literature cited

Blain, S., S. Bonnet, and C. Guieu. 2008. Dissolved iron distribution in the tropical and sub tropical South Eastern Pacific. Biogeosciences 5:269-280.

Johnson, K.S., R.M. Gordon, and K.H. Coale. 1997. What controls dissolved iron concentrations in the world ocean? Authors' closing comments. Mar. Chem. 57:181-186.

Appendices

Appendix A1. Hydrographic and biogeochemical data in surface waters from November 2002 CalCOFI survey cruise stations including CalCOFI line and station numbers (line and sta; see Fig. 4.1 for station map), latitude and longitude in degrees (lat and long), temperature °C (temp), salinity in psu (sal), µg L^{-1} chlorophyll a (chl), µM nitrate (nit), and nM dissolved iron (dFe).

line	sta	lat	long	temp	sal	chl	nit	dFe
77	49	35.088	-120.778	12.9	33.40	1.54	8.1	7.75
77	51	35.020	-120.918	13.8	33.32	0.89	4.0	0.52
77	55	34.888	-121.198	15.2	33.40	0.97	0.4	0.17
77	60	34.718	-121.550	15.2	33.35	0.96	0.2	0.24
77	70	34.387	-122.248	15.2	33.35	0.92	0.2	0.09
77	80	34.055	-122.945	14.2	32.96	1.10	0.2	0.13
80	51	34.450	-120.525	15.3	33.31	1.32	0.1	0.83
80	55	34.317	-120.800	15.7	33.39	0.40	0.2	0.38
80	60	34.150	-121.152	14.5	33.38	1.61	1.4	0.17
80	80	33.480	-122.533	16.0	33.31	0.31	0.1	0.09
82	47	34.273	-120.028	15.9	33.33	0.95	0.1	1.05
83	41	34.227	-119.408	16.0	33.37	1.13	0.4	1.81
83	42	34.180	-119.508	16.2	33.34	0.93	0.1	4.75
83	55	33.747	-120.415	16.2	33.39	0.30	0.1	0.13
83	110	31.913	-124.168	17.6	33.08	0.13	0.1	0.10
87	33	33.888	-118.492	17.0	33.40	0.31	0.1	1.37
87	35	33.823	-118.630	16.4	33.32	0.88	0.1	3.39
87	50	33.322	-119.667	15.6	33.35	0.91	0.2	0.30
87	60	32.995	-120.347	16.6	33.40	0.34	0.1	0.12
87	90	31.990	-122.395	17.5	33.03	0.11	0.1	0.14
90	28	33.483	-117.767	17.6	33.38	0.55	0.1	1.94
90	30	33.418	-117.902	16.8	33.42	0.28	0.1	0.16
90	37	33.187	-118.390	17.0	33.36	0.17	0.2	0.22
90	60	32.417	-119.958	16.7	33.35	0.19	0.1	0.22
90	80	31.748	-121.313	16.4	33.15	0.17	0.2	0.19
90	90	31.417	-121.990	17.0	33.10	0.13	0.1	0.07
90	110	30.747	-123.333	17.6	33.11	0.10	0.1	0.13
93	28	32.908	-117.397	17.5	33.47	0.29	0.0	0.31
93	60	31.850	-119.567	17.3	33.45	0.25	0.0	0.24
93	100	30.512	-122.255	17.7	33.13	0.11	0.1	0.08
93	120	29.850	-123.585	19.0	33.34	0.11	0.1	0.07

Appendix A2. Hydrographic and biogeochemical data in surface waters from January/February 2003 CalCOFI survey cruise stations including CalCOFI line and station numbers (line and sta; see Fig. 4.1 for station map), latitude and longitude in degrees (lat and long), temperature °C (temp), salinity in psu (sal), µg L^{-1} chlorophyll a (chl), µM nitrate (nit), and nM dissolved iron (dFe).

line	sta	lat	long	temp	sal	chl	nit	dFe
77	49	35.088	-120.778	14.1	33.19	0.39	1.3	3.06
77	51	35.020	-120.918	14.3	33.30	0.53	1.2	2.44
77	55	34.888	-121.198	14.5	33.23	0.62	0.6	2.55
77	70	34.387	-122.248	14.1	33.06	1.71	0.1	0.96
80	100	32.812	-123.903	14.6	32.59	0.26	0.0	0.39
82	47	34.273	-120.028	15.1	33.41	0.50	0.1	0.96
83	40.6	34.227	-119.408	15.1	33.39	0.53	0.0	5.24
83	42	34.180	-119.508	15.2	33.37	0.29	0.1	0.80
83	55	33.747	-120.415	14.6	33.37	0.66	0.1	0.28
83	70	33.245	-121.438	14.9	33.01	0.25	0.1	0.19
83	90	32.580	-122.813	15.3	32.86	0.15	0.1	0.26
87	33	33.888	-118.492	15.5	33.41	0.46	0.1	4.44
87	45	33.488	-119.317	14.5	33.34	0.94	0.7	0.70
87	55	33.158	-120.012	14.8	33.00	0.31	0.0	0.25
87	80	32.317	-121.710	14.9	32.90	0.18	0.0	0.50
90	28	33.483	-117.767	15.8	33.38	0.33	0.1	2.28
90	30	33.418	-117.902	16.0	33.38	0.41	0.1	1.31
90	37	33.187	-118.390	15.8	33.41	0.25	0.1	0.45
90	53	32.653	-119.482	14.7	33.25	0.48	0.0	0.10
90	70	32.083	-120.638	15.0	33.08	0.19	0.0	0.24
90	110	30.747	-123.333	15.8	33.01	0.15	0.1	0.20
93	28	32.908	-117.397	15.9	33.40	0.21	0.0	4.00
93	30	32.845	-117.533	15.8	33.39	0.23	0.1	1.57
93	40	32.510	-118.215	15.9	33.41	0.18	0.1	1.57
93	50	32.180	-118.893	15.2	33.24	0.18	0.0	0.45
93	80	31.173	-120.923	15.4	33.18	0.16	0.0	0.33

Appendix A3. Hydrographic and biogeochemical data in surface waters from April 2003 CalCOFI survey cruise stations including CalCOFI line and station numbers (line and sta; see Fig. 4.1 for station map), latitude and longitude in degrees (lat and long), temperature °C (temp), salinity in psu (sal), µg L^{-1} chlorophyll a (chl), µM nitrate (nit), and nM dissolved iron (dFe).

line	sta	lat	long	temp	sal	chl	nit	dFe
77	49	35.088	-120.778	11.3	33.73	6.18	10.7	3.47
77	51	35.020	-120.918	11.4	33.54	9.06	9.3	0.28
77	55	34.888	-121.198	12.0	33.16	3.43	6.4	0.16
77	100	33.388	-124.323	15.5	32.85	0.08	0.0	0.14
80	51	34.450	-120.525	12.3	33.65	33.34	0.3	8.20
80	55	34.317	-120.800	13.3	33.32	2.55	1.4	1.70
80	60	34.150	-121.152	13.3	33.17	6.65	0.1	0.16
82	47	34.273	-120.028	12.4	33.49	12.60	1.4	0.21
83	42	34.180	-119.508	12.3	33.59	7.32	6.9	0.34
83	51	33.873	-120.133	11.9	33.61	2.74	11.0	3.08
83	55	33.747	-120.415	13.3	33.36	2.88	0.8	0.34
83	60	33.578	-120.757	13.3	33.06	6.02	0.1	0.49
83	70	33.245	-121.438	14.9	33.11	0.29	0.1	0.05
83	100	32.242	-123.492	14.9	32.81	0.15	0.1	0.11
87	33	33.888	-118.492	13.7	33.54	8.87	0.2	0.75
87	35	33.823	-118.630	14.7	33.48	0.89	0.1	0.53
87	45	33.488	-119.317	12.7	33.43	9.17	3.3	0.26
87	50	33.322	-119.667	12.7	33.39	10.35	3.9	1.97
87	55	33.158	-120.012	13.5	33.22	2.99	2.3	0.23
87	70	32.655	-121.040	14.6	33.19	1.64	0.1	0.13
87	90	31.990	-122.395	15.0	33.09	0.30	0.0	0.10
90	28	33.483	-117.767	14.5	33.42	5.22	0.4	0.19
90	30	33.418	-117.902	15.4	33.41	0.51	0.1	0.76
90	37	33.187	-118.390	14.1	33.41	0.67	0.1	0.22
90	53	32.653	-119.482	14.9	33.23	0.76	0.2	0.51
90	90	31.417	-121.990	15.1	33.04	0.15	0.0	0.34
93	26.5	32.950	-117.307	15.4	33.35	1.20	0.9	2.30
93	28	32.908	-117.397	15.1	33.34	0.75	0.7	0.62
93	30	32.845	-117.533	15.5	33.26	0.27	0.0	0.47

Appendix A4. Hydrographic and biogeochemical data in surface waters from July 2003 CalCOFI survey cruise stations including CalCOFI line and station numbers (line and sta; see Fig. 4.1 for station map), latitude and longitude in degrees (lat and long), temperature °C (temp), salinity in psu (sal), µg L^{-1} chlorophyll a (chl), µM nitrate (nit), and nM dissolved iron (dFe).

line	sta	lat	long	temp	sal	chl	nit	dFe
77	49	35.088	-120.778	15.6	33.57	5.57	0.2	0.72
77	55	34.888	-121.198	15.4	33.18	0.52	3.3	0.20
77	70	34.387	-122.248	17.2	33.01	0.25	0.1	0.34
77	100	33.388	-124.323	18.1	32.94	0.11	0.0	0.33
80	51	34.450	-120.525	17.1	33.45	3.50	0.0	3.40
80	55	34.317	-120.800	17.3	33.47	1.45	0.0	1.04
80	70	33.820	-121.838	16.4	33.10	0.38	1.8	0.27
80	80	33.480	-122.533	16.2	32.96	0.41	2.2	0.28
82	47	34.273	-120.028	19.4	33.48	1.83	0.0	0.76
83	51	33.873	-120.133	17.6	33.42	2.32	0.0	1.02
83	55	33.747	-120.415	17.7	33.49	1.83	0.2	0.72
83	80	32.907	-122.123	17.2	32.89	0.26	0.0	0.33
87	33	33.888	-118.492	22.5	33.55	2.59	0.1	1.17
87	35	33.823	-118.630	22.9	33.58	3.29	0.0	1.38
87	55	33.158	-120.012	16.8	33.51	2.09	0.1	0.55
87	70	32.655	-121.040	17.1	32.93	0.33	0.0	0.35
90	28	33.483	-117.767	20.5	33.51	1.03	0.0	0.56
90	37	33.187	-118.390	19.7	33.52	0.51	0.2	0.10
90	53	32.653	-119.482	15.7	33.10	0.64	0.9	0.05
90	70	32.083	-120.638	15.8	33.20	0.44	1.1	0.49
90	90	31.417	-121.990	17.1	32.86	0.20	0.1	0.37
93	28	32.908	-117.397	20.2	33.42	0.52	0.1	0.75
93	30	32.845	-117.533	20.2	33.49	0.45	0.1	0.59
93	40	32.510	-118.215	19.2	33.32	0.35	0.0	0.54
93	50	32.180	-118.893	18.6	33.56	0.35	0.0	0.41
93	55	32.012	-119.233	17.1	33.32	0.57	0.1	0.34
93	60	31.850	-119.567	18.1	33.17	0.09	0.1	0.24
93	80	31.173	-120.923	16.8	33.07	0.31	0.2	0.42
93	110	30.180	-122.923	19.0	33.16	0.08	0.3	0.27

Appendix A5. Hydrographic and biogeochemical data in surface waters from Mar/April 2004 CalCOFI survey cruise stations including CalCOFI line and station numbers (line and sta; see Fig. 4.1 for station map), latitude and longitude in degrees (lat and long), temperature °C (temp), salinity in psu (sal), µg L^{-1} chlorophyll a (chl), µM nitrate (nit), and nM dissolved iron (dFe).

line	sta	lat	long	temp	sal	chl	nit	dFe
77	49	35.088	-120.778	10.6	33.63	9.17	15.3	1.90
77	51	35.020	-120.918	10.8	33.49	9.01	14.0	0.38
77	55	34.888	-121.198	12.0	33.24	0.15	7.5	0.32
77	60	34.718	-121.550	12.7	33.18	0.85	3.1	0.39
77	70	34.387	-122.248	13.9	33.05	0.75	0.3	0.20
77	100	33.388	-124.323	14.0	32.93	0.52	0.0	0.29
80	51	34.450	-120.525	13.4	33.34	8.86	1.1	2.80
80	55	34.317	-120.800	12.2	33.51	5.52	10.9	2.70
80	60	34.150	-121.152	12.4	33.46	11.64	6.1	0.79
80	80	33.480	-122.533	14.2	33.05	0.85	0.5	0.76
82	47	34.273	-120.028	14.7	33.35	3.78	0.6	2.20
83	51	33.873	-120.133	13.4	33.29	3.26	3.7	3.00
83	55	33.747	-120.415	13.4	33.28	3.89	2.7	2.60
83	60	33.578	-120.757	13.0	33.22	2.42	4.5	0.58
87	33	33.888	-118.492	16.2	33.19	2.75	0.2	3.40
87	35	33.823	-118.630	15.9	33.17	0.31	0.1	0.90
87	45	33.488	-119.317	15.2	33.19	0.82	0.0	0.31
87	55	33.158	-120.012	13.9	33.23	1.89	1.5	0.50
87	100	31.657	-123.070	15.6	33.10	0.08	0.0	0.17
90	28	33.483	-117.767	15.7	33.17	5.30	0.7	4.00
90	30	33.418	-117.902	16.0	33.16	0.31	0.0	0.39
90	37	33.187	-118.390	15.9	33.18	0.20	0.0	0.22
90	53	32.653	-119.482	13.3	33.02	0.43	2.2	0.55
90	60	32.417	-119.958	13.4	33.07	1.30	0.7	0.38
90	110	30.747	-123.333	15.7	33.00	0.08	0.1	0.15
93	26.6	32.950	-117.307	15.5	33.09	1.92	0.0	2.70
93	28	32.908	-117.397	16.2	33.09	1.33	0.0	2.40
93	30	32.845	-117.533	15.7	33.13	0.59	0.0	0.56
93	40	32.510	-118.215	15.3	33.17	0.27	0.0	0.25
93	50	32.180	-118.893	14.7	33.07	0.27	0.0	0.27
93	60	31.850	-119.567	14.6	33.09	0.29	0.0	0.11
93	100	30.512	-122.255	15.6	33.01	0.08	0.0	0.18
93	120	29.850	-123.585	16.0	33.02	0.09	0.0	0.17

Appendix A6. Hydrographic and biogeochemical data in surface waters from July 2004 CalCOFI survey cruise stations including CalCOFI line and station numbers (line and sta; see Fig. 4.1 for station map), latitude and longitude in degrees (lat and long), temperature °C (temp), salinity in psu (sal), µg L^{-1} chlorophyll a (chl), µM nitrate (nit), and nM dissolved iron (dFe).

line	sta	lat	long	temp	sal	chl	nit	dFe
77	49	35.088	-120.778	13.0	33.59	17.59	4.7	1.60
77	51	35.020	-120.918	16.0	33.55	4.63	2.1	0.87
77	70	34.387	-122.248	17.4	33.07	0.29	1.9	0.19
77	100	33.388	-124.323	18.7	32.87	0.12	0.0	0.18
80	51	34.450	-120.525	12.5	33.50	8.45	8.8	4.00
80	70	33.820	-121.838	17.7	33.34	0.26	3.4	0.44
82	47	34.273	-120.028	16.2	33.51	2.27	0.1	1.20
83	40.6	34.227	-119.408	18.3	33.39	2.14	0.0	0.50
83	60	33.578	-120.757	15.9	33.45	0.53	2.0	0.44
83	110	31.913	-124.168	19.7	32.83	0.08	0.0	0.09
87	33	33.888	-118.492	20.5	33.40	0.81	0.0	1.30
87	35	33.823	-118.630	21.2	33.49	0.43	0.0	0.54
87	45	33.488	-119.317	16.1	33.47	0.55	3.2	0.46
87	70	32.655	-121.040	16.9	33.09	0.26	1.1	0.20
90	28	33.483	-117.767	20.7	33.46	0.40	0.0	0.74
90	30	33.418	-117.902	21.5	33.48	0.32	0.0	0.26
90	37	33.187	-118.390	20.3	33.44	0.27	0.0	0.31
90	53	32.653	-119.482	17.4	33.54	0.34	2.1	0.31
90	60	32.417	-119.958	16.5	33.43	0.39	2.0	0.17
93	50	32.180	-118.893	17.6	33.36	0.34	0.0	0.22
93	80	31.173	-120.923	16.6	32.95	0.27	0.3	0.09
93	110	30.180	-122.923	18.7	33.06	0.09	0.0	0.27

Appendix B1. Hydrographic and biogeochemical profile data from October 2006 CalCOFI cruise stations including CalCOFI line and station numbers (line and sta; see Fig. 4.1 for station map), latitude and longitude in degrees (lat and long), temperature °C (temp), salinity in psu (sal), oxygen saturation (%O_2 sat), µg L^{-1} chlorophyll a (chl), µM nitrate (nit), and nM dissolved iron (dFe).

line	sta	lat	long	depth	temp	sal	%O_2 sat	chl	nit	dFe
83	42	34.180	-119.508	10	17.8	33.45	108	1.68	0.0	2.23
83	42	34.180	-119.508	40	14.3	33.31	97	0.64	0.9	0.28
83	42	34.180	-119.508	75	11.4	33.47	68	0.10	14.1	2.09
83	51	33.873	-120.133	10	16.5	33.49	104	1.47	0.6	3.98
83	51	33.873	-120.133	30	15.6	33.47	97	1.42	2.3	3.46
83	51	33.873	-120.133	70	11.5	33.59	58	0.20	16.5	4.50
83	60	33.578	-120.757	10	15.8	33.41	103	0.77	0.1	0.33
83	60	33.578	-120.757	50	12.3	33.15	89	0.26	5.5	0.99
83	60	33.578	-120.757	100	10.1	33.76	47	0.05	22.2	3.46
83	60	33.578	-120.757	200	9.3	34.12	29	0.01	28.2	2.17
83	70	33.245	-121.438	10	16.4	33.10	102	0.33	0.1	0.16
83	70	33.245	-121.438	50	15.5	33.23	103	0.58	0.1	0.26
83	70	33.245	-121.438	100	11.9	33.49	78	0.10	9.7	0.20
83	70	33.245	-121.438	200	8.9	34.01	38	N.D.	27.4	0.64
83	90	32.580	-122.813	10	17.7	33.21	102	0.15	0.0	0.20
83	90	32.580	-122.813	65	14.8	33.20	103	0.40	0.0	0.33
83	90	32.580	-122.813	150	9.7	33.68	57	0.02	20.8	0.55
83	90	32.580	-122.813	250	8.0	34.13	22	N.D.	33.0	0.88

Appendix B2. Hydrographic and biogeochemical profile data from April 2007 CCE-LTER drifter study including study and day number (study and day), latitude and longitude in degrees (lat and long), temperature °C (temp), salinity in psu (sal), µg L^{-1} chlorophyll a (chl), µM nitrate (nit), and nM dissolved iron (dFe).

cycle	day	lat	long	depth	temp	sal	chl	nit	dFe
1	1	34.268	-120.876	20	12.19	33.60	2.18	7.6	1.47
1	1	34.268	-120.876	60	10.71	33.58	0.16	15.5	1.33
1	1	34.268	-120.876	100	8.71	33.94	0.16	12.4	1.75
1	1	34.268	-120.876	200	7.81	34.03	0.16	27.8	0.92
1	4.5	34.358	-121.075	10	12.49	33.47	1.21	4.7	0.33
1	4.5	34.358	-121.075	45	11.52	33.71	1.70	11.6	1.40
1	4.5	34.358	-121.075	100	10.42	33.65	0.19	22.4	1.13
1	4.5	34.358	-121.075	150	9.08	33.87	0.19	22.4	1.13
1	4.5	34.358	-121.075	200	N.D.	N.D.	0.19	26.5	1.13
4	4	33.742	-121.001	15	12.50	33.44	0.68	8.0	0.33
4	4	33.742	-121.001	60	12.19	33.61	1.60	13.2	1.40
4	4	33.742	-121.001	100	11.70	33.68	0.39	19.7	0.73
4	4	33.742	-121.001	200	N.D.	N.D.	0.39	25.4	0.96

Appendix B3. Hydrographic and biogeochemical profile data from July 2007 DCM stations including CalCOFI line and station numbers (line and sta; see Fig. 4.1 for station map), latitude and longitude in degrees (lat and long), temperature °C (temp), salinity in psu (sal), oxygen saturation (%O_2 sat), µg L^{-1} chlorophyll a derived from in situ fluorometer (chl), µM nitrate (nit), and nM dissolved iron (dFe).

line	sta	lat	long	depth	temp	sal	%O_2 sat	chl	nit	dFe
93	40	32.510	-118.215	10	19.4	33.76	124	0.20	0.0	0.09
93	40	32.510	-118.215	30	14.0	33.62	126	0.62	0.6	0.08
93	40	32.510	-118.215	40	12.7	33.60	113	0.69	5.7	0.08
93	40	32.510	-118.215	50	12.0	33.63	104	0.43	12.1	0.12
93	40	32.510	-118.215	70	10.6	33.72	88	0.18	16.8	0.14
93	40	32.510	-118.215	100	9.7	33.87	79	0.16	21.1	0.52
93	40	32.510	-118.215	150	9.2	34.02	73	0.15	25.6	0.91
93	40	32.510	-118.215	250	8.3	34.20	60	0.15	31.0	1.00
93	60	31.850	-119.567	10	16.5	33.66	125	0.81	0.6	0.04
93	60	31.850	-119.567	15	16.4	33.67	125	0.94	0.7	0.11
93	60	31.850	-119.567	30	15.2	33.61	123	0.66	1.9	0.21
93	60	31.850	-119.567	75	11.7	33.62	101	0.22	13.9	0.20
93	60	31.850	-119.567	100	10.6	33.68	91	0.17	18.5	0.26
93	60	31.850	-119.567	150	9.1	33.93	84	0.15	23.0	0.39
93	60	31.850	-119.567	250	7.5	34.09	64	0.15	31.4	0.70
93	80	31.173	-120.923	15	17.8	33.41	124	0.26	0.3	0.16
93	80	31.173	-120.923	62	14.2	33.26	125	0.54	0.2	0.16
93	80	31.173	-120.923	70	14.1	33.35	123	0.55	0.6	0.05
93	80	31.173	-120.923	75	13.6	33.36	120	0.42	2.1	0.15
93	80	31.173	-120.923	100	12.2	33.40	111	0.22	5.8	0.45
93	80	31.173	-120.923	250	8.2	34.06	71	0.15	30.4	0.78
93	110	30.180	-122.923	20	19.4	33.42	122	0.14	0.0	0.09
93	110	30.180	-122.923	40	18.0	33.53	123	0.14	0.0	0.03
93	110	30.180	-122.923	60	16.9	33.50	124	0.15	0.0	0.05
93	110	30.180	-122.923	80	15.9	33.45	125	0.18	0.0	0.06
93	110	30.180	-122.923	110	15.4	33.59	122	0.25	0.0	0.02
93	110	30.180	-122.923	130	15.2	33.77	120	0.30	0.8	0.10
93	110	30.180	-122.923	150	14.2	33.75	115	0.23	1.0	0.01
93	110	30.180	-122.923	250	9.0	33.93	89	0.14	21.2	0.18
93	120	29.850	-123.585	20	19.2	33.32	122	0.15	0.0	0.18
93	120	29.850	-123.585	50	16.8	33.34	124	0.15	0.5	0.11
93	120	29.850	-123.585	75	15.7	33.39	124	0.19	0.5	0.10
93	120	29.850	-123.585	95	15.6	33.62	122	0.25	0.2	0.09
93	120	29.850	-123.585	115	14.7	33.56	119	0.29	1.0	0.11
93	120	29.850	-123.585	130	14.5	33.71	117	0.25	2.9	0.09
93	120	29.850	-123.585	250	9.2	33.92	89	0.14	24.4	0.29